Final Technical Report No. GR 69-11

JET FUEL DECONTAMINATION STUDIES

September, 1969

Contract No. DA 44-009-AMC-1165(T)

Task No. 1M643324D59209, U. S. Army
Engineer Research and Development Laboratories,
Fort Belvoir, Virginia

Report prepared by

H. A. Beatty

ETHYL CORPORATION
1600 West Eight Mile Road
Ferndale, Michigan 48220

U. S. Government Agencies may obtain copies of this report directly from Defense Documentation Center (DDC). Other qualified DDC users should request through Commander, USAMERDC Ft. Belvoir, Virginia

PREFACE

This study has been undertaken by Ethyl Corporation's Research Laboratories in Ferndale, Michigan, on behalf of the U.S. Army Mobility Equipment Research and Development Center, Fort Belvoir, Virginia 22060, under Contract No. DA-44-009-AMC-1165(T).

The contract became effective 10 June 1965 and the termination date is 9 September 1969. The present Final Report summarizes the experimental work carried out during this period.

The Contracting Officer's Representatives have in turn been Messrs. John C. Estabrooke, Robert N. Brown, Edward Russell, and William R. Williams.

Overall responsibility for the project has been in the hands of Dr. E. B. Rifkin, Associate Director, Petroleum Chemicals Research, and Dr. M. E. Gluckstein or Mr. U. A. Lehikoinen, Research Supervisors. The work was planned and supervised by Dr. H. A. Beatty, Research Advisor, and has been carried out principally by Mr. E. P. Balda and in part by Mr. R. G. Lyben and Mr. D. C. Hargis.

TABLE OF CONTENTS

TABLE OF CONTENTS - Continued

LIST OF TABLES

LIST OF TABLES - Continued

LIST OF FIGURES

SUMMARY

This report covers four years of laboratory bench research on coalescer media for removal of free water from JP-5 and diesel fuels. The objective was to investigate the basic physico-chemical factors and hydraulic mechanism involved in the coalescence process, and to design coalescer mats of greater effectiveness for fuel containing corrosion inhibitors or other surfactants.

Measurements were made of contact angles of water on surfaces submerged in fuels, and of water-fuel interfacial tensions. Capillarity and flow resistance of coalescer media and electrokinetic behavior of water suspensions were examined. A careful study was made of the attachment, growth, and detachment of water droplets on single fibers in a flowing suspension. Most of this work was done with JP-5 containing a variety of surfactants; Jet A, CITE, and diesel fuels were also used. The WSIM of all fuels was determined.

Based on these data and the literature, calculations were made and correlations were established. Unfortunately, the results of this basic work proved to be of little value as a guide to the selection of effective coalescer media.

All coalescence was done using a water separometer to prepare and pump the suspensions of 0.1 to 1% water and to monitor the effluent fuel. Tests of experimental mats in the separometer cell were useful for screening materials and indicating important process variables. However, it became evident that these tests were not adequate to predict the performance of coalescer media under realistic conditions of greater mat depth and lower fuel flow rate.

Accordingly, cells were made having 0.5 inch or greater diameter, with provision for variation in depth and packing density of the mat layers and for visual observation of the downstream mat surface. These cells reached equilibrium performance in 20 to 40 minutes at a flow velocity of 1 cm/sec, and gave significant results that could be expected to anticipate the behavior in full scale filter/coalescer elements. To obtain discrimination between different mats, it was generally necessary to add a strong surfactant to the fuel.

The principal observations and conclusions from this study were:

1. Tests of an individual material were of no value whatever in defining its usefulness in a combination coalescer mat. Effective coalescence was obtained only in combination mats in which the fiber diameter and porosity increased progressively from the upstream to the downstream side.

2. The overall process evidently required: (a) complete attachment of inflowing droplets onto fiber surfaces, (b) collection of the attached water

into rivulets that joined together into streams during flow through the mat, and (c) unhampered discharge in drop form at the downstream surface. Visual observations of the first two stages were difficult to make, but gave support to this mechanism.

3. Surfactants may impede one or all of these processes, by modifying both the water-solid and water-fuel interfacial tensions. Sulfonates such as Petronate L were far worse than corrosion inhibitors such as Santolene C. Antiicer greatly reduced the effect of both kinds of surfactants.

4. Preferred materials were: for the upstream layer, resin-coated 1 to 5 μ glass wool. For the intermediate layers, the best materials were natural sponge, a sintered plate of steel shavings, 8 to 12 μ steel wool, 16-μ carbon felt, 40 to 50 μ nylon or dacron felts, a porous carbon plate, and 6 to 24 μ coated glass wool. At the outer surface, a layer of uncoated glass or quartz wool promoted formation of large drops, but tended to cause "grapeing"; this was prevented by an outer skin of 100-pore polyurethane foam. Steel wool and nylon felt also gave good results with only a 16-mesh glass or PVC screen as the outer skin. In surfactant fuel, a good experimental mat was far superior to plugs cut out of commercial elements. Altogether, it was clear that the nature and even the surface texture of the materials was not nearly as important as the dimensions, structure, and packing density.

5. No electrokinetic effects could be detected in the coalescer cells. However, the presence of methacrylate (Plexiglas) surface on the cell wall on upstream sometimes gave a greatly improved performance. This was not reproducible.

6. Addition of two types of organic dye to the water gave a market improvement in coalescence. Addition of acidic ferrous chloride was harmful.

7. Diesel No. 2 oils, even when additive-free, gave poor coalescence; additives made them worse. Purification with silica or charcoal gave an oil of WSIM = 99 although the fuel-water IFT was raised only slightly to 17 dyne. Using this oil, a good mat gave perfect coalescence for 8 minutes but then the performance became very poor.

8. Two cells in tandem gave wellnigh complete coalescence, where one cell alone was quite inadequate.

9. It may be possible to design a superior envelope to replace the present-day high-cost outer canister screens.

Finally, after a number of structural failures, a satisfactory group of full scale experimental filter/coalescer elements was delivered to Fort Belvoir for testing.

INTRODUCTION

It has long been recognized (refs. 4, 7, 11) that faulty performance of filter/coalescer elements is likely to occur with fuels containing surfactants. Diesel fuels, many JP-4's, and some JP-5's contain natural surfactant components. Clean fuels may become contaminated with sulfonates at the refinery or in pipeline transit. Finally, the desired addition of corrosion inhibitors increases the surface activity to some degree.

Much effort has been made to determine how and why these sufactants interfere with the coalescence of water (for example, see refs. 3, 13, 19, 28). However, the knowledge gained to date has provided no specific solution to the problem. The development of filter/separator units (recently reviewed by Redmon and by Stark, refs. 22, 23, 30) has largely been directed toward mechanical improvements designed to reduce size and weight and increase throughput.

Various empirical modifications of the filter/coalescer elements have been made by their manufacturers. However there has been but little basic research aimed at improved coalescer media and design. Early work of Langdon (ref. 17) sponsored by the Army showed some promise of accomplishing this. Jefferson (ref. 12) has recently indicated the Army's current efforts in this direction, including work by Ethyl Corporation.

The present final report gives the salient results of Ethyl's four years of laboratory study of the coalescence of free water in JP-5 fuel. Previously, the following seven semiannual interim reports were issued:

Ethyl No.	Date	AD No.
GR 66-1	January 1966	476 384 L
GR 66-30	July 1966	815 527 L
GR 67-2	January 1967	815 528 L
GR 67-28	July 1967	818 061 L
GR 68-3	January 1968	826 454 L
GR 68-33	July 1968	835 249 L
GR 69-1	January 1969	846 399 L

Also reference will be made to Ethyl Report No. GR 65-1, March 1965 (AD No. 465 647 L) covering a preliminary short term contract, No. DA-44-009-AMC-576 (T).

The objective of the project, in essence, was to gain a better understanding of the dynamics of the water coalescence and detachment process, and thereby to develop new coalescer mats that would give better performance on surface active fuels of low WSIM. We did not study the filtration of solid particles--a different problem, outside the scope of the contract. Thus, in the final assembly of a few full size experimental filter/coalescer elements, we used a commercial element with its inner filtering section intact and modified only the outer layer to a depth of 7/16 in.

All of our own laboratory observations of coalescence were made in small size cells, the later ones having a realistic mat depth and fuel flow velocity. Experience elsewhere (ref. 5) has shown that such cells match full size elements in performance, as would be expected. Thus we avoided the costly and time-consuming fabrication of many full size elements and operation of a single element test loop. Instead, the few elements we finally made were sent to Fort Belvoir for testing.

The following record is divided according to subject matter, and so is not entirely in chronological order. The first two chapters briefly describe the principal materials and equipment used. Following are sections giving observations of physical and electrostatic properties of additive fuels and coalescer media, and the preparation and analysis of water droplet suspensions. Then come the actual experiments on coalescence, beginning with single fiber studies and continuing with the major part of the project, the study of fiber mats. The latter includes visual observations, standard WSIM determinations, exploration of other mat media in the water separometer cell, tests in larger cells at realistic low flow rates using contaminated fuel, and finally some observations of the action of detached outer screens. A description of the construction and performance of a few full size elements terminates the experimental part. A final chapter gives general conclusions and recommendations.

All significant data not previously reported are given in detail in Sections IV and V of the chapter on Coalescence in Fiber Mats. Previously reported data and conclusions are either given in detail or summarized, as seems fit.

During the course of the project, a considerable number of pertinent reports, journal articles, and patents have been collected and studied. No attempt will be made here to list and critically review all these publications. To do so would be a major task, not called for in the present contract. However, reference will be made to a number of reports of particular interest that are listed in the Bibliography.

MATERIALS

I. FUELS

Most of the coalescence study used high quality JP-5 of WSIM 99-100, first from Sun Oil and then from Ashland Oil. A few tests were made with CITE, Jet A, and three diesel fuels. Bayol 35 reference fuel was used in the contact angle, single fiber, and porosity studies, as well as in the routine washing and occasional checking of the water separometer.

JP-5 and Jet A, unlike JP-4, are usually low in surface activity, insofar as this is shown by the WSIM. However, they may often become contaminated at the refinery or in transit. Much of the filter/separator difficulty at airports is ascribed to delivery from common carrier pipelines that have been contaminated by products from low grade refineries. Degradation may also occur in storage. In our final drum of Sun Oil JP-5, the WSIM suddenly dropped from 100 to 80 for no known reason. One drum from a different company had a WSIM of 45; it was discarded with no further ado.

At this time (1967) the source of supply was shifted to Ashland oil. Two drums of their JP-5 had a distinct color and a WSIM of only 80. The fuel was treated with silica gel which removed the color and raised the WSIM to 99. After using this purified fuel for a time, we obtained a supply of "Bronoco 140", a high quality, narrow boiling kerosene refined by Ashland Oil and used by them in their own company jet aircraft. It fully meets MIL-F-5624G, grade JP-5, and ASTM Jet A specifications, although the viscosity is a little lower than normal. This fuel was used from December 1967 to date.

Diesel fuels are notoriously variable in ease of removal of water. The WSIM is not a satisfactory measure of this, being usually low, and it does not correlate with emulsification tendency (ref. 18). The three fuels used in our study cover a wide range of quality.

It can be concluded that all fuels used for experimental purposes, particularly those from drums or smaller containers, should periodically be checked in the water separometer to assure constant quality. Even the Bayol 35 reference fuel is not above suspicion: the first two drums of this that we received were contaminated, having a WSIM of about 55. Subsequent drums gave values of 94 and 98, in agreement with the average of 96 found by the CRC (ref. 9).

Table 1 lists the pertinent properties of the fuels used. The Great Northern and Delta fuels were straightrun No. 2 diesel oils; the JP-5 fuels were free from additives. Note that a WSIM of 100^+ means that the meter continued to read 100 even when the flow rate was raised to 180-190 ml/min.

TABLE 1

PROPERTIES OF FUELS USED

	Density		Viscosity		
	API	d 77F	cs 100F	cp 77F	WSIM
Ashland Bronoco 140	46.9	.786	--	1.14	99
Ashland JP-5 as recd.	43.0	.805	--	1.53	80
same, purified	--	--	--	--	99
Sun Oil JP-5	43.6	.801	--	1.35	$99\text{-}100^+$
Gulf Oil Jet A	44.1	.799	--	1.47	99
CITE (USAMERDC)	41.3	.810	1.73	1.8	94
Humble Bayol 35	--	.774	2.40	2.42	96
Delta No. 2 diesel	35.0	.844	3.04	3.06	81
Great Northern No. 2	29.7	.868	2.95	3.4	31
NATO F-75 marine diesel	33.5	.849	3.5	4.2	21

II. ADDITIVES

Apart from surfactants, the only additive used in JP-5 was 0.15 vol.% of the standard methoxyethanol antiicer of military specification grade (Phillips 55MB or Union Carbide UCAR 500). Two diesel fuel additives used were Delta's FOA 208 (a dispersant and metal deactivator) and Ethyl's MPA-D (a multipurpose additive). Table 2 lists the surfactants used.

TABLE 2

STRUCTURE OF SURFACTANTS

Santolene C	A 50% hydrocarbon solution of a cross-linked dimer of linoleic acid, $C_{17}H_{31}COOH$. Source: Monsanto.
RP-2	A mixture containing 25% octyl phosphate esters and 55% octyl amines and alcohols and 20% hydrocarbon diluent (Ref. 5). Source: duPont.
AFA-1	Similar to RP-2. Source: duPont.
Petronate L	A sodium alkyl aryl petroleum sulfonate, molecular weight 415-430, having both oleophilic and hydrophilic properties: its basic structure is $R-\langle O \rangle-SO_2ONa$. Source: Sonneborn.

Continued

TABLE 2 - Continued

Pyronate 30	Similar to Petronate L, but completely water-soluble, and insoluble in oil. Source: Sonneborn.
Aerosol OT	Sodium dioctyl sulfosuccinate: $ROCOCH_2CH(COOR)SO_2ONa$, R = 2-ethylhexyl. A powerful wetting agent. Source: American Cyanamide.
Igepal CO-530	Nonylphenoxypoly(ethyleneoxy)ethanol: $R-C_6H_4-O(CH_2CH_2O)_nCH_2CH_2OH$, R = nonyl. A non-ionic agent, with balanced oil-water solubility. Source: General Aniline and Film.
Katapol PN-430	A polyoxyethylated alkylamine: $RNH(CH_2CH_2O)_nCH_2CH_2OH$; alkyl group not identified. This is a cationic, oil and water-soluble wetting agent. Source: General Aniline and Film.
Igepon T-33	Sodium N-methyl-N-oleyltaurate: $RCON(Me)CH_2CH_2SO_2ONa$, R = $C_{17}H_{33}$. A versatile, water-soluble, and oil-insoluble, anionic surfactant. Source: General Aniline and Film.

III. COALESCER MEDIA

A wide variety of coalescer materials were investigated. For convenience in tabulations etc. these are designated by FM (filter media) numbers. Certain metal specimens from Huyck Metals already carried an FM (fibermetal) number and these were retained by us. Other solid materials used, such as contact angle plates, retainer screens, etc. are not numbered and listed here but are described in the text. Table 3 lists the FM materials that were actually tested. Many other materials were procured, but were unsuitable for use because of high flow resistance or other reasons.

TABLE 3

COALESCER MATERIALS

Description	FM No.	Structure	Fiber diam. μ	Source
Glass Fiber, uncoated	0	wool	0.5-0.8	Johns-Manville
	1	"	3-8	Owens-Corning
Glass Fiber, resin-coated				
Standard WS coarse	-	wool	5-20	Emcee
fine	-	"	2-5	"
Commercial A coarse	3	"	6-24	mfg. of element
fine	4	"	1-5	"
B-1 coarse	-	"	6-24	coml. element
B-2 coarse	-	"	3-40	"
fine	-	"	1-5	"
B-3 coarse	-	"	3-15	"
Filter material	72	mat	1-2	Amer. Air Filter
Organic Polymers				
Acrilan 1656	46	wool	25	Chemstrand
158B	47	"	5-20	"
needle punched	48	fabric		"
Cotton	5	wool	15-40	--
Dacron	56	staple	45	duPont
	86	fabric	23-70	Borosites Ind.
	98	felt	12	Amer. Felt
Dacron-Vinyon	84	paper	35-57	Borosites Ind.
Dynel	85	felt	35-70	" "
Nylon 0555 SA	8	monofil.	125	duPont
--	9	"	25	Chemstrand
--	11	"	50	"
1409-53-7	12	felt	--	duPont
1687-122	13	fabric	--	"
1770-8-B	16	"	--	"
1840-15-3	19	"	--	"
-6	21	"	--	"
-7	22	"	--	"
--	49	monofil.	10-14	Chemstrand
--	74	felt	40-52	Amer. Felt
--	93	"	23-57	AFCO Filter Products
Plexiglas	69	chips	--	F. B. Wright

Continued

TABLE 3 - Continued

Description	FM No.	Structure	Fiber diam. μ	Source
Granular Solids				
Carbon, sintered	65	porous plate	--	section of a crucible
Chromosorb P	101	granules	--	stock
Alumina, adsorbent	102	80-200 mesh	--	Fisher Scientific
Sea sand, fine	103		--	"
Miscellaneous				
Quartz	67	wool	2-14	Thermal Amer. Quartz
Carbon	75	felt	16	Carborundum Co.
Cellulose	90	sponge	--	--
Natural sponge	91	network	22-31	--

Sintered "Fibermetal" Plates

Description	FM No.	Thickness in.	Mfg. Spec. % voids	Mfg. Spec. med. pore size μ	Obsvd. ΔP cm	Source
347 Stainless steel	123	1/25	35	85	3.7	Huyck Metals
" "	225	1/16	80	20	64	"
" "	250	1/10	78	40	6.8	"
" "	627	1/25	55	14	21.0	"
302 " "	1102	1/16	80	27	16.6	"
430 " "	1307	1/8	80	235	1.2	"
Nickel	131	1	82	60	10.1	"
Copper on steel	901	1/2	80	530	0.5	"
Copper	1006	1/8	80	46	1.0	"

EQUIPMENT

I. WATER SEPAROMETER

A standard water separometer was used as a convenient means of preparing, pumping, and metering the flow of fuel-water suspensions and measuring the turbidity of the effluent fuel. The standard coalescer cell and fallout chamber could be replaced by any of the several experimental cells described below. Certain other modifications were made. An accurate pressure gauge was installed; a tee was inserted directly above the turbidimeter to allow withdrawal of samples at that point; and an open standpipe was attached to a tee at the fuel outlet and extended to a point 2 in. below the top level of the cabinet. The purpose of this was to eliminate the suction resulting from the fact that the fuel outlet delivery tube extended to a point well below the bottom level of the cabinet. At low fuel flow rates, this suction reduced the pressure at the coalescer cell to below atmospheric and thus tended to draw air into the experimental cells (which were not completely airtight).

Routine maintenance involved replacement of the flow control needle valve if its operation became erratic, renewal of the turbidimeter lamp if the meter reading for clear fuel fluctuated, and replacement of the fuel pump if its output fell below 400 ml/min. At one point in the program, the WSIM of clear fuel fell from 99-100 to about 95 and the index for a well-standardized inferior mat fell from 78 to about 53. After a lengthy and tedious search, the apparent cause of the trouble was found to be a small piece of tramp plastic material that had become lodged in the outlet line from the fuel reservoir. When this obstruction was removed, the standard ratings at once returned to normal and stayed there. This episode emphasizes the importance of making frequent check runs on the machine.

Operation of the separometer was carried out exactly as specified in the CRC manual (ref. 9) and the prescribed flushing procedure was followed after each run, regardless of the cleanliness of the fuel used. One modification made was to leave the machine loaded with isopropanol, rather than empty, whenever it was shut down. Our experience has been that meticulous operation consistently gives reliable results. Although WSIM values are notoriously of low precision, we obtained satisfactory reproducibility in a number of cases where four or more replicate runs were made at widely separated intervals for

the purpose of checking performance. Our values of 95-100 are good to ±1 unit; at the level of about 75-80, the variation is ±4; at about 40, it may be as great as ±10.

II. COALESCER AND OBSERVATION CELLS

1. Modified Separometer Cell

The standard modified No. 2 separometer cell was used in the earlier part of the program. It has a mat depth of 1/16 inch and open area of 0.1 cm^2, giving a linear fuel flow velocity of 25 cm/sec at the standard flow rate of 150 ml/min. In some cases the mat depth was increased by the insertion of spacers below the cap.

Although this was a satisfactory research tool, the conditions under which it is used (thin depth of mat and high linear flow rate) are much too severe to be realistic. (In a full scale filter/coalescer element, the mat depth may be 5/8 inch and the velocity at the outer surface is only 0.86 cm/sec at a flow rate of 20 gal/min.) For these reasons subsequent work was done with larger cells, while continuing to use the separometer to prepare, pump, and meter the suspensions.

2. Glass Tube Coalescer Cell

A few preliminary experiments were made using the simple assembly illustrated in Figure 1. This cell had a useful mat area of 3.80 cm^2, giving linear velocities up to 0.83 cm/sec at the maximum flow rate of 190 ml/min; the mat depth could be varied as desired. The test results (GR 68-33) showed that a satisfactory discrimination between different mats or different fuels could be obtained, even at the low linear flow rate. Accordingly, we proceeded to construct and use the following cells.

3. Plexiglas 0.5-inch Coalescer Cell

This prototype cell, illustrated in Figure 2 from GR 68-33, had an exposed mat diameter of 0.5 inch and area of 1.27 cm^2, giving a maximum linear flow of 2.5 cm/sec at 190 ml/min. or 1.0 cm/sec at 75 ml/min. The incorporation of the perforated support disks allowed the packing density of each layer of the mat to be varied independently. Tests showed that these thin disks had no adverse effect on the performance of a composite mat. Doubtless the fibers on each side of a disk were in physical contact, owing to their elasticity under compression.

FIGURE 1

GLASS TUBE CELL

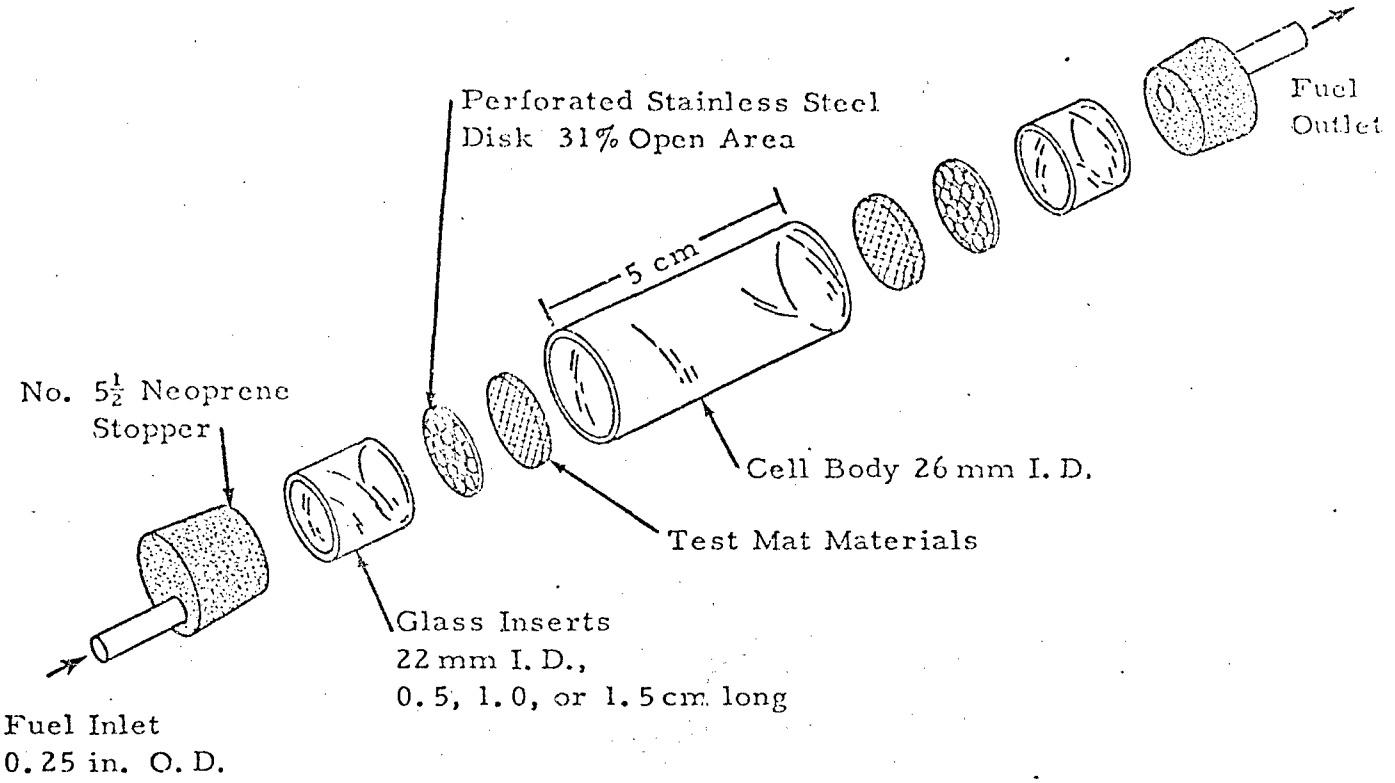

FIGURE 2

PLEXIGLAS CELL

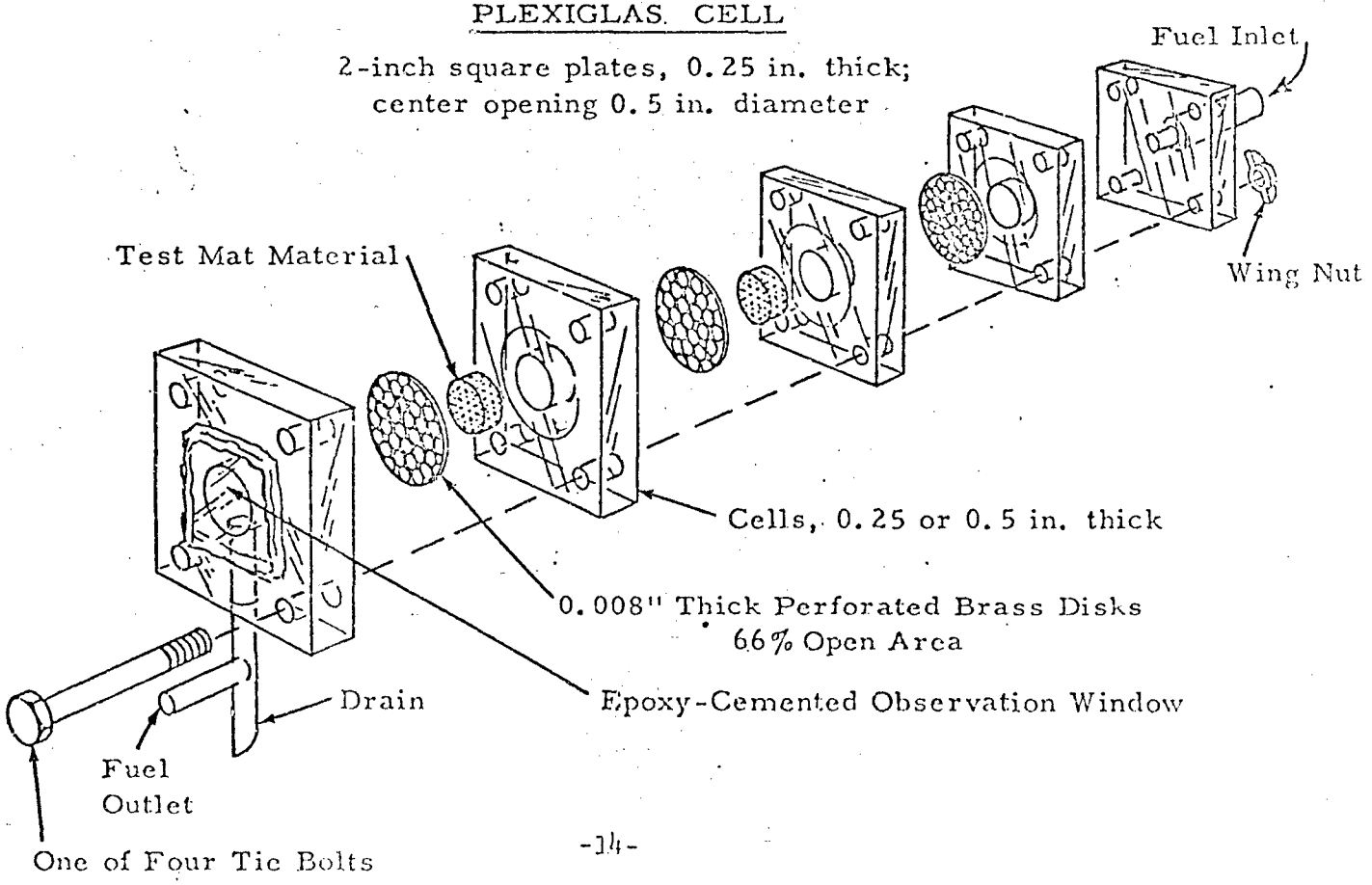

4. Steel 0.5-Inch Coalescer Cell

This was constructed much like the Plexiglas cell, using circular stainless steel or brass plates of 2 inch diameter and various depths from 1/32 to 1/2 inch. The opening again was 0.5 inch in diameter and the shallow recess to hold the support disks was 1 inch in diameter. No sealant was used between the plates, since they were flat enough to fit together with little if any leakage. The downstream layer of the mat was retained by a 1/4-inch plat whose opening tapered out to 1 inch diameter. Cushioned against this by a neopreme O-ring was a glass fallout and observation chamber 1.2 inch long an 1 inch in diameter, with a flat glass window cemented onto the end. It was h in place by a Plexiglas collar, through which passed the four tie bolts that held the entire cell together. Narrow water drain and fuel outflow tubes were fused into the bottom and top, respectively, of the glass cell close to the steel retainer plate.

The glass chamber allowed a very good view of the entire half-inch diameter downstream disengagement surface of the coalescer mat. The relative number and size of the detached water drops could readily be observed. The flow path of the fuel in the chamber was such that large water drops had an opportunity to fall out, while small droplets were swept along into the fue outlet line as described in GR 69-1.

5. Separator Screen Observation Cell

One objective of the program was to study possible replacement of the external 5-inch canister screen that surrounds each element in a filter/separator. In order to observe the behavior of such screens, a simple cell (not previously described) was set up as shown in Figure 3. The standard flow velocity at the inner surface of a canister (i.d. 4.82 inches) is redu to 0.67 cm/sec. Thus it was feasible to increase the diameter of the test section to 0.75 inch and obtain better visibility; the corresponding stand flow rate is 11¼ ml/min. By adjusting the surfactant content of the fuel the flow velocity, it was possible to deliver a stream of small and medium size water droplets that would traverse the fallout chamber and impinge o screen.

FIGURE 3

SEPARATOR SCREEN OBSERVATION CELL
Full Scale

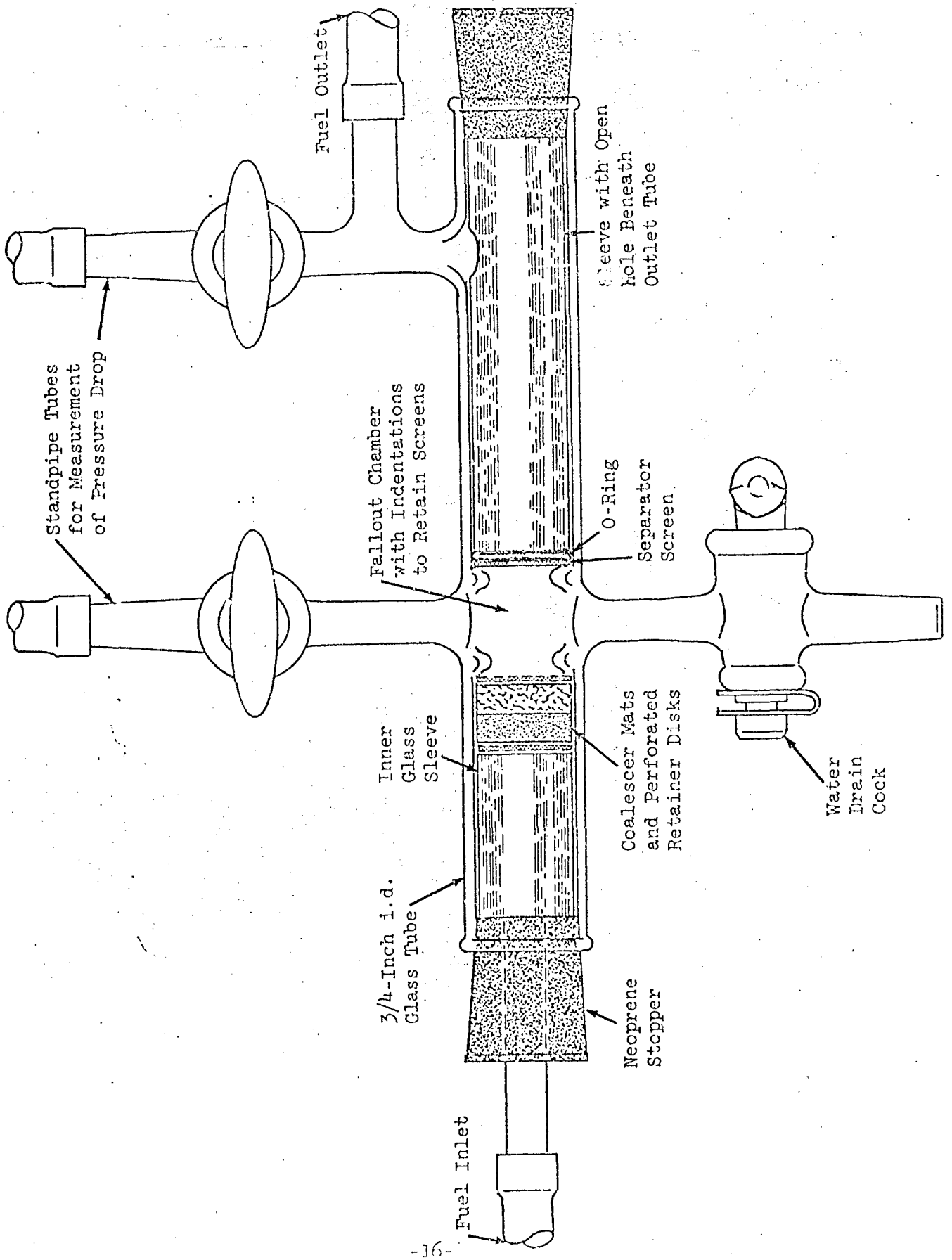

6. Other Observation Cells

The cell used in the single fiber studies will be described in the section dealing with that part of the program.

Also a special cell used to view a cross section of a mat pressed against a side window will be discussed in the section devoted to visual observations.

III. OTHER EQUIPMENT

Other than the foregoing, the various items of equipment used during the program require no special description. They will be mentioned as required in subsequent sections. Included in this category are the facilities used for measurement of contact angle, interfacial tension, flow resistance, porosity, electrostatic behavior, water content and drop size, fiber diameter, etc.

PHYSICAL PROPERTIES

I. CONTACT ANGLES ON FLAT PLATES

1. Equipment and Procedure

The contact angles were measured by a conventional procedure, as described in detail in Report GR 65-1. The test plate was supported horizontally on a pedestal in a movable glass or Plexiglas tank filled with the test fuel. Drops of distilled water were slowly delivered onto the plate from a fixed hypodermic syringe with a 27-ga. needle whose flat tip was 1 mm above the plate. The drop size was from 2 to 4 mm diameter. Often, after making the measurement, the size of the drop was increased and the measurement was repeated. Except as noted, all data reported are for these advancing angles. To measure receding angles, water was slowly retracted into the syringe until the edge of the drop was seen to retreat abruptly.

The angles were observed at 50X by a monocular microscope fitted with a simple goniometer having a precision of 1° or better. Proper back lighting gave a sharp silhouette of the drop and its reflected image.

For each measurement, two or more separate drops were placed on the plate. Each drop was observed at least three times, at intervals, and both limbs of the drop were measured. Thus each value reported is an average of at least 12 measurements. A pair of values represents two separate experiments, each on a fresh plate. The indicated precision of each reported value is ±2°.

2. Preparation and Handling of Test Plates

As described in GR 66-30, plates were prepared of the following materials: glass, nylon, phenoxy resin (Monsanto 556), polyvinylchloride, Kel-F (polychlorotrifluoroethylene), polyethylene, and polypropylene. For those polymers that were used in the single fiber studies described below, the identical filaments were used in the preparation of the plates.

Measurements on glass are notoriously difficult to reproduce, because of the ready contamination of its high energy surface. Using clean tools, ordinary microscope slides were cleaned by one of two methods: (1) washing in hot chromic acid, or (2) scrubbing with fine alumina in water. In either case, the slides were thoroughly rinsed in hot tap water and distilled water,

and the wet plates were immediately placed in a bath of clean JP-5 and stored there.

Nylon 66 filament was used to prepare both a solid plate and a film on an aluminum plate having rounded edges. A smooth, adherent film was obtained from a 3% solution in formic acid. The solid plate was obtained from a layer of chopped filament pressed between sheets of smooth aluminum foil in a Pasadena hydraulic press held at 220°C and 20,000 lb ram force for 5 min. The resulting smooth plate was stored in JP-5.

Attempts to mold a solid phenoxy resin plate were unsuccessful, but an adequate film on glass with rounded edges was obtained from a 50% solution of the resin in ethanol. After spin drying for 5 min, the plate was heated at 185°C for 30 min.

PVC, polyethylene, and polypropylene plates were prepared from chopped filaments in the hot press, as described above. The conditions were established by preliminary trials. They were: for PVC, 35,000 lb at 145°; for polyethylene, 32,000 lb at 150°; for polypropylene, 34,000 lb at 205°. Satisfactory plates were obtained and, without further treatment, were stored in JP-5.

A small plate of solid Kel-F was furnished by 3-M Company. It had a somewhat rough surface. It was used both as received and after carefully polishing on a wheel with alumina. The polishing did no damage and gave a smooth, clean surface.

Prior to a measurement, the plates were transferred directly from the JP-5 storage tank to a tank containing the fuel mixture to be studied and were allowed to stand there for at least 3 hours and usually overnight before the water drops were added. After each observation in surfactant-containing fuel, the plates (other than glass) were thoroughly rinsed with acetone followed by hot tap water and distilled water, before being returned to the JP-5 storage tank. The glass plates were discarded. The tanks were kept covered, to exclude dust and reduce evaporation. A few drops of surplus water were added to each fuel tank, to maintain saturation.

3. Effect of Surfactants in JP-5

Most of the observations were made using JP-5 fuel with various surfactant additives. Table 4 gives these data.

In clear JP-5, the angles varied from 60° on glass to about 170° on the polyolefins. Nylon gave an unexpectedly low angle, 84-89°. For the phenoxy resin, the reported value of 110° is a little lower than that observed in the previous study. Polishing the Kel-F plate raised the angle from 150° to a more reasonable value of 160°, indicating that the surface of the plate as received was contaminated.

The effects of the different surfactants were highly variable and showed no consistent pattern. A few individual results, notably for AFA-1 and Katapol on polished glass, remain questionable. Three results that were clearly erroneous were discarded and the measurements were repeated, giving widely different values. Usually, however, the reproducibility was quite satisfactory.

The data clearly show that the effects of surfactants are highly specific with respect to the solid surface material. In general, the three corrosion inhibitors give higher angles on all surfaces. The sulfonates and other powerful surfactants tend to give lower angles on glass and Kel-F, but higher angles on nylon and PVC. The effect of Igepon T-33 added to the water is comparable with that of sulfonates added to the fuel.

The effects of surfactant concentration are variable. In at least two instances (Santolene with PVC, and RP-2 with glass), a low concentration decreased the contact angle, but a high concentration raised it. The question of equilibrium at very low concentrations is discussed below.

TABLE 4

CONTACT ANGLES OF WATER ON FLAT PLATES UNDER JP-5

Fuel additive	Concn. ppm	Glass		Nylon film	Phenoxy resin	PVC	Kel-F		Poly-ethylene	Poly-propylene
		washed	polished				rough	polished		
None		59	63, 60	89[1]	110	145[2]	150	159, 161	165	173
Santolene C	5.6	60		123, 129	104	136			171	
	56	74		118	120	164			171	
RP-2	7.1	54		107						
	71	79		106	121	165				
AFA-1	5.6	51		107						
	56	54	120?	119	138	170		169		
Aerosol OT	0.2	42	63	84		153	147		169	173
	1	60	63	89						
	1[3]		79	139	102	154				
Petronate L	1		75	119	110	155		134		
Katapol PN-430	1	57		114						
	50	68	100?	130	127	161		151		
Igepal CO-530	10		96	128	126	161		153		
Igepon T-33	1		49	125	106	158				
in water	10		57	127	111	163				

Notes

1. The solid nylon plate gave 84°.
2. Another plate made from a different sample also gave 145°.
3. The fuel-additive blend had previously been shaken with 0.1% water and allowed to settle overnight.

4. Measurements in Other Fuels

Table 5 gives a comparison of the results for JP-5, CITE, and NATO F-75 diesel fuels, with and without 56 ppm Santolene C, on four different surfaces. The relatively "impure" CITE and diesel fuels, as expected, gave higher angles than JP-5, except on the phenoxy resin surface. The pronounced effect of the Santolene C in diesel fuel is noteworthy.

TABLE 5

CONTACT ANGLES IN JP-5, CITE, AND DIESEL FUELS

Fuel	Additive, ppm	Glass polished	Nylon film	Nylon plate	Phenoxy resin	PVC
JP-5	none	63, 60	89	84	110	145
CITE	none	89	120	118	100	162
Diesel	none	95, 99[1]	110	107	116	150
JP-5	56 Santolene C	74[2]	118		120	164
CITE	56 Santolene C	114	136		102	164
Diesel	56 Santolene C	165, 165[1]	162	163	161	163

Notes

1. Angle was unchanged on standing 1.5-2 hr.
2. Washed glass plate.

5. Establishment of Equilibrium

In general, the contact angles remained unchanged when the drop was allowed to stand for a considerable period, provided the fuel was saturated and the tank was covered to prevent loss of water vapor. This constancy was observed in our previous experience (GR 65-1) and in several instances in the present work, such as noted above in Table 5. Weatherford (ref. 31) has shown that the initial spreading of the drop occurs at a rapid though measureable rate.

There remained the question of whether equilibrium was quickly established in fuels containing surfactants, particularly at the low additive concentration of 1 ppm. There is evidence in the literature that, in a static system, it may take an hour or more for a drop of water to come to equilibrium

with fuel containing such a low concentration of solute, although at 50-100 ppm equilibrium should be reached in a matter of seconds. The present experiments with fuel containing 1 ppm Aerosol OT showed no evidence of a time delay. However, these results are not regarded as conclusive. For it was observed that water which had been equilibrated with 1000 times its volume of JP-5 containing 1 ppm Aerosol OT gave a contact angle on glass 14° higher than pure water.

The equilibrium contact angle in theory is not affected by the gravitational force resulting from the difference in density of the water drop and the surrounding fuel. A factor that does enter in, however, is the tendency of the drops to "stick" on the plate and therefore not spread to the full extent that they should. In that event, a drop resting on top of a plate should show a somewhat higher contact angle than the identical drop hanging beneath the plate. This was confirmed in several instances, by carefully turning the plate and its attached drop upside down in the fuel bath. The "stickiness" of the drops enabled this to be done without disturbance. Some fairly large decreases in the apparent contact angle were observed, as shown in Table 6.

TABLE 6

EFFECT OF GRAVITY ON CONTACT ANGLES

Plate	Additive	Concn. ppm	Contact angle	
			sessile drop	pendant drop
glass	none	--	60	55
Kel-F polished	none	--	161	154
Phenoxy resin	RP-2	71	121	109
	none	--	130	120
	Santolene C	56	120	112

A number of observations were made of both advancing and receding contact angles of a given water drop. The difference between these angles reflects not only the stickiness of the drops but also the change in the film of adsorbed material on the solid surface. The results obtained, given in Table 7, show differences in the range from 10 to 40° on both glass and nylon. From the one observation of clear fuel on nylon, together with previous data for clear fuels on glass, it appears that the presence of surfactants minimizes the differences between the advancing and receding angles.

TABLE 7

COMPARISON OF ADVANCING AND RECEDING CONTACT ANGLES IN JP-5 FUEL

Surface material	Fuel additive	Concn. ppm	Contact angle advancing	Contact angle receding
Glass, washed	Santolene C	56	74	57
	RP-2	71	79	56
	AFA-1	5.6	51	32
		56	54	37
	Aerosol OT	1	60	52
Nylon-plate -film	none	--	84	75
	RP-2	7.1	107	76
	AFA-1	5.6	107	65
	Aerosol OT	0.2	84	65
		1	89	65
	Katapol PN-430	1	114	89

6. Discussion

Altogether, it is evident that these flat-plate contact angles are highly specific with respect to individual fuel components and surface materials. They cannot reliably be predicted, but have to be determined as needed. Notwithstanding, these angles are a fundamental measure of the adhesion of a drop to a surface. This will be considered further in the following section dealing with the work of adhesion.

The relation of flat-plate contact angles to the adhesion of drops on cylindrical filaments will be discussed later, in the section describing the single fiber studies.

II. INTERFACIAL TENSION AND SOLUBILITY

1. IFT of Surfactant Fuels vs. Distilled Water

Measurements of various fuel-surfactant blends and also pure n-heptane against distilled water were obtained at 24 ±1° by the duNouy ring method (GR 66-1 and 66-30). The procedure of ASTM D971-50 was followed exactly, except for the fact the ordinary laboratory distilled water supply was used without extra purification. This was preferable since the same water supply

was used in the other parts of the program. The values of the surface tension of the several bottles of water used ranged from 65 to 69, indicating a very slight degree of contamination. Likewise, the interfacial tension of pure heptane against the laboratory water was 47.3, compared with the literature value of 50.8 against pure water at the same temperature.

This small departure from absolute purity in no way affected the conclusions drawn from the data; on the contrary, it provided the correct value to use in calculations. The fuel-surfactant mixtures used were part of the same 1-gal blends that had been put through the water separometer and care was taken to avoid contamination in removing the samples. The values reported are averages of from two to four separate determinations. Their deviation from the mean was generally well below the 2% allowed by the ASTM method. Only one of the reported values appears far out of line.

Table 8 shows the average values of the interfacial tensions observed. For convenience in comparison, the corresponding WSIM values of the blends are also given.

TABLE 8

INTERFACIAL TENSIONS

	Additive	Concentration ppm	Concentration lb./1000bbl	IFT dyne/cm	WSIM
Bayol, drum 1	None			48.1	55
Bayol, drum 3	None			45.0	94
JP-5	None			44.1	99
	Santolene C	56	16	35.5	63
		5.6	1.6	42.2	96
	RP-2	71	20	24.8	25
		7.1	2	39.7	65*
		1.4	0.4	42.0	93
	AFA-1	56	16	21.4	69
		5.6	1.6	37.3	83
	Aerosol OT	1		43.6	53
		0.2		43.7	94
	Petronate L	1		44.2	61
		0.2		43.0	97
	Igepal CO-530	10		28.8	83
	Katapol PN-430	50		16.6	57
		1		40.9	95

Continued

TABLE 8 - Continued

Fuel	Additive	Concentration ppm	Concentration lb./1000bbl	IFT dyne/cm	WSIM
JP-5 + Antiicer	None			43.7	93
	RP-2	7.1	2	38.2	67
	Petronate L	1		43.5	80
CITE	None			43.0	95
	Santolene C	56	16	38.2	69
	RP-2	7.1	2	40.4	65
	AFA-1	5.6	1.6	39.2	85*
Jet A	None			46.7	98
	Santolene C	56	16	41.9	47
	RP-2	7.1	2	42.5	65
	AFA-1	5.6	1.6	38.6	89
Diesel, NATO F-75	None			34.8	21
	Santolene C	56	16	32.8	18

*Estimated.

Several conclusions are evident from these data. (1) The contamination that drastically lowered the WSIM of the drum 1 of Bayol did not show up in its IFT; also the low WSIM of the marine diesel fuel was not reflected in its IFT (see also ref. 16). (2) The various surfactants had much the same effect in the different fuels of high IFT. (3) There is no good correlation between the effect of a surfactant on the IFT and WSIM. (4) In particular, the lack of any appreciable effect of 1 ppm of Aerosol OT or Petronate L on the IFT appeared to be fallacious. This could be ascribed to a failure to reach equilibrium in the ASTM method, as discussed above in the contact angle measurements. Accordingly the following experiments were made; some of them were reported in GR 69-1.

2. IFT and Solubility of Water in Equilibrated Mixtures

JP-5 (Bronoco 140) containing additives was equilibrated with 0.1% water by pumping in the separometer. The resulting suspension was transferred to an Erlenmeyer flask and allowed to stand quietly for a long time. After decanting the now clear fuel, the settled water was removed with the aid of a separatory funnel. The IFT of this water against a sample of the decanted fuel was determined by the standard method, using a small size cup and ring. Also, the unequilibrated IFT of the original clear fuel against deionized water was measured. In like manner, samples of the non-additive Great Northern

No. 2 fuel oil, before and after treatment with silica gel, were equilibrat with 5% water and the IFT's of the two phases were determined. Finally, th water content of the equilibrated JP-5 fuel samples was measured by the Kar Fischer method. The results are given in Table 9.

TABLE 9

INTERFACIAL TENSION OF EQUILIBRATED FUEL-WATER

Fuel	Additives, ppm	IFT dyne/cm	Water in fuel, ppm
JP-5	None (no equilibration)	43.0	80
	56 Santolene C + 10 Aerosol OT	0.59	<10
	56 San. C + 10 AOT + 1500 antiicer	0.84	<10
	56 San. C + 3 Petronate L + 1500 antiicer	1.20	60
Diesel as rec'd.	None	14.9	--
purified	None	17.5	--

The concentrations of Petronate L and Aerosol OT used in these tests were 3 to 10 times higher than those reported in Table 8, in order to dupli cate the mixtures used in coalescence experiments. Despite this difference it is clear that these powerful surfactants give a very low IFT after equi bration with a small amount of water. For fuels containing such additives, it follows that conventional IFT measurements made against pure water are meaningless.

The addition of antiicer had no significant effect on the lowering o the IFT. Also, purification of the diesel fuel had almost no effect, alth it raised the WSIM from 31 to 97.

The very low solubility of water in the fuel treated with Aerosol OT surprising, but we have no reason to question the validity of the measurem

III. WORK OF ADHESION

From the contact angle and interfacial tension data given above (Tab 4, 5, and 8), we can calculate the work of adhesion of water on the solid faces submerged in fuel. The basic relations are

$$\gamma_{sf} = \gamma_{sw} + \gamma_{wf} \cos \theta$$

and $$W = \gamma_{wf} (1 + \cos \theta)$$

where the γ's are the IFT's between the surface, s; fuel, f; and water, w; θ is the contact angle and W is the work of adhesion in ergs/cm^2.

Any change in the fuel components will, in general, change each of these γ's. In particular, γ_{sw} may be changed drastically. This is because the surface in contact with the water is not necessarily the original substrate material. On the contrary, it is generally a layer of components previously adsorbed from the fuel, a layer that is not completely displaced by pure water (refs. 1, 3, 28, 32).

Moreover, different fuel components do not necessarily have parallel effects on the different γ's. Each polar group in a fuel component has its own specific degree of attraction to each different solid surface and to water. Thus, for example, the CITE fuel gave lower angles than the diesel fuel on glass and phenoxy resin, but higher angles on nylon and PVC. Similarly, 10 ppm Igepal and 71 ppm RP-2 in JP-5 gave about the same reduction in IFT and increase in contact angle on phenoxy resin and PVC, but the Igepal gave a much greater increase in the angles on glass and nylon than did the RP-2.

The net result is that the work of adhesion, W, of water on the surface varies widely with the type of surfactant in the fuel, as well as with the nature of the surface material. Table 10 summarizes the values of θ and W for all fuels on the three surfaces of higher energy (glass, nylon, and phenoxy resin). On PVC and the lower energy surfaces, θ is high and hence W is very small in all cases.

For each surface a plot of W vs γ_{wf} gives widely scattered points, showing a marked specificity of the effects of different fuel components and additives.

TABLE 10

COMPARATIVE RESULTS ON FLAT SURFACES

Values of interfacial tension, γ_{wf}, contact angle of water, θ, and work of adhesion of water on solid, $W = \gamma_{wf}(1 + \cos\theta)$. Data for the last six fuels listed are from the previous study, report GR 65-1.

Fuel and Additive (ppm)	γ_{wf}	Glass		Nylon		Phenoxy	
		θ	W	θ	W	θ	W
JP-5 - clear	44.1	60	66	89	45	110	29
56 Santolene C	35.5	74	45	118	19	120	18
71 RP-2	24.8	79	30	106	18	121	13
56 AFA-1	21.4	54	34	119	11	138	6
10 Igepal CO-530	28.8	96	26	128	11	126	12
50 Katapol PN-430	16.6	68	23	130	6	127	7
CITE - clear	43.0	89	44	120	22	100	36
56 Santolene C	38.2	114	23	136	11	102	30
NATO F-75 diesel - clear	34.8	97	31	110	23	116	20
56 Santolene C	32.8	165	1	162	2	161	2
Kerosene clear	43.4	42	76			122	20
CITE clear	41.0	--	--			122	19
Diesel clear	38.3	72	50			135	11
JP-5 clear	38.1	51	62			124	17
JP-4 clear	40.5	46	69			122	19
56 Santolene C	29.5	117	16			136	8

IV. POROSITY AND PRESSURE DROP

1. Capillarity Theory

The porosity and capillary properties of each layer in a coalescer mat are a major factor in determining its performance (refs. 5, 25, 26, 27). We spent some effort in attempts to characterize this behavior for different coalescer media. Details are given in GR 67-2, 67-28, and 68-3.

The rate of rise of liquid in a uniform, vertical capillary tube open to air is:

$$\frac{dh}{dt} = \frac{1}{8\eta h} \quad (2R\gamma - R^2\rho gh)$$

where h is the height reached in time t; η, γ, and ρ are the viscosity, surface tension, and density of the liquid; and R is the capillary radius. This ignores the inertia of the liquid and viscosity of air, and assumes a liquid-solid

contact angle of zero (which is the case for fuels on coalescer media).

To test this relation for a liquid of known properties, experimental observations of h are plotted against t, and the slope of the resulting curve at various points is determined and plotted against 1/h. The resulting points should give a straight line, whose slope and intercept provide separate values of R that should be in agreement.

We have found it better to multiply the equation by 2h and therefore to plot h^2 vs. t, measure dh^2/dt, and plot it against h. (The advantage is that h^2 vs. t gives a curve that has a finite slope at h = 0 and is flatter throughout.)

In a felt or wool-like mat of more or less randomly oriented fibers, such as a glass coalescer mat, it is obvious that there will not be a uniform pore size, but rather flow channels varying in dimension. The observed rate of rise in a vertical mat represents an integration of the local variations.

This subject has been discussed in an important paper by Peek and McLean on the "Capillary Penetration of Fibrous Materials" (ref. 21). They assume that inertial effects can be ignored, and that R and R^2 in the preceding expression for dh/dt must be replaced by two functions A and B, whose value is determined by the distribution of pore sizes. If it is assumed that the pore radius varies uniformly over a certain range, that range can then be determined from the straight line plot of dh/dt vs 1/h. (In any case, if the data can be extrapolated to give the maximum rise where dh/dt = 0, an average equivalent value of R can be obtained from the usual relation, $R = 2\gamma/\rho g h_{max}$. Details of the computation of the minimum (R_1) and maximum (R_2) pore radius are given in GR 67-2.

Further consideration was given in GR 67-28 to the assumption that a coalescer mat might be represented as a 3-dimensional random array of long straight cylinders. The calculations showed that this model is incorrect, since it gives a modal cell size much smaller than the average pore radius determined by the rate of capillary rise. Indeed visual inspection clearly shows that the fibers in a typical glass mat are by no means randomly arrayed but tend to lie in parallel planes and are to some degree bunched together.

2. Capillarity Measurements

Measurements were made on four samples of glass wool and six granular materials packed into 10-mm i.d. graduated tubes, and on strips cut from nylon,

polyethylene, polyvinylchloride, and steel fibermetal filter materials suspended inside a glass shield tube. To prepare uniform columns of glass wool is not easy. Best results were obtained by spreading out the bats in sheets and cutting out a large number of 10-mm diameter disks with a cork borer. After weighing, these were carefully inserted one at a time into the tube and were tamped down to give the desired packing density. The packing was held in place by inserts cut from 1-hole rubber stoppers.

The lower end of the packed column or strip was immersed in Bayol 35, dyed green for better visibility. At the same moment a timer was started. The time was recorded for every 0.25 cm increase in capillary height until the rate became very slow. In the glass-packed columns, despite the effort to obtain a uniform packing, the capillary rise was by no means as uniform and easy to follow as it was in the granular and strip materials. Many void spaces remained unfilled and it was difficult to estimate the level reached at a given time. However, one duplicate pair of runs showed very close overall agreement.

For satisfactory differentiation of the h^2 vs. t curve by drawing tangents at a number of points, it was necessary to draw a truly smooth curve of constantly decreasing slope through the data points on 11 x 17 in. graph paper. This is facilitated by having points at frequent intervals. Apart from this requirement, the method is simple and easy to carry out. The tests were usually terminated after 0.5 to 2 hours.

After plotting dh^2/dt vs. h, a straight line was drawn through the more reliable points (those at the higher values of h). This was extrapolated to zero to obtain an estimate of h_{max} and hence R_{avg}. The values of R_1 and R_2 were computed as indicated above.

The results of these experiments are summarized in Table 11. For the granular materials, the rate of rise data were erratic and failed to extrapolate to give the maximum height that was actually observed after long standing. Hence, for these materials, only the latter values are reported in the table. It should be noted that, while these materials would hardly be practical for use in filter/coalescer elements, we hoped their performance might be helpful in defining optimum characteristics for the downstream layer of the coalescer mats.

TABLE 11

PORE SIZES COMPUTED FROM RATE OF CAPILLARY RISE

Material	FM No.	Packing density, g/cm³	% Void est.	Rate constants[1] a	Rate constants[1] b	h_{max} est., cm.	Calcd. pore radius, microns R_1	Calcd. pore radius, microns R_2	Calcd. pore radius, microns R_{avg}
Uncoated glass	1	0.159	93	0.180	0.021	8.7	19	213	76
Coml. A glass, coarse	3	.344	85	.3045	.0300	10.15	20	159	64
Coml. A glass, fine	4	.032	98.5	.0936	.0144	6.5	18	303	101
Coml. A glass, fine	4	.064	97	.0766	.0074	10.35	12	185	63
Nylon	21	.32 est.	72	.468	.024	19.5	14	62	33
Steel	627	3.61	53	.122	.0044	28	7	56	23
Polyethylene	54	0.596	35	.071	.0072	9.8	13	13	67
PVC	29	0.485	65	.161	.0133	12.1	14	143	54
Magnesium	--	0.72	59	--	--	10.3[2]	--	--	63
Tungsten carbide	--	1.85	88	--	--	7.0	--	--	94
Steel	57	0.70	91	--	--	9.5	--	--	69
Alumina	102	0.95	73	--	--	20.2[3]	--	--	32
Sea Sand	103	1.56	44	--	--	12.5	--	--	52
Chromosorb	101	0.43	71	--	--	13.2[3]	--	--	50

1. Constants of the straight line, $dh^2/dt = a-bh$.
2. Reached 13 cm on long standing.
3. Reached >21 cm on long standing.

From these data several facts are evident. First, in comparison with glass and the other polymers, the Nylon fabric is in a class by itself, as might be expected from its structure: its threads of closely packed, parallel-oriented filaments exert a strong capillary action, even though the overall density is not high. Among the glass packings, there is no major difference in the minimum R values, and the average R can be taken as representative of the material. Compression of the FM 4 fine glass decreased the several values of R more than might have been expected. The closely packed FM 627 steel fibermetal had the strongest capillary action of all the materials tested,

whereas the loosely packed FM 57 steel shavings were relatively weak.

In general, there is no clear-cut correlation between the porosity (as measured by R_{avg}) and the packing density or % void space. This is not unexpected, in view of the diversity in structure of the materials.

3. Pressure Drop

In general, coalescer mats prepared for use in the water separometer or larger cells were characterized by their resistance to air flow. Using an accurate flowmeter and vertical water manometer, the ΔP across a cell and mat was measured to the nearest millimeter. If significant, a blank correction for the empty cell and line was subtracted.

Originally, the measurements were made in the No. 1 unmodified separometer cell at 8 lit/min air flow, in accordance with standard practice (ref. 9). Later (GR 68-3), in order to save time, the measurements were made directly in the cell that was to be used for the coalescence -- either the No. 2 modified or one of the larger experimental cells. These cells were rated at 1 lit/min air flow. The relation between the ΔP at 8 lit/min in No. 1 cell and 1 lit/min in No. 2 cell is not linear, and moreover depends on the nature of the mat material. For comparison of the reported data, the following equivalents will suffice:

Mat	ΔP, cm water	
	No. 1, 8 lit/min	No. 2, 1 lit/min
Standard fine + coarse	29.7	64
2 Standard coarse	5.9	7.5

With fuel flowing, the actual pressure drop across the standard fine + coarse mats in the No. 2 cell is essentially in linear proportion to the flow rate. It is 6 psi at the standard rate of 150 ml/min. In the 0.5-inch cell, a mat having a moderately high air flow ΔP of 30 cm showed a fuel flow pressure drop of 2.5 psi at the standard flow rate of 75 ml/min.

The various ΔP values for the individual mats used will be recorded later in the tables of coalescence performance data.

In general, for the different coalescer media, it was not possible to make a general prediction of pressure drop from fiber fiameter and packing density. This was precluded by the wide variation of diameter within a given glass mat, and by the differences in mat structure of different materials.

As an example of the latter effect, wide variations in pressure drop were observed for three granular materials and nylon FM-21 filter when packed in the No. 1 cell to give essentially equal void space (72-76%). The ΔP's observed were: magnesium 4.7, nylon 7.1, Chromosorb 14.1, and aluminia 30.5 cm.

In GR 67-2, data are given for the ΔP's of four different glass mats and two nylon structures (cloth and filament), each packed over a wide range of densities in the No. 1 cell. For each material, the relation is nearly linear at low densities, which is approximately as expected for viscous flow through capillary channels or pores. At high packing density, the volume occupied by the fibers becomes a factor, and the pressure drop rises above the straight line.

A somewhat detailed study was made (GR 67-28) of the standard fine and coarse glass mats, separately or in combination, over a wide range of packing densities in the No. 1 cell. The data, given in Table 12, were accurately correlated by the relations $\Delta P = W_c \left[15.7 + (1.16 + 87.4\ W_c)/V\right]$ and $\Delta P = W_f\ (237 + 3570\ W_f/V)$, where W_c and W_f are the coarse and fine mat weights in grams and V is the cell volume in cubic centimeters (1/16 inch depth = 0.843 cc). For a combination of fine and coarse glass, ΔP is the sum of the values computed separately, allowing half of the total volume for each component.

We anticipated that there might be a simple relationship between the flow resistance of the fine and coarse fibers, but this evidently was not the case. The ratio of the fiber diameters is approximately 1 to 4, so that for equal weights, the fine mats have about 4 times the surface area and 16 times the total length of fiber. But for equal weights in a given volume, the above formulas give a ratio of the flow resistances varying from 15 to 1 up to 41 to 1, as the packing density varies from zero to infinity; at a typical density of 0.1 g/cc, the ratio is 23 to 1.

Thus in general it appears that, in flow resistance, the fiber mats are intermediate in character between screens and capillary channels, and that the degree of resistance varies with both the diameter of the fibers and the average distances between them.

TABLE 12

PRESSURE DROP OF STANDARD GLASS MATS

In cm. of water for 8 lit/min air flow in the unmodified separometer cell.

Depth of cell, in.	Number of mats	Packing density g/cm^3	ΔP, cm	No. of detns.
1/16	1 coarse (85 mg)	0.101	2.2	2
	2 "	.202	5.9 ± 0.5	27
	3 "	.303	11.0	1
	1 fine (44 mg)	.052	17.0	6
	2 "	.104	52.4	1
	1 fine + 1 coarse	.153	29.7 ± 1.5	28
1/8	1 coarse	.050	1.8	2
	2 "	.101	4.8	1
	1 coarse + 1 fine	.076	21.9	2
5/32	1 coarse	.040	1.65	2
	2 "	.081	4.0	1
	1 coarse + 1 fine	.061	18.7	1
7/32	1 coarse	.029	1.6	2
	2 "	.058	3.5	1
	1 coarse + 1 fine	.044	16.4	1

ELECTROKINETIC PROPERTIES

I. GENERAL OBSERVATIONS

It is well recognized that electrostatic charges can have a major effect on phase separation in suspensions, and Bitten (ref. 5) concludes that "the electrokinetics of fuel flowing through a fiber bed is a little understood phenomenon that may play a vital role in the coalescence mechanism." However, in an important study by Reiman of Arthur D. Little, Inc., under contract from the Air Force (ref. 24), it was concluded "that filter/separators function primarily by mechanical means and that electrostatic charges will not significantly affect their operation."

Our limited observations in this area tend to confirm the latter conclusion. One possible exception to this is the effect of Plexiglas surfaces described below.

A few experiments reported in GR 66-1 showed that charged water droplets injected into kerosene quickly lost their charge. On sedimentation of a suspension between parallel electrode plates 1.2 cm apart, charged to a potential difference of 90 volts, there was no effect; at 300 volts, some of the droplets were attracted to the negative electrode. When the electrode eventually became partly covered by water, many of the droplets attracted to it impinged on a previously attached drop and were instantly repelled therefrom. (This is due to the rapid neutralization of the induced positive charge on the leading surface of the droplet, leaving it with a net negative charge.)

In other experiments (GR 66-1), saturated fuel with or without free water in suspension, flowed rapidly over various coalescer media loosely packed in a Teflon tube. In the absence of free water, substantial voltages were measured in the effluent; with water droplets present, the voltages were much lower.

During the single fiber study described in a later section, one experiment was made in which the wire frame holding nylon filaments was charged to -3500 volts and a wire screen wrapped around the outside of the glass observation cell was charged to +3500 volts. There was no indication that this field had any effect on the adherence of droplets to the filament. However, the subsequent growth rate and size of the attached drops was greatly increased. This was more pronounced on a 125-μ than on a 25-μ filament. The detachment of the large drops appeared to be unaffected.

In the same series of single fiber studies, it was observed that polyvinylchloride filaments had a pronounced tendency to pick up stray fibers from the fuel stream. This is clearly visible in one of the photographs shown in the section describing those studies. This may well be the result of electrostatic attraction, and may be related to the ready adherence of water droplets on these filaments.

In an experiment reported in GR 68-3, an electrically insulated Plexiglas cell was made with the same internal dimensions as the No. 2 separometer cell. It was operated in the normal manner, using fuel containing 0.1% water and 25 ppm Santolene C; the mat comprised standard fine glass and FM 235 steel wool. By means of an alligator clamp and a 0.001-inch brass shim, the steel mat could be grounded or insulated at will. There was not the slightest observable effect on the performance of the cell when the mat was alternately insulated and grounded; the meter reading remained constant at 84.

II. EFFECT OF PLEXIGLAS

Up to this point in the program, we had no reason to suspect that electrokinetic effects were significant in the operation of the cells. However, a group of similar runs made in the 0.5-inch Plexiglas and steel cells (GR 68-33) showed a startling difference in performance. In each case, the mat comprised 8 std. fine and 4 std. coarse glass disks compressed to a depth of 0.5 inch; the fuel contained 0.1% water, 25 ppm Santolene C, and 1 ppm Aerosol OT. Two runs in the Plexiglas cell each gave 8-min. indexes of 97, while 4 runs in the steel cell gave readings from 71 to 79 with an average of 74.

In view of these results, an initial series of experiments was made in which perforated Plexiglas disks were placed upstream of the coalescer mat material. Three different disks were made and tested. All were two inches in diameter. One had 1/16 inch diameter perforations and was 1/4 inch thick; the other two had 1/32 inch diameter perforations and were 1/4 and 1/16 inch thick respectively. The mats were contained in the steel cell.

With operating conditions as above, the same beneficial effect was observed with the No. 1 disk in place: two runs gave indexes of 98. When the mat was replaced by a 1-inch deep plug cut from a commercial element, the Plexiglas disk raised the index from 54 to 75.

Then a much better glass mat was used; it alone gave an index of 95. The next run with this mat, made with the No. 2 disk in place, was unique --

it gave by far the best coalescence ever observed visually, even better than the runs with AFR dye (described later). All the water emerged in two or three massive drops that slowly grew in size until they flowed down the surface of the mat into the pool at the bottom of the observation chamber; there were no small droplets at all. However, five subsequent tests using each of the disks completely failed to reproduce this extraordinary result; there was no indication of any effect whatsoever.

When the same test was carried out with a layer of the porous polyvinylchloride sheet FM 64 as the outer skin, the results were completely reversed. In the absence of Plexiglas, coalescence was quite good, but with the No. 2 disk upstream, severe grapeing occurred -- a phenomenon that had never before been observed in the half-inch cell.

With glass-steel mats there was no evidence of any specific effect of the Plexiglas; coalescence was good in all these runs.

One experiment with the NATO F-75 diesel fuel indicated a marked improvement by the Plexiglas. The two mats involved in this comparison were by no means alike, the one used with Plexiglas being presumably inferior.

Some further effort was made to confirm or extend these findings, but with no conspicuous success (GR 69-1).

To obtain upstream surface area greater than provided by the No. 1 perforated disk, three porous sintered disks were prepared from pulverized FM 69 pellets; one of these contained FM 57 stainless steel shavings of very fine size. The material was thoroughly mixed with sodium chloride in a mortar and poured into an annular brass mold of 1 inch i.d. placed on a bed of sand or on a fine wire screen. The mixture was then packed down to a depth of 0.25 inch and was heated in an oven for 45 min. at 150 C. Then the assembly was transferred to a pan of cold water, to dissolve the salt, and the now rigid porous disk was rinsed in hot and cold water and dried in air. In the composite disk, the steel shavings did not become coated with the polymer. The particle size and composition was as follows:

Disk No.	FM 69 mesh size	Composition, by Wt. FM-69	Steel	Salt
4	30-60	100	0	25
5	<60	78	22	30
6	20-30	100	0	100

These disks, together with the No. 1 perforated plate previously use were tested upstream of a glass mat of 6/32 inch FM 4 plus 8/32 inch FM 3; the fuel contained antiicer, 56 ppm Santolene C, and 3 ppm Aerosol OT. Th results were as follows:

Disk No.	ΔP cm	Rating 8 min	Rating 26 min
None	28	100	96
No. 1	31	100	99
No. 4	45	100	98
No. 5	33	92	89
No. 6	28	100	97

The inferior performance of the No. 5 disk is perhaps noteworthy. The oth disks showed no significant effect. Also two other runs were made using t No. 1 disk with a more severe fuel containing Petronate L. Neither showed indication of benefit from the Plexiglas.

We concluded that this capricious effect of the Plexiglas surface wa rants further consideration. It presumably involved an electrostatic or electrokinetic action, and this will better be investigated in other contr research programs now underway.

I. PREPARATION

A major part of the proposed study was observation of the adhesion, growth, and detachment of water droplets on single or crossed fibers suspended in a flowing fuel stream. For this purpose, it was desirable to prepare a suspension of droplets of controlled size and concentration, free from extraneous electrostatic charges. The customary method of preparation by shearing action in a pump or blender produces suspensions having a wide range of drop sizes, and it does induce electrostatic charges that take a certain time to dissipate. Accordingly, a number of other methods were investigated (GK 66-1). Some of these proved to be adequate, though not as good as desired.

Cooling kerosene saturated with water at 100° or adding water dissolved in alcohols or benzene was quite unsatisfactory. A fine slurry of ice ground under cold kerosene added to a beaker of kerosene at room temperature gave a suspension of quite uniform sized droplets, but they were about 25 μ in diameter -- somewhat larger than desired. It was concluded that the method is intrinsically effective, but is certainly not very practicable.

A hypodermic needle vibrating at its resonant frequency is known to produce a stream of very uniform droplets, of diameters down to 30 μ. We were unable to make smaller droplets, and in any event the rate of delivery would be low. Likewise, it is well known that a succession of uniform drops can be obtained from a capillary or needle charged to a high voltage. After a number of trials, we concluded that this method had promise but that considerable development would be required to adapt it to a continuous fuel flow system.

Three other methods proved to be more useful.

The liquid jet method used a very rapid discharge of water from a hypodermic syringe through a No. 25 needle submerged in kerosene. This gave many very small droplets which remained in suspension for hours. The overall drop size distribution covered a wide range, however. The method is useful for rapid preparation of a batch of suspension for use in experiments, but is not suitable for continuous production of uniform sized droplets.

Injection of live steam through a capillary jet beneath the surface of kerosene gave a milky white suspension of small droplets that showed no visible sedimentation in one hour. The temperature rise was trivial. Since this

method would be adaptable to a flow system, we set up a boiler that delivered 0.4 g/min of steam superheated to 125°. A suspension of 2.3% water in Bayol 35 was prepared in 30 sec. Droplet size measurements, made as described below, showed that this equipment did not give as good a size distribution as expected, there being a substantial number of droplets in the 20 to 80 μ range. Doubtless a better and more uniform suspension could be obtained by modifying the manner of injecting the steam. Instead of doing so, we used the following simple method to provide the suspensions for the single fiber flow studies.

The vapor condensation method (GR 66-30) gave an adequate droplet size distribution, was easy to operate, and had good reproducibility. Air at a flow rate of 600 ml/min (at 24°, 741 mm) passed through a water saturator maintained at 56° and thence through a warm 0.25-inch copper delivery tube. The exit of this tube was located 6 mm above the surface of a reservoir of saturated Bayol 35 at 24°. The warm air-vapor stream was rapidly cooled by the fuel and the surplus water condensed out in droplet form at the rate of 54 mg/min. This rate was calculated and was also measured in a special run. The droplet size distribution is given below. When the moist air stream was delivered 6 mm below the surface of the fuel, the bulk of the water condensed into droplets of less than 5 μ and the fuel was too opalescent for satisfactory observation.

II. DROP SIZE AND TURBIDITY

1. Size Distribution of Suspensions

A 0.5-ml sample of a water-fuel suspension was placed in a sample cup for microscopic observation and counting. The cup was a short section of 22-mm i.d. glass tubing cemented with silicate onto a polyethylene film on a microscope slide. The droplets would soon fall through the 1.3-mm depth of fuel in the cup and rest on the film without spreading. Each particle count covered a circular area 1.4 mm in diameter. A photomicrograph was taken at 100X or 210X on Polaroid 3000 film with 1/30 sec. exposure under strong illumination. With the aid of a calibrated grid in the eyepiece, the size distribution on three random areas was then counted at leisure.

The submerged air-vapor jet, like the steam jet, gave many droplets in the 1-10 μ range and a number of larger ones up to a maximum of 30 μ. There were also a number of "clouds" of droplets too small to be individually visible.

On the other hand, the above-surface air-vapor jet gave only droplets in the range from 3 to 30 μ. Evidently very small droplets cannot penetrate the fuel-air interface, but instead coalesce there. The numerical distribution over this range was almost flat, as shown by the following numbers:

Droplet diameter, μ -	<3	3-5	5-9	9-13	13-17	17-25	25-30	>30
Percentage observed -	0	8	28	20	20	20	4	0

This size distribution and concentration proved to be very satisfactory for the flow studies, and was adopted without modification.

A sample taken from the separometer, after the standard procedure for preparation of the suspension, showed the following size distribution:

Droplet diameter, μ	0-5	5-10	10-40	>40
Percentage	51	42	7	0

2. Calibration of the Turbidimeter

Suspensions of various amounts of water in clear fuel were prepared as usual in the separometer. They were then pumped at the standard flow rate (150 ml/min) directly from the tank to the turbidimeter, bypassing the coalescer cell and fallout chamber. The readings were:

% Water input	0	.02	.05	.10	.10*	.25	.50	1.00
Meter reading	100	88	41	18	11	7	8	3

* fuel contained 60 ppm Santolene C, giving a finer dispersion.

As anticipated, these data indicate a linear relation between the water content and the negative logarithm of the index or meter reading, 7.6 x % water = 2 - log index, which holds up to at least 0.1% water; lower values of the index are of no practical interest. For example, with an input of 0.1%, an index of 70 indicates that only 80% of the water has been removed.

If the effluent water droplets from a coalescer cell happen to be smaller than the average input, then the amount of water in the effluent will be less than estimated from the index.

On the other hand, it has become recognized by Hazlett (ref. 10) that the effluent droplets, although just too small to fall out, may be large enough (about 20 to 50 μ) to be clearly visible to the eye. These have little or no effect on the meter reading, unless present in high concentration. Hazlett has shown that several hundred parts per million of free water may be present in this form without lowering the index below 90, and we have

observed a substantial number of such droplets in an effluent that still gave an index of 100. The smaller, invisible droplets which appear as a haze are the ones that have a marked effect on the index.

Thus the separometer index (or any other similar meter) gives only an indication of the amount of finely divided free water in a fuel. It cannot be relied on to measure the total free water content.

The above calibration assumes that all the water input is suspended in the fuel, and that none disappears by solution or by hangup in the system. Since any fuel is normally more or less saturated with dissolved water, any further amount going into solution will be negligible. When the input water is carefully injected in the specified manner, we believe that the amount of "natural coalescence" occurring in the equipment is much less than indicated in the CRC study (ref. 9).

The basis for this belief is a test reported in GR 67-28. A 0.1% water suspension in clear fuel was prepared as usual, and was then pumped at 150 ml/min through a jumper leading to the turbidimeter and the outlet line was led back to the reservoir -- altogether a long flow path. The index remained constant at 17 ±1 for 55 min, then slowly rose to 39 at 130 min. This clearly shows a high degree of stability of the suspension.

III. ANALYSIS OF WATER CONTENT

1. Treated Pad Methods

The reliable measurement of free water in fuel has always been a troublesome problem. The simple turbidimetric method is not always satisfactory, for the reasons discussed above. The Karl Fischer method has long been abandoned since it has to measure the usually small difference between total water in the sample and dissolved water in a separate sample of the same fuel saturated at exactly the same temperature.

The Navy AEL fluorescent pad method has been evaluated by Brown, Johnston and others (refs. 8, 14, 15), and equipment is commercially available. We tried this method, but found it quite unsatisfactory for fuels containing water droplets of substantial size and amount. A pad method based on electrical conductivity recently published by Bitten (ref. 6) appears promising; we did not take the time to try it.

2. Water Soluble Dye Methods

Hazlett (ref. 10) has proposed to make the suspensions using water containing 0.8% of a fuel-insoluble dye, Acid Fuchsin Red. Then a sample of effluent fuel from a coalescer is extracted with a small amount of acidified water. This is separated by centrifuging and its optical density at 545 nm is measured by a spectrophotometer. The method is easily capable of detecting 1 ppm of free water in the fuel.

We tested this method using the 0.5-inch steel cell and observation chamber (GR 68-33). With an all-glass mat, two runs with clear fuel and no dye gave indexes of 100. Visual observation showed the water falling from the downstream surface in large drops. Addition of dye to the water gave an index of 98 and similar drop detachment. These tests of all-glass mats were then continued with the addition of Santolene C and Aerosol OT to the fuel. The results were unexpected and startling: the dye promoted coalescence to a marked degree. It maintained the detachment of the water in large drops, in conspicuous contrast to the small drops normally observed with the additives in the fuel. With 25 ppm Santolene C plus 1 ppm Aerosol OT in the fuel, the index was 71 to 79 in four runs without dye, and 99 in each of two runs with dye. Using twice as much surfactant, the corresponding figures were 68 and 97.

The same effects were observed with glass-plus-steel mats. Although these gave a high index with or with or without dye, the difference in drop size was readily apparent.

In an effort to overcome this activity, we shifted to the use of Indigo Carmine as the dye, using a crude colorimetric procedure. A standard solution containing 0.36% Indigo Carmine in distilled water was prepared. A series of color standards was made by dilution and placed in small test tubes. The standard solution was used to make the 0.1% water suspension in the separometer. After eight minutes of running, a 300-ml sample of the effluent fuel was caught in a separatory funnel from a line downstream from the turbidity chamber. To this, 3 ml of distilled water was added and shaken several times vigorously. The water layer was then separated and visually compared to the color standards, to provide a rough estimate of the free water content in ppm.

This method was used for a number of runs. It finally became evident, however, that the Indigo Carmine also affected the coalescer operation, though nowhere near as strongly as the Fuchsin dye. Also, the initial appearance of water at the downstream face was greatly delayed by the dye. We therefore abandoned it.

One more unsuccessful attempt was made to use a tracer to measure the free water in the effluent fuel (GR 69-1). The water used to make the suspension contained 1% iron as ferrous chloride and 0.1% of hydrochloric acid. A 200-ml sample of effluent fuel was extracted with two 3-ml portions of aqueous hydroxylamine sulfate by shaking in a separatory funnel. The extract was drained into a small test tube and treated with 1,10-phenanthroline solution to form the red-colored ferrous complex. Blank tests showed that this simple procedure would readily permit direct visual estimation of as little as 1 ppm free water in the fuel. However, for no evident reason, the ferrous solution had a very drastic inhibitory effect on the coalescence.

After these experiences, we gave up further efforts to make quantitative measurements of the free water in the effluent. Instead, the performance ratings of the later runs was expressed by the meter reading followed by a letter code for the visual observation, as follows:

A** - Same as A, with fallout from the mat in massive globules.

A* - Same as A, with fallout in large drops, 1 mm or more in diameter.

A - No droplets visible in effluent fuel.

AH - No droplets but slight stream of haze visible.

B - Very few visible droplets; meter 99-100.

C - Considerable number of droplets, but meter still 99-100.

D - Many droplets; meter 90-99.

E - Haze evident; meter about 75-95.

F - Very poor coalescer; meter below 75.

G - Almost no fallout; haze present at outset, and meter down to about 20-40.

I. PRELIMINARY EXPERIMENTS AND CALCULATIONS (GR 66-1)

1. Initial Observations

At the outset of the program, we observed the gravity-free behavior of massive drops of water suspended in a density gradient between two mixtures of chlorobenzene and xylene. The mixtures had densities at room temperature of 1.005 and 0.990. They were contained in a 16-oz square bottle.

The effects of surface tension were readily observed with drops floating freely in the column. They could be pushed about by metal or glass rods, undergoing considerable elastic deformation and recovery, without adhesion. Drops moved against one another would usually bounce or slide away. Small drops would coalesce much more readily than large ones, usually after the characteristic time delay. On the other hand, when a drop was touched with the end of a glass rod that had been broken off and not polished, the drop adhered instantly. The sharp points or edges of the glass penetrate the intervening organic liquid film and make immediate contact with the water. Once contact is established, the drop spreads very rapidly over the surface.

Photographs were taken of both side and end views of drops adhering to clean rods of aluminum, copper, stainless steel, and glass, each about 5 mm in diameter. In air, the clean rods were readily wetted by water. However, after the dry rods were immersed in the organic fluid it was not easy to obtain adhesion of water drops, even on the glass rod. To overcome this difficulty, a very small drop of water was placed on the desired spot on the rod before lowering it into the density gradient column. Then a medium or large size drop of water (diam. 3 to 15 mm) was added from a pipette onto the same spot, where it adhered readily. The water used with the glass rod was colored with phenol red, to give better contrast. The shape of these drops is described below.

One experiment was made to observe the behavior of drops on a lattice. A piece of 3/16-inch mesh stainless steel wire screen was supported horizontally in the density gradient bottle, and a large drop of colored water was placed on it. The drop seemed to be attached at just one point where the wires crossed, but it adhered very tenaciously. The plane of the screen was then titled 30° and the drop was pushed with a glass rod. Considerable force seemed to be required to dislodge the drop.

2. Shape of Drops on Spherical and Cylindrical Surfaces

A liquid drop adhering to a solid sphere forms a spherical segment, and the contact angle is the angle between the radii of the sphere and the segment at the circular line of intersection. In GR 66-1, we showed that the basic contact angle equation for a drop of water, w, on a surface, s, submerged in fuel, f,

$$\gamma_{sf} - \gamma_{sw} = \gamma_{wf} \cos\theta$$

is equally valid for a drop on a sphere as well as a flat surface.

For the adhesion of a drop on a cylindrical rod, such as a fiber, the geometry involved is highly complicated and no longer permits simple mathematical solution (refs. 20, 27, 29). The contact angles are not uniform around the periphery of the solid-water interface (unless the rod is enveloped), and the water-fuel interface is not necessarily spherical. As a result, a precise determination of the interfacial areas for minimum surface free energy of a given size drop on a rod of unit radius becomes a problem of extreme difficulty. Only when the drop is large enough and its contact angle is low enough will it evelop the rod and take on the symmetrical shape of an unduloid.

For the solid materials used in the present work, the normal contact angles are generally high (between 90° and 180°), so that the drops did not envelop the cylinders and retained a nearly spherical water-fuel interface.

The photographs of large drops adhering to copper, steel, aluminum, and glass rods, obtained as described above, were analyzed. Testing with a compass showed that all the drop profiles were indistinguishable from circles, except for the axial profile of the drop on glass which began to show the unduloid curvature as noted above. After carefully measuring the radii of these circles and the distance of their centers from the axis of the rods, the corresponding contact angles were calculated as indicated below. The angles at the extreme points along the length of the rod (side view) and along its circumference (end view) are denoted θ_1 and θ_2 respectively. Let the radius of the rod equal unity, and the radius of curvature of the drop profile equal r, and the minimum distance from the center of the drop to the surface of the rod equal s. Then $\cos\theta_1 = s/r$ and $\cos\theta_2 = [1 + r^2 - (1 + s)^2]/2r$. The value of θ_1 for the drop on glass was estimated by drawing tangents. The observed angles were as follows:

Material	Drop No.	Radius of curvature, r, of drop profile (radius of rod = 1.00)	Contact angles θ_1	θ_2	$\theta_1-\theta_2$
Aluminum	1	2.64	146	115	31
Steel	1	2.10	140	109	31
	2	0.60	121	107	14
Copper	1	2.20	137	102	35
	2	0.68	130	117	13
Glass	1	1.90	50±4	32	18

These data illustrate the fact that small drops have a greater tendency to adhere to a curved surface than large ones do -- as was indicated by the visual observations. Also, the difference between the two contact angles depends on both r and h.

When the radius of the drop is much larger than that of the cylinder, the profiles resemble that shown in Figure 4. Values of θ_1 for such drops are given below in the section dealing with drop detachment.

3. Decrease in Free Energy on Attachment

For a drop of given size, the free energy decrease resulting from attachment on a cylinder of unit radius will invariably have a value intermediate between that on a flat plate and on a sphere of unit radius. This fact suffices to give an adequate approximation for the cylinder. The calculation of the relative water-fuel interfacial areas and surface free energies was detailed in GR 66-1, and the results are shown in Figures 5 and 6. In these figures, A_o and A_{wf} are the water-fuel interfacial areas before and after attachment, and $-\Delta F$ is the total change in surface free energies at all three interfaces as determined by the contact angle.

From these figures, it is apparent that the attachment of relatively large drops causes very little change in water-fuel area and total free energy, especially on surfaces giving a high contact angle. On the other hand, for relatively small drops the free energy of attachment on a cylinder must be close to that on a flat plate.

FIGURE 4

FIGURE OF A LARGE DROP ON NYLON FILAMENT
F/D = 0.05; L/D = 0.66

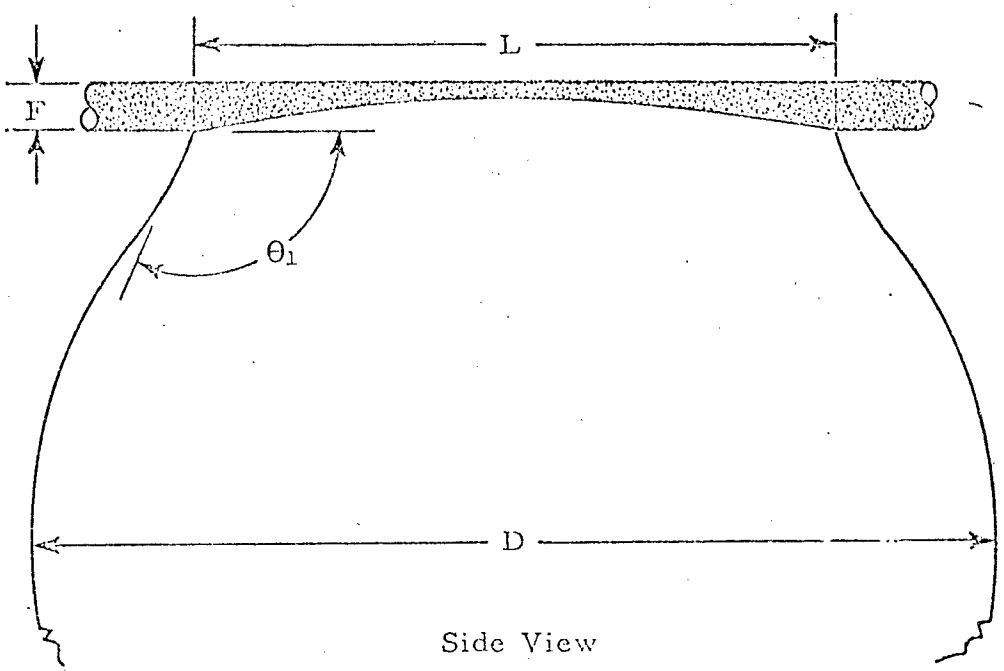

Side View

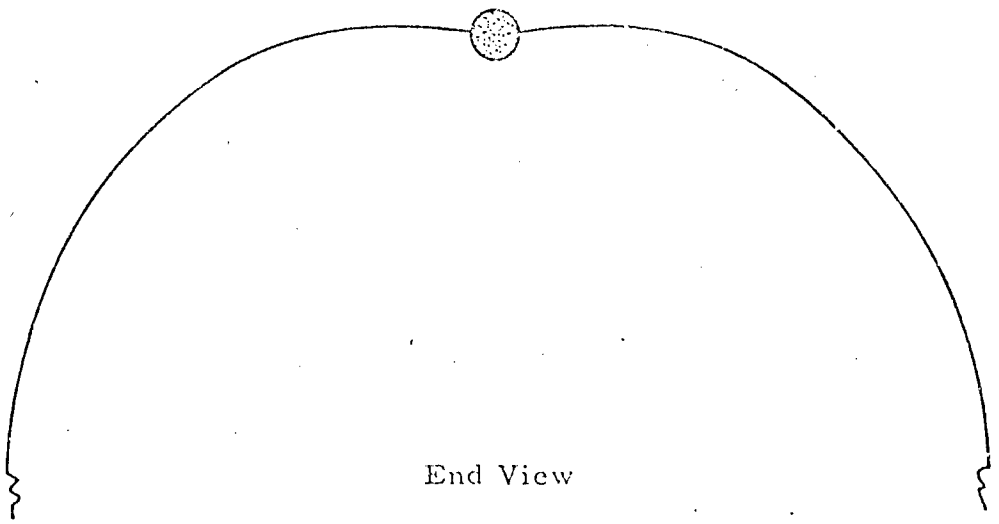

End View

Figure 5

RELATIVE WATER-FUEL INTERFACIAL AREA, A_{wf}/A_o, FOR DIFFERENT SIZED DROPS ON A SPHERICAL SURFACE

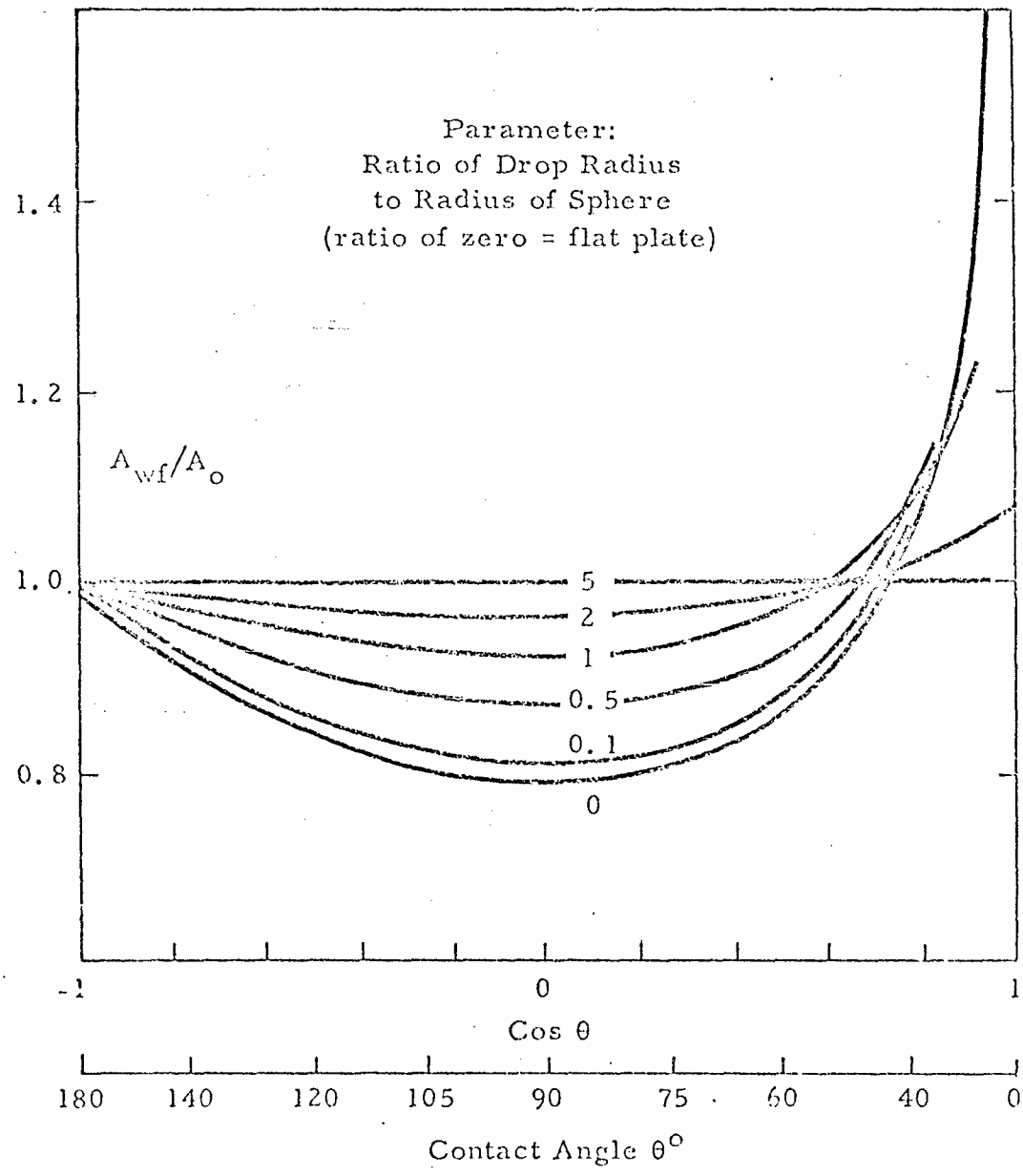

Figure 6

RELATIVE DECREASE IN SURFACE FREE ENERGY $-\Delta F/(A_{o\gamma wf})$, FOR DIFFERENT SIZED DROPS ON A SPHERICAL SURFACE

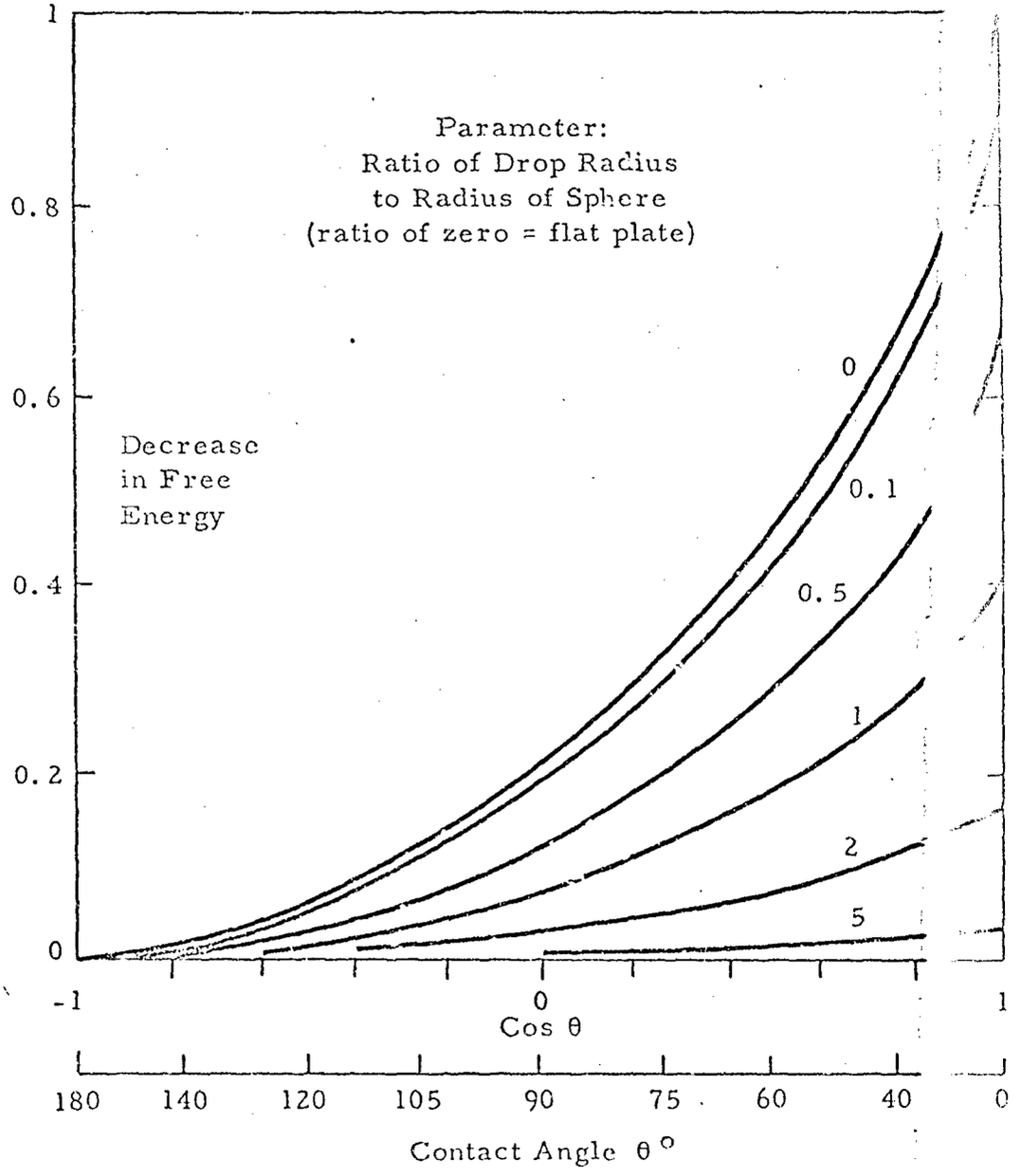

4. Decrease in Free Energy on Coalescence

It is obvious that coalescence of water droplets will invariably result in a substantial decrease in surface free energy. The probability that coalescence will occur in a given situation is therefore dependent on hydrodynamic rather than thermodynamic considerations. Consider two spherical water drops, surrounded by fuel, having radii r_1 and r_2 and total surface area A_o, that coalesce to form a single drop of radius r and area A. As shown in GR 66-1, $-\Delta F = (A_o - A)\,\gamma_{wf}$, or $-\Delta F/A_o\,\gamma_{wf} = 1 - \dfrac{r^2}{r_1^2 + r_2^2}$ where $r^2 = (r_1^3 : r_2^3)^{2/3}$. For several values of r_2/r_1, the relative energy decreases are as follows:

r_1	r_1	$r_1^2 + r_2^2$	r^2	$-\Delta A/4\pi$	$-\Delta F/A_o\gamma_{wf}$
1	1	2	1.587	0.413	0.2063
1	2	5	4.327	0.673	0.1346
1	5	26	25.133	0.867	0.0333
1	10	101	100.066	0.934	0.0092

Thus, coalescence of two drops of equal size gives an energy decrease of 20.6%, the same as obtained on adhesion on a flat surface at 90° contact angle. Coalescence of a small drop with a larger one gives a lower percentage energy change for the system as a whole; at the same time, as the next-to-last column shows, the surface area of the smaller drop almost completely disappears, so that from its viewpoint, the energy change is very high.

When one drop coalesces with another drop already fixed on a surface, the resulting decrease in surface free energy is slightly greater than if the same drops had coalesced in the free state as described above. This assumes, of course, that the resulting larger drop on the surface spreads in such manner as to minimize its free energy. The difference in favor of coalescence with a fixed drop compared with a free drop is not large enough to be of importance; it is the kinetic factors that are paramount in determining the growth of fixed drops.

II. OBSERVATIONS IN A FLOWING SUSPENSION (GR 66-30)

1. Single Filament Observation Cell

All experiments on individual fibers used the observation cell shown at half scale in Figure 7. Here the fuel was recirculated through a small water coalescer, a variable speed pulse pump, and a flowmeter. The coalescer was a small chamber packed with fine glass fiber. The "Man-stat" plastic pump delivered fuel at any desired rate up to 1200 ml/min. If this flow was spread over the entire cross-sectional area of the 40-mm i.d. cell, the linear flow rate in the cell averaged 1.6 cm/sec. If, preferably, the flow was restricted to a 10-mm diameter stream, as indicated in Figure 7, the maximum flow velocity became 25.6 cm/sec. The cell was normally operated at a flow of 78 ml/min or 1.65 cm/sec. This gave a laminar streamline from the feed tube to the outlet, surrounded by motionless, unclouded fuel.

The test filaments were illuminated by a spotlight behind one window and were observed through the opposite window by a monocular microscope. For the drop attachment and growth study, 20 photographs were taken at intervals in each run using 1/60 sec. exposure of 35-mm Kodak Tri X Pan film; the magnification on the strip film was 10X. A 220-μ square grid in the microscope provided a scale for size measurement of the adhering drops. The drops in the fuel stream moved too rapidly to be visible. For the detachment study, the drop was photographed with a Polaroid camera at a magnification of 26X or 79X.

2. Attachment and Growth Study

Filaments of 10 to 25 μ diameter of cotton, uncoated glass, phenoxy-coated glass, nylon, and polyvinylchloride, and 125-275 μ filaments of nylon, polyethylene, polypropylene, and copper were used. These were drawn taut and cemented onto a frame as shown in Figure 7, touching at the point of intersection. Usually the photographs were taken at 5-min intervals for 100 min; in later runs, the first four pictures were taken at 1-min intervals and the final ones at 10-min intervals to give 100 min total.

The fuel was undiluted Bayol 35. The fact that its viscosity is somewhat higher than that of jet fuel was not objectionable, since none of the conclusions drawn would be altered thereby. In some of the runs one of the following surfactants was added at a concentration of 60 ppm: Santolene C, AFA-1, RP-2, Aerosol OT, Petronate L, Igepal CO-530, and Katapol PN-430.

FIGURE 7

OBSERVATION CELL FOR FLOW STUDIES

1/2 Scale

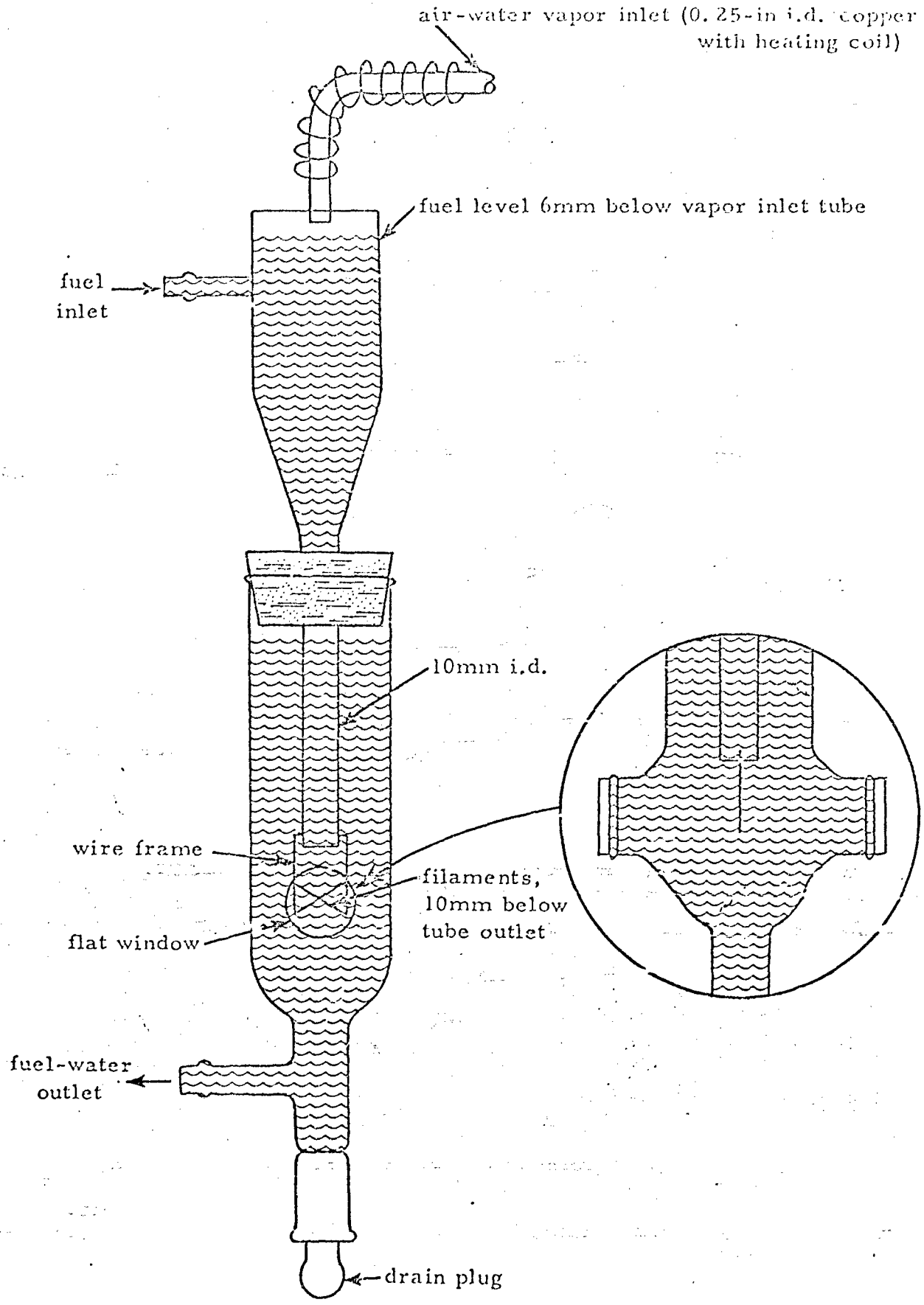

Also, Aerosol OT was used at 1 or 2 ppm.

Figures 8-13 give a representative selection from the total of 66 runs made. They show, in order, uncoated glass, polyvinylchloride, and 25-μ nylon in clear fuel, and nylon in fuel containing Santolene C or Aerosol OT at 60 or 1 ppm. In the latter two runs, the initial pictures are at 1-min intervals. The direction of fuel flow is from right to left on the page (i.e. from bottom to top of the film) owing to reversal in the microscope.

Detailed visual examination of consecutive frames in these and the other photographs gave a good qualitative picture of the overall coalescence process. For a closer examination and calculation of the rate of increase in size of attached drops, enlarged positive prints giving a magnification of 80X were made for a number of the runs. The following conclusions were drawn.

The relative ease of attachment of the flowing droplets onto the bare filament surface was appraised qualitatively by comparison of corresponding frames in the several photographs. The rate at which the filaments became well covered with attached drops near the start of each run was one good index. Another was the amount of filament left uncovered near the end of the run, as a result of lateral coalescence of adjoining drops.

From these comparisons, it was concluded that in clear fuel the ease of adherence decreases in the following order; PVC > nylon > glass, cotton > phenoxy coating >>> polyethylene > polypropylene > copper. In a special experiment using glass coated with silver or with an alkyl titanate, there was no adherence at all.

Santolene C in the fuel had no marked effect on the adherence on cotton, glass, nylon, phenoxy coating, or PVC. With other surfactants, the adherence on nylon decreased in the following order: Santolene C > RP-2 > AFA-1 > 1 ppm AOT >> Igepal, Katapol, AOT, Petronate. The adherence on the other four surfaces was similarly decreased by AFA-1 and AOT.

Adherence on 26 and 125 μ nylon appeared about the same. Reducing the flow rate one-half or increasing it three-fold had very little effect on the initial adherence, except that the attached droplets tended to be smaller in size at the higher flow rate.

It was not possible to determine with certainty whether small (3 μ) and large (30 μ) droplets were attached with equal readiness. The indications were, however, that the larger 10 to 30-μ droplets predominated at the lower flow rates. This result is entirely reasonable when one considers the pattern

FIGURE 5 - GLASS

FIGURE 9 - POLYVINYLCHLORIDE

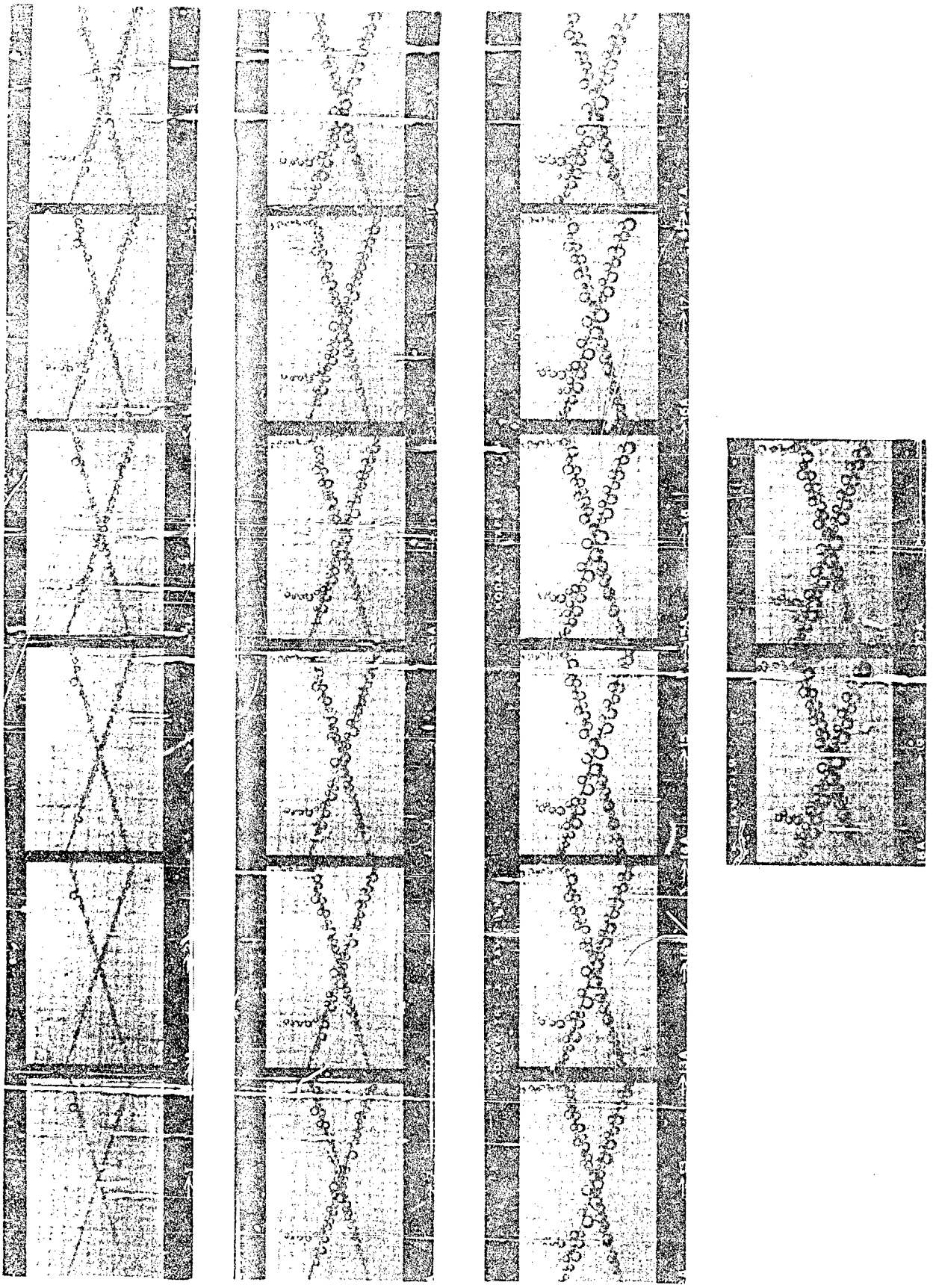

FIGURE 10 - NYLON

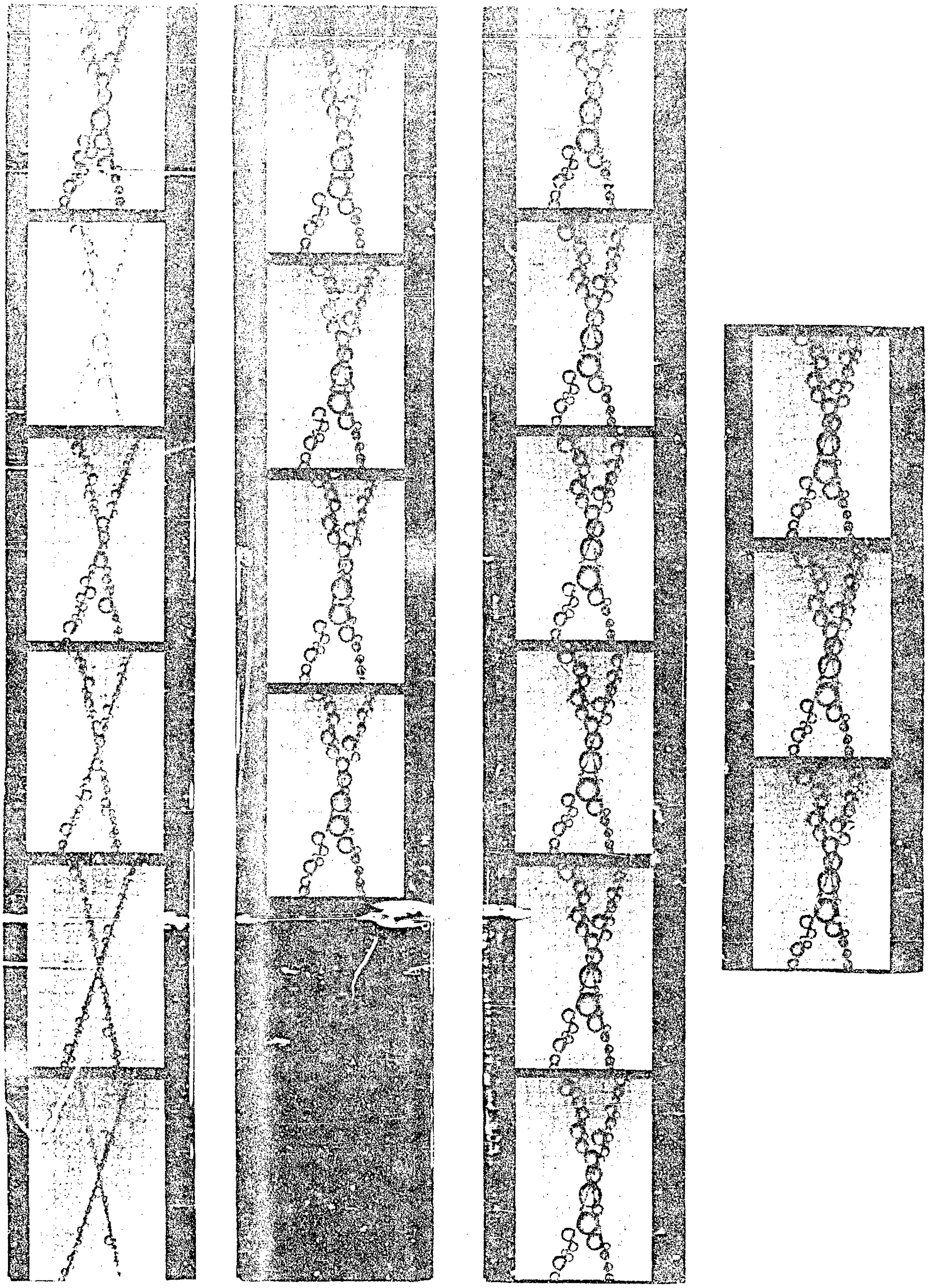

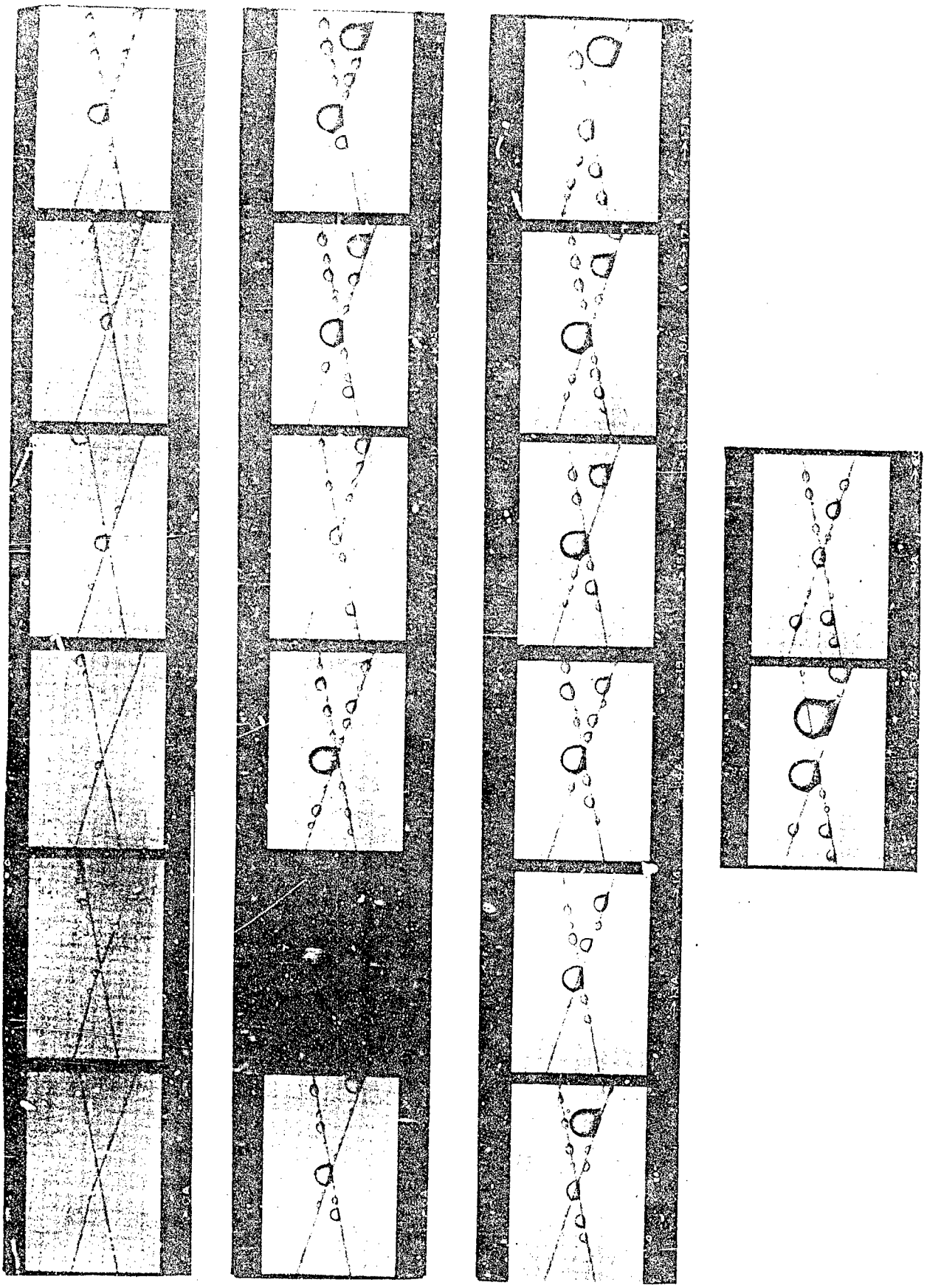

FIGURE 17 - NYLON - 3 FPM AIRFLOW

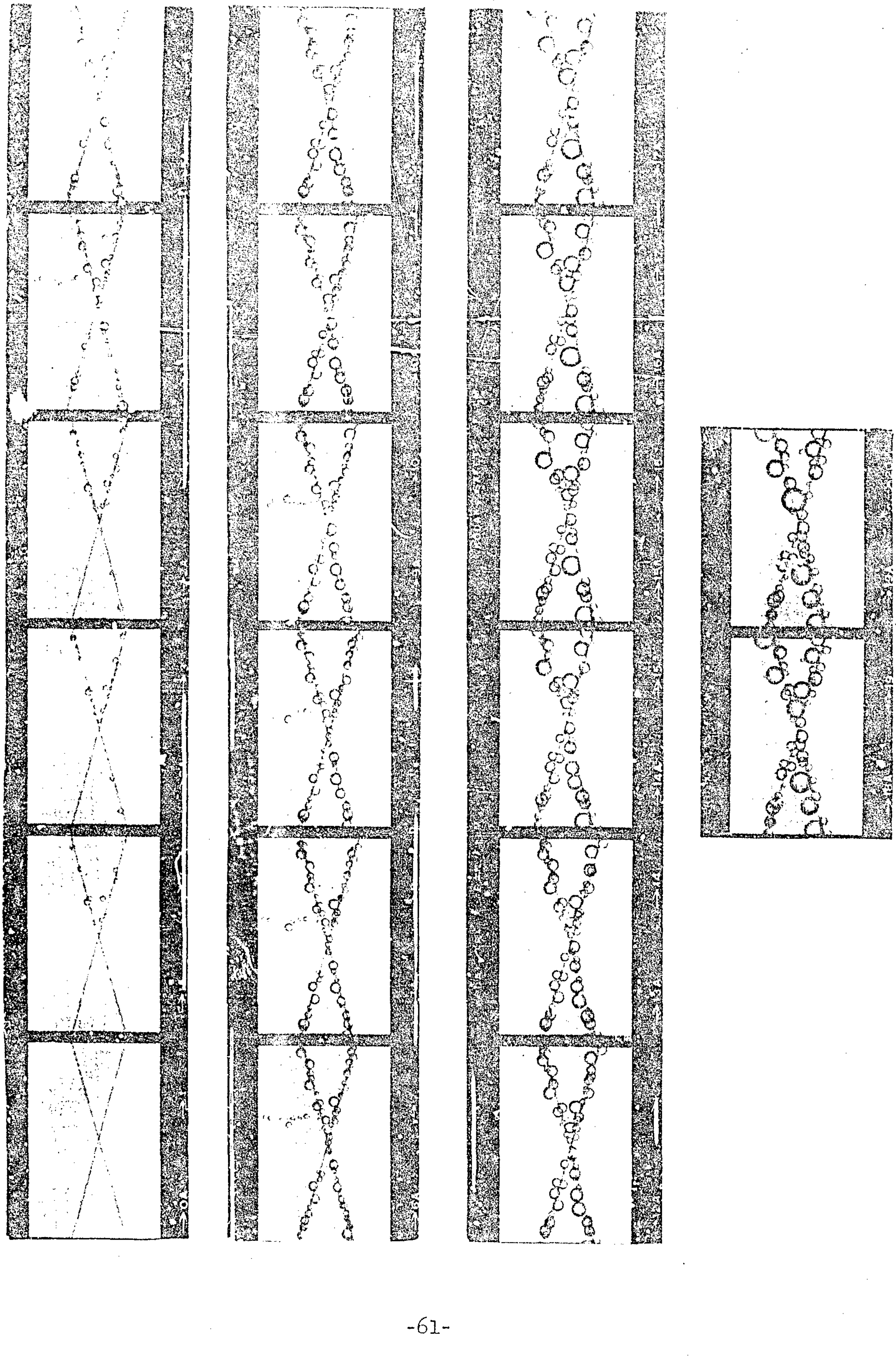

of the fuel flow streamlines across the filament. The larger droplets with relatively high inertia have a much greater likelihood of making the strong impact against the surface that is required for adherence.

At best, however, only a very small fraction of the approaching droplets managed to adhere, as the following rough calculations show. Assuming a flat distribution curve of droplet diameter from 3 to 30 μ, the mass mean diameter is equal to $((1/27) \int_3^{30} n^3\, dn)^{1/3} = 19.6\ \mu$, and the weight of this mean drop is 3.93×10^{-9} g. At a concentration of 890 ppm or 6.9×10^{-4} g/ml in the fuel, and a fuel flow velocity of 1.65 cm/sec, the droplet delivery rate was 1.74×10^7 droplets per minute per cm^2 of cross-sectional area of fuel flow. The corresponding area of a 1-mm length of 25 μ filament is 2.5×10^{-4} cm^2. Then the number of droplets approaching that area was 4350 per minute. But the number of attached drops observed on 1 mm of filament in the first 5-min frame was only about 40 on PVC and 10 on glass. Even if 5 or 10 times as many droplets adhered to form the drops visible in the photographs, it is evident that less than 1% of the closely-approaching droplets became attached.

The adherence and spreading on nylon in the presence of the four powerful surfactants was not anticipated from the flat-plate contact angles. With 50-60 ppm of Katapol in the fuel, the value of θ was 130° but the angle θ_1 on the filament was extremely low. Igepal, AOT (at 60 ppm), and Petronate gave similar behavior on the filament (See Figure 12). There was only a slight tendency for drops to remain fixed and grow. Instead, they would slide along the surface in the downstream direction (despite the slight angle of inclination); Figure 12 clearly shows the difference between the advancing and receding angles of the drops. Alternatively, the drops might grow to some extent, then drain away in a liquid film on the filament surface.

In view of this behavior, it was not possible to make any quantitative appraisal of the ease of adherence of the droplets in the fuel containing these surfactants. The total amount of attached water visible in the photographs was distinctly less with the four strong surfactants than it was with Santolene C, or AOT at 1 ppm, or clear fuel. However, much of the attached water may have disappeared from view by downstream travel or drop detachment.

The growth of drops by coalescence occurred both by impingment of droplets from the fuel stream and by lateral coalescence of adjoining drops. The rates of growth by accretion from the fuel were computed as follows. In the 80X enlargements, individual drops were selected that appeared to have had no

growth by lateral coalescence. Their apparent diameters in consecutive frames (usually from 5 to 20 mm on the enlargement) were measured under a magnifying glass to the nearest 0.1 mm and were plotted against time. Generally, straight lines were obtained. Occasionally there was an abrupt increase in diameter during a 5-min interval, undoubtedly caused by a lateral coalescence that could not be seen in the photomicrograph. The slopes of selected straight lines were:

Filament material	Fuel	Drop diameter increase μ/min x 100
cotton	clear	87, 119
glass	clear	45, 72, 90, 99
"	+ San. C	50, 113
nylon	clear	68, 93, 99
PVC	clear	84, 91
"	+ San. C	93

Obviously, individual drops on the same surface grew at somewhat different rates. This was ascribed to their location with respect to adjoining drops and to the filament, and the consequent local variations in the fuel flow streamlines. In one instance, a drop attached to a stray fiber on the downstream side of the filament grew at a rate several times as great as normal, perhaps because of a local vortex effect. On the whole, however, the growth rate was essentially uniform for the different filament materials and fuels, the average rate being about 0.9 μ/min.

Thus, if dD/dt is constant, it follows that the volumetric growth rate, $(\pi/6)dD^3/dt$, was proportional to D^2 -- that is, to the drop area exposed to the fuel stream. This seemed reasonable.

It was immediately evident that only a small fraction of the fuel stream droplets that came into proximity to the attached drop ever coalesced with it. This is in accord with the large-scale observations previously reported, as well as with an abundance of the information in the literature. If a droplet in "proximity" be defined as one in a cylindrical element of the fuel stream of diameter D equal to that of the attached drop, then the rate of approach of proximate droplets, under standard feed and flow conditions, was $(6.9 \times 10^{-4}$ g/ml$)(1.65$ cm/sec$)(\pi D^2/4$ cm$^2) = 9.0 \times 10^{-4} D^2$ g/sec. And if $dD/dt =$ 0.9 μ/min, the mass growth rate of the attached drop was $(\pi/6)(3D^2)(0.9 \times 10^{-4})(1/60) = 2.3 \times 10^{-6} D^2$ g/sec, or only 0.25% of the approach rate. Clearly, most of the oncoming droplets were swept past the attached drop in the fuel

streamlines, or else struck and bounced away from it.

Lateral coalescence in the absence of surfactants evidently occurred only when an oncoming droplet in the stream became wedged between closely adjoining drops and acted as a bridge between them. This was favored by a low contact angle, as on glass and 125-μ nylon, where the terminal points of attachment of the adjoining drops along the length of the filament were close together. In general, this growth rate increased with increase in fuel flow rate and with decrease in filament diameter.

With surfactants in the fuel, a variety of growth patterns were observed on 26-μ nylon. Santolene C and 1 ppm AOT had no marked effect. RP-2 gave a somewhat lower rate; AFA-1 gave a very much lower rate with little or no lateral coalescence. The AFA-1 had the same inhibitory action on glass and phenoxy coating as on nylon; however on PVC the adherence was good and the growth rate was not so greatly reduced.

The more powerful surfactants, as shown in Figure 12 (page 60) had an abnormal effect. The small attached droplets evidently slid along the filament until they reached a favorable point, usually at the intersection of the filaments, where they coalesced to form a large drop. Because of the low adherence rate, the total amount of water accumulated was small. Moreover, the large drops thus formed were very readily detached in comparison with normal drops. With 60 ppm AOT in the fuel, an exactly similar behavior to that on nylon was observed on glass and phenoxy coating and even on the cottom filament.

One matter of interest was a contamination of the equipment that occurred during one stage in the program. This was noteworthy, not only because of the interesting phenomena that it produced, but also because it suggested the possibility that interaction between different types of surfactants may have profound effects. The contamination occurred after a series of runs with various fuel additives and it persisted for 11 consecutive runs, until finally the entire fuel loop was dismantled and chemically cleaned. The observable effect was a formation of increasingly larger water droplets from the air-vapor stream at the upper surface of the fuel reservoir. Instead of a maximum diameter of 30 μ, the droplet size increased to hundreds of microns. This was indicative of an increase in interfacial tensions, which is not explicable on any evident basis. Moreover, in one of these defective runs, the large droplets that became attached to the filament were seen to be of the "grape" type, containing many small fuel droplets within the water drop.

3. Detachment Study and Contact Angles

An extensive series of observations was made to determine the fuel flow rate required to detach a drop of given size from a given filament.

The same observation cell and fuel flow loop was used, but there was no continual water feed. Instead, before starting the fuel flow, a single relatively large drop of water was placed on the filament and photographed at 26X.

Then the fuel pump was turned on at a low rate. With the drop under visual observation, the fuel flow rate was gradually increased until detachment occurred or until a rate of 520 ml/min (seven times standard) was reached. The fuel was Bayol 35, clear or with 60 ppm Santolene C. In one group of runs with Santolene C, the drops were equilibrated for 5 to 15 min with the fuel at a low flow rate, before measuring the detachment rate.

In addition, a set of measurements of only the drop dimensions and contact angle was made at the higher magnification of 79X.

Six different filament materials were examined, each at two or more different diameters. Overall, the drop diameters ranged from 3 to 100 times the filament diameter. Usually a single, horizontal filament was used. A few observations were made with inclined or vertical filaments, or with the drop placed at the intersection of two crossed filaments. Tables 13-16 give the data obtained.

Consider first the shape of the drops. In the vicinity of the filament, the drop shape visibly departed from the spherical, as illustrated above in Figure 4. Nevertheless, an entirely adequate definition of the shape was afforded by the two dimensionless ratios, F/D and L/D, where F and D are the filament and drop diameters and L is the axial length of attachment. For a given filament material and a given fuel, the relation between F, D, and L was shown by simply plotting L/D vs. F/D, as described in GR 66-30. These ratios could be correlated with the flat plate contact angle as shown in Figure 14.

It is evident that this plot gave a very satisfactory correlation between F, L, D, and θ over the range of interest from 60° to 150°. At values of θ higher than that of PVC, the curves all must fall abruptly to L/D = 0 at θ = 180°. The photographs of drops on the two polyolefins were inadequate to define this region, but this is not of practical interest.

This correlation has one consequence of considerable practical importance. It implies that any material available in filament form can be directly

TABLE 13

FLOW RATE REQUIRED FOR DROP DETACHMENT IN CLEAR BAYOL

Lengths are given in microns. Flow rates are ml/min (100 ml/min = 2.12 cm/sec linear rate); * indicates no detachment at 530 ml/min.

Filament material	Filament diam. F	Drop diam. D	Attachment length L	F/D	L/D	Contact angle θ_1	Detach. flow rate
cotton	19	845	--	0.022	--	--	*
		947	606	.020	0.64	129,130	440
		1110	670	.017	.60	130,132	470
		1150	663	.016	.58	132,133	340
glass	15	420	231	.036	.55	130,133	*
		576	277	.026	.48	141,140	460
		769	330	.020	.43	144,146	360
		962	405	.016	.42	143,146	310
	27	724	--	.037	--	--	*
		871	--	.030	--	--	430
		932	708	.028	.76	118,122	390
		1025	689	.026	.67	125,125	380
		1125	883	.024	.78	117,121	360
phenoxy-coated glass	11	648	242	.018	.37	149,151	260
		678	280	.017	.41	150,147	310
		928	341	.012	.37	148,148	410
		970	307	.012	.32	152,149	220
	23	576	292	.033	.51	--	530
		735	420	.031	.57	136,134	510
		818	428	.028	.52	140,137	420
		932	474	.024	.51	140,138	310
		1230	489	.018	.40	149,147	280
nylon	26	636	436	.042	.68	128,125	*
		750	466	.035	.62	129,133	480
		894	481	.030	.54	139,140	410
		977	553	.027	.57	134,137	390
		1100	606	.024	.55	134,135	380
	42	754	492	.055	.65	--	*
		883	583	.047	.66	127,126	480
		1125	739	.037	.66	126,127	410
	133	1480	1155	.090	.78	--	*
PVC	15	564	277	.027	.49	139,143	520
		670	250	.022	.37	149,149	390
		708	258	.021	.36	148,150	370
		947	307	.016	.32	151,152	280
		992	417	.015	.42	144,143	420
poly-ethylene	300	902	318	.332	.35	161,159	*
		958	280	.312	.29	157,161	430
		1120	273	.245	.22	165,163	290

TABLE 14

FLOW RATE REQUIRED FOR DROP DETACHMENT IN BAYOL CONTAINING 60 PIM SANTOLENE C

Lengths are given in microns. Flow rates are ml/min (100 ml/min = 2.12 cm/sec linear rate); * indicates no detachment at 530 ml/min.

Filament material	Filament diam. F	Drop diam. D	Attachment length L	F/D	L/D	Contact angle θ_1	Detach. flow rate
cotton	13	424	95	0.036	0.22	--	250
		468	114	.027	.24	156,157	230
	15	582	203	.026	.35	158,154	220
glass	9	443	139	.020	.31	159,158	260
		614	253	.014	.41	147,145	230
		709	291	.012	.41	146,146	190
	32	582	506	.054	.87	109,111	*
	28	798	658	.035	.83	115,114	420
	32	829	658	.038	.79	116,117	400
	27	1100	772	.024	.70	115,114	330
phenoxy-coated glass	13	549	152	.028	.28	151,152	220
		563	158	.022	.28	165,165	220
		646	241	.020	.37	--	270
		734	291	.017	.40	147,149	230
		861	266	.015	.31	155,154	200
	23	494	329	.046	.67	126,125	500
		791	399	.029	.50	140,140	300
		975	424	.024	.44	141,143	250
nylon	10	500	203	.020	.40	149,150	340
		804	316	.012	.39	146,148	280
		1060	228	.009	.22	159,159	160
		1070	304	.009	.28	153,152	170
	26	487	291	.052	.60	134,133	400
		810	443	.031	.55	134,135	330
		1100	519	.023	.47	139,140	220
	(1)	610	284	.044	.47	140,145	350
		758	375	.035	.50	141,140	300
		928	500	.028	.54	134,135	250
		1000	455	.026	.45	137,139	230
	(2)	572	352	.046	.62	135,129	430
		826	326	.032	.39	145,148	260
		955	477	.028	.50	138,140	220

Continued on next page.

TABLE 14 — Continued

Filament material	Filament diam. F	Drop diam. D	Attachment length L	F/D	L/D	Contact angle θ_1	Detach. flow rate
nylon	(3)	261	174	.101	.67	---	390
		462	265	.057	.57	136,139	290
		572	288	.046	.50	136,140	250
		792	337	.033	.43	146,147	220
		795	405	.033	.51	136,138	200
		860	417	.031	.48	140,142	230
		936	417	.028	.45	140,141	170
	33	468	329	.070	.70	124,124	530
		747	468	.044	.63	130,132	360
		924	494	.036	.53	136,138	290
	30	500	196	.061	.39	154,156	400
		855	392	.036	.46	143,149	290
		950	481	.032	.51	139,138	260
	127	1180	893	.108	.76	121,118	*
	124	1190	747	.104	.63	130,137	500
		1215	886	.102	.73	121,121	*
		1440	1075	.086	.75	123,129	380
PVC	19	341	--	.067	--	--	340
		614	--	.037	--	--	210
		836	266	.023	.32	155,157	140
poly-ethylene	275	766	532	.359	.69	125,123	*
		1100	497	.262	.45	140,144	440
		1215	633	.226	.52	134,135	460

Notes

1. The drop was equilibrated by exposure to a fuel flow of 100 ml/min, for a period of 5 min.
2. Ditto, 10 min.
3. Ditto, 15 min.

TABLE 15

FLOW RATE REQUIRED FOR DROP DETACHMENT FROM FILAMENTS INCLINED AT VARIOUS ANGLES AND FROM A ROUGH-SURFACE FILAMENT

Filament 26-μ nylon in Bayol containing 60 ppm Santolene C, except as noted. Lengths are given in microns. Flow rates are ml/min (100 ml/min = 2.12 cm/sec linear rate); * indicates no detachment at 530 ml/min.

Angle of filament above horizontal, deg.	Notes	Drop diam. D	Attachment length L	F/D	L/D	Detach. flow rate
17		402	---	0.066	--	420
		409	---	.065	--	450
		580	---	.046	--	280
		636	345	.042	0.54	260
		640	394	.041	.61	290
		788	428	.034	.54	260
		841	428	.032	.51	250
20	1	636	409	.042	.64	380
		640	455	.042	.71	390
		814	466	.032	.57	300
		936	568	.028	.61	290
		1125	549	.024	.49	230
20, intersecting	1,2	989	---	.030	--	*
		1030	---	.029	--	510
		1410	---	.021	--	470
		1465	---	.020	--	440
30		383	---	.079	--	270
		727	436	.042	.60	190
		902	504	.034	.56	120
32		424	311	.062	.73	340
		487	---	.054	--	260
		655	424	.040	.65	220
		795	470	.034	.59	160
42		398	---	.067	--	250
		409	---	.074	--	260
		443	---	.060	--	180
		462	322	.066	.70	250
		636	398	.042	.63	120
		769	455	.040	.59	140

Continued on next page.

TABLE 15 - Continued

Angle of filament above horizontal, deg.	Notes	Drop diam. D	Attachment length L	F/D	L/D	Detach. flow rate
90	3	333	246	.091	.74	330
		352	235	.086	.67	340
		500	356	.060	.71	270
		773	508	.039	.66	160
		917	576	.033	.63	60?
90	4	436	216	.070	.50	255
		553	277	.055	.50	230
		667	322	.046	.48	190
0, rough surface	5	500	---	.060	--	370
		682	---	.044	--	260
		1057	---	.029	--	170

Notes

1. Clear Bayol.
2. Drop at intersection of two crossed filaments, each at 20° angle.
3. Drop on side of vertical filament.
4. Drop at lower end of filament; attachment occurs along one side.
5. Surface of filament abraded by drawing it between sheets of No. 400 emery paper.

TABLE 16

ADDITIONAL MEASUREMENTS OF DIMENSIONS AND CONTACT ANGLE OF DROPS ON FILAMENTS

Lengths are given in microns. Filaments are submerged in clear Bayol 35, except as noted.

Filament material	Filament diam. F	Drop diam. D	Attachment length L	F/D	L/D	Contact angle θ_1
cotton	14	1160	627	0.012	0.54	136,135
		703	481	.020	.69	127,126
		766	487	.018	.64	129,130
		715	468	.020	.65	126,129
glass	8	873	354	.009	.41	145,148
		646	316	.012	.40	138,143
		753	329	.010	.44	147,148
	20	728	633	.028	.87	113,115
		1020	652	.020	.64	129,129
		930	620	.022	.67	127,129
		924	620	.022	.67	125,125
phenoxy-coated glass	13	772	424	.016	.55	135,140
		1030	424	.012	.41	143,147
		823	424	.015	.52	138,139
	28	1100	532	.025	.48	136,141
	32	810	532	.039	.66	141,134
		924	586	.034	.64	131,130
nylon	25	975	582	.026	.60	132,134
		886	513	.028	.58	133,135
		582	386	.044	.66	126,127
		867	500	.029	.58	132,137
	38	880	582	.043	.66	130,127
		937	551	.040	.59	136,134
		747	481	.051	.64	134,131
	124	987	873	.126	.88	104,113
		797	658	.156	.82	111,112
		722	639	.172	.89	103,117
PVC	8	797	203	.010	.25	156,157
		703	171	.018	.24	161,157
		582	139	.022	.24	159,161
polyethylene	275	1100	443	.250	.40	
nylon[1]	25	601	310	.042	.52	142,143
		797	367	.032	.46	143,143
	(2)	1070	443	.024	.41	141,145
		1050	418	.024	.41	144,145

Notes

1. Filament in Bayol 35 containing 60 ppm Santolene C.
2. Measurements made at the beginning and end of a 1-hour immersion in fuel flowing at a linear rate of 2.1 cm/sec; measurements at intervening 5-min intervals were in line with these data. The decrease in D and L indicates gradual evaporation of the water drop.

FIGURE 14

CORRELATION OF DIMENSIONS OF LARGE DROPS WITH FLAT-PLATE CONTACT ANGLES ON FIVE DIFFERENT SURFACES

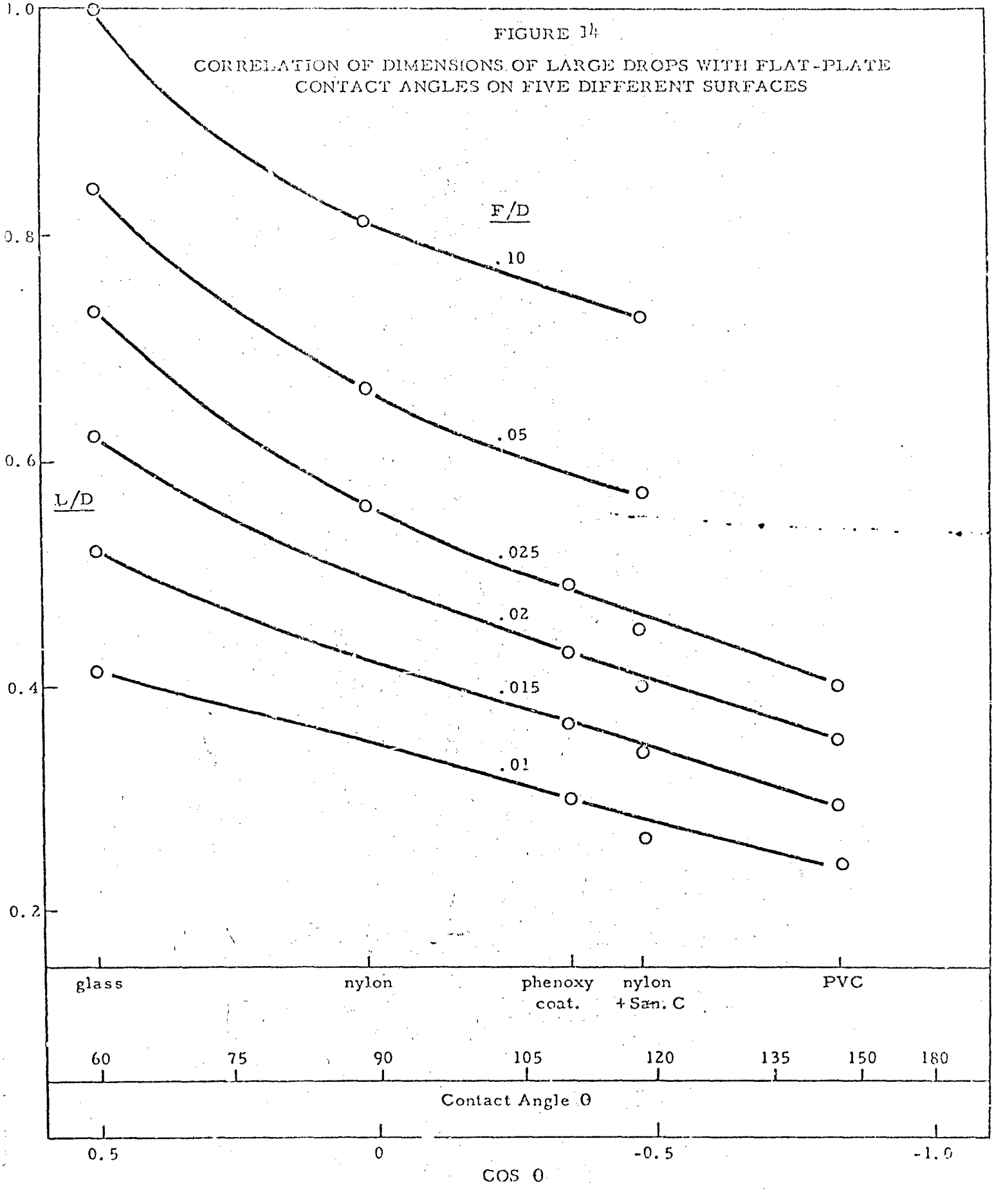

characterized by measurement of F, L, and D in a given fuel. It does not have to be converted to a flat plate for a measurement of θ. The measurement of L and D can readily be made for a number of drops attached to a filament of known F. With suitable equipment, this can be done as quickly as a measurement of θ.

Some consideration was given to the significance of the sideview contact angle θ_1 observed for large drops on filaments. Since the drops profile is not circular at the point of contact (as shown in Figure 4 on page 49), θ_1 is not directly determined by L/D. Empirically, it was found that a single straight line correlates θ_1 in degrees vs. L/D, for all observed data, regardless of surface material or fuel composition. This fortuitous relationship had no evident significance. The noteworthy fact was that, even on cotton and uncoated glass filaments, large drops gave high contact angles like that shown in Figure 4. Thus, the drops did not spontaneously spread and envelop the filament. The same was true in the drop attachment on glass, as shown above in Figure 8 (page 56).

With respect to the detachment force, qualitatively the results were in accord with general expectations. Detachment occurred more readily from small than from large diameter filaments of a given material; more readily from low-energy than from high-energy surfaces; more readily in fuel containing Santolene C than in clear fuel; and (as noted above) very much more readily in fuel containing the more powerful surfactants.

The visual observations of the process were of some interest. As the fuel flow rate was increased, the drop at first remained unchanged. At a rate equal to about 80% of the detachment rate, the length of attachment began to decrease and was finally only 50% of its original value. This reduction was very nearly the same in all cases. On approaching the critical flow rate, oscillating motion of the drop became visible. The final breakaway was too abrupt to be observable. It generally left one very small residual droplet attached to the filament, as would be expected.

A principal objective of this phase of the work was to determine whether the force required to detach a drop from a filament could be correlated with the dimensions and properties of the assembly.

A drop of diameter D cm suspended in a down-flowing laminar stream of fuel of viscosity μ = 2.0 cp and linear velocity U is subjected to two forces: (1) a hydrodynamic force equal to 3 DμU, and (2) the force of gravity, $(\pi/6)D^3\Delta\rho g$, where $\Delta\rho$ = 0.22, the difference in density of the two liquids. (The force of gravity is trivial compared with the water-fuel interfacial tension, so that the drop remains nearly spherical as shown above. However, this force is of the same order of magnitude as the hydrodynamic force and therefore cannot be ignored.) Then the total force acting on the drop is 0.19 DU + 113 D^3 dynes.

Owing to the complex geometry of the assembly, it seemed hopeless to attempt an exact calculation of the force of adhesion that holds the drop on the filament. Instead, since energy = force x distance, it was assumed that this force must be proportional to a specific energy of adhesion multiplied by the area of filament wetted by the drop, and divided by a characteristic length of "stretching" required to effect detachment. The wetted area should be approximately proportional to the product of filament diameter, F, and length of attachment, L. The stretching length is presumably proportional to F.

This simple assumption proved to give a surprisingly good correlation of the observations. When the detachment force, 0.19 DU + 113 D^3, was plotted against L for each drop, all the points for a given surface, both with and without Santolene C in the fuel, fell as close as could be expected to a straight line passing through the origin.

Figure 15 illustrates this correlation for glass filaments varying over 3-fold in diameter, with drops varying 20-fold in weight, and in the two different fuels. The slope of the line is 3.7 dyne/cm (or erg/cm^2). This is an order of magnitude lower than the specific work of adhesion, W, given in Table 10 (66 erg/cm^2 in clear fuel and 45 erg/cm^2 in fuel containing Santolene C). The reason for this seeming disappearance of W in the correlation is that it appears indirectly, by determining the value of L for a given drop diameter D.

Similar correlations were obtained for the other five surface materials. These slopes of these correlation lines varied more than 2-fold, as follows: glass 3.7, phenoxy coating 4.4, cotton 4.9, nylon 6.1, PVC 8.8, polyethylene 9.9 in clear fuel and 6.8 in Santolene C fuel. There was some trend toward increasing slope with decreasing surface energy of the materials, but that

FIGURE 15

DETACHMENT FORCE VS. LENGTH OF ATTACHMENT

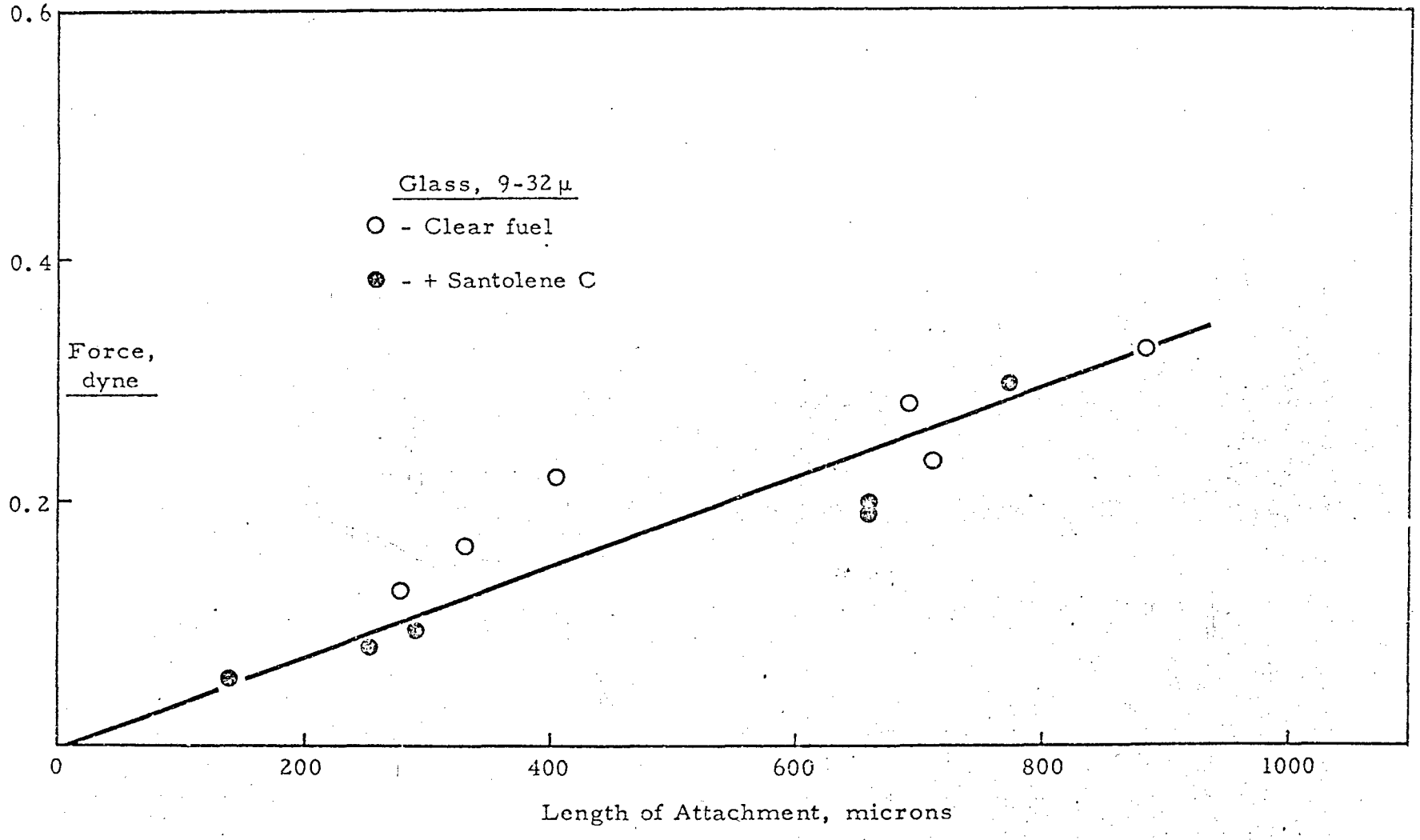

correlation was very poor. It seemed probable that these slopes represent a residual effect of W (or Θ) which had not been manifested in the value of L. Thus for a given drop size on filaments of about equal diameter, the detachment flow rate varied but little with the nature of the filament material, over the range of interest from cotton to PVC. Only on filaments of very low surface energy, such as polyethylene, did detachment become very much easier.

Of particular interest are the data in Table 15 (page 69), on detachment flow rates of drops on inclined, intersecting, and abraded nylon filaments.

At inclinations of 17-42°, the detachment force was considerably lower than predicted. Moreover, the drops showed no evidence of sliding downward along the filament -- a conspicuous illustration of their inherent reluctance to moving or "stickiness." This behavior is confirmed by recent experiments of Somer (ref. 29), who observed drops on filaments in air, and had to employ much larger drops to find angles at which sliding occurs. He also noted that even on a vertical filament, small drops would not slide down.

This reluctance of drops to move along or become detached from a vertical filament was clearly indicated by the data presented here. At a sufficient flow rate, the drops placed on the side of a vertical filament would slide down to the unattached lower end, but would hang there until a higher flow rate finally caused detachment. This adhesion may have been increased by the fact that the end of the filament was somewhat ragged.

On the other hand, the drops placed on a horizontal, abraded filament were detached much more readily than from a smooth surface. This was unexpected, and warrants further investigation.

The adhesion of a drop at the intersection of two crossed filaments was, as anticipated, somewhat stronger than on a single filament. The difference was not great, however. Thus, for the three drops on crossed nylon filaments whose detachment flow rate is listed in Table 15, the values of L calculated from the correlation equation are 690,110, and 1140 μ, respectively. These values are only 15-30% greater than expected for the same size drops on single filaments.

COALESCENCE IN FIBER MATS

I. VISUAL OBSERVATIONS

1. Upstream and Downstream Surfaces

Normally no effort was made to observe the upstream face of a mat, because of the dense haze in the inflowing suspension. Using a fine glass fiber layer upstream, it is evident (as described below) that the fibers become heavily laden with small adherent water droplets, in a manner like that shown in the single fiber observations in the preceding section. This accumulation of water in the upstream layer is confirmed by the analyses made by Bitten (ref. 5) of the amount of water in sucessive layers of a mat.

Direct visual observation of the downstream surface was readily made in the 0.5-inch cell described in the section on equipment. For this purpose, the outer layer of the mat was usually retained by a layer of 16-mesh fiber glass screen which left nearly all the mat surface open to view. A variety of water detachment processes was observed, depending on the fuel, mat, flow rate, and water content employed.

With 0.1% water input and with a fuel and mat giving exceptional coalescence, all the water emerged from only two or three channels. These were usually in the lower half of the mat, suggesting a tendency to downward flow within the mat. The emergent water formed massive globules several millimeters in diameter which eventually became detached and slid down the face of the mat. Under more normal conditions, the channels were more numerous and were widely distributed over the face, and their location sometimes varied during the course of a run. The emergent water detached in drops of about 1 mm diameter which quickly fell to the bottom of the cell. This behavior was typical of a good mat of 14/32 inch depth with fuel containing 0.1% water, antiicer, and Santolene C, at the standard flow velocity of 1 cm/sec.

When Aerosol OT or Petronate L "poison" was added to the same fuel, the emergent droplets were considerably smaller and varied in size. The majority of them were large enough to fall out along a parabolic path in the observation chamber, but the smaller ones of about 20 to 50 μ diameter were swept along in the upflowing fuel stream. It was quite clear that these droplets were not formed by breakup of a larger mass at the outer surface, but came from the interior of the mat. Frequently, the droplets emerged in Rayleigh

chains, as described by Hazlett (ref. 10). These small droplets showed very little tendency to fallout in a large diameter horizontal glass tube between the observation cell and the entrance to the turbidimeter.

Under still more adverse conditions (inadequate mat or abnormally high flow rate), the poisoned fuel effluent contained a substantial haze of droplets too small to be visible. This clearly indicated a breakdown in the efficiency of the droplet attachment process in the upstream layers of the mat.

The ratings used to describe these visual observations of drop size, varying from A** to G, have been tabulated above, page 45, in the section on water suspension analysis.

2. Lateral Observation of a Cross Section

Motion pictures have been taken by R. N. Brown at USA MERDC, Fort Belvoir, showing in operation a vertical cross section taken from a full scale filter/coalescer element and pressed against a window. After viewing these, we followed the same principle in an attempt to obtain a photomicrographic view of coalescence across a 1/16-inch composite fine and coarse glass mat.

The cell, described in GR 68-3, was a closed box fitted with several windows and with fuel inlet and outlet tubes. The mat was confined between two Plexiglas plates closely fitted in grooves. The flow through the mat was limited to a semicircular opening of 2.5 mm radius in the plates against one window. Each side of this opening was back lighted at a 45° angle.

JP-5 fuel containing 0.1% water dyed green, with or without the addition of 25 ppm of Santolene C, was delivered at a flow rate of 40 ml/min. This gave a velocity at the face of the mat of 6.7 cm/sec. The suspension was pumped from the separometer and the effluent fuel was recycled to the fuel reservoir, so that a run could be continued for 100 min. Polaroid pictures, usually at 20X, were taken at intervals.

This type of setup suffers from the fact that one can see only the mat structure immediately adjacent to the window, and there the fluid flow is probably not the same as it is in the interior. However, there seems to be no better way of obtaining an inside view of the process.

On the whole, the results of this effort were not very illuminating. The edge of the mat was, perhaps, pressed too tightly against the window, which tended to increase its depth and flow resistance at that surface. Without dye in the water it was impossible to follow its progress through the mat. Even when dyed water was used, the individual small droplets and rivulets in the interior were not clearly evident.

Many photographs were taken. The most instructive were those in Figure 16 showing the formation and progression of a large channel through the downstream coarse glass layer. The fuel used contained Santolene C. The first picture shows that the upstream fine glass quickly became loaded with attached droplets, so that it appears as a completely dark area. The next two pictures show the marked contrast between the droplet content of the fine and coarse layers, and the formation of a channel or rivulet in the coarse layer. In the last picture, a large 1.4-mm drop is about to become detached. Drops continued to emerge from this channel at the rate of one every 15 sec. Meanwhile numerous small droplets were also emerging from the mat, since it was incapable of complete coalescence in the Santolene C fuel.

In the absence of Santolene C, no small droplets were observed in the effluent. Many large drops were seen to form and become detached at the downstream surface, although the channels that produced them were not visible in the photographs. Also, after 100 min of operation, some massive drops of water had accumulated on the upstream surface.

After studying the entire collection of photographs, we concluded that the most significant step in the process occurred at the junction between the fine and coarse glass layers. Here the surfactant content of the fuel determined whether the water was expelled from the fine glass in droplets that flowed through the coarse glass without further coalescence, or whether it collected into large channels, or whether it did both as in Figure 16.

II. WSIM MEASUREMENTS

1. Base Fuels

It is generally agreed that the WSIM is a useful (though not precise) measure of a non-additive fuel's freedom from those natural components that are likely to cause trouble in filter/separators.

The WSIM's of the base fuels as received, that were used in the present work are listed above in Table 1 (page 7) in the section on materials. It is

FIGURE 16

CROSS SECTION OF MAT BEHIND A WINDOW

Standard fine plus coarse glass in JP-5 with 25 ppm Santolene C. Flow from left to right. Enlargement 22X.

Upstream layer at 3 min.

Midsection at 4 min.

Downstream layer at 5 min.

Same at later intervals

evident that a "clean" jet fuel will have a WSIM of 98 or better. In contrast, a "dirty" jet fuel may have a WSIM of 80 or below, and normal diesel fuel is likely to have a still much lower rating even when free from additives.

We found that these dirty fuels can be cleaned up by treatment with assorbents. Silica gel at room temperature was commonly used for this purpose. This reaised the WSIM to a level close to 100, as shown by the following data:

Fuel	Adsorbent	WSIM	
		Original	Treated
Ashland JP-5	Silica gel	80	99
Degraded Sun JP-5	"	80	100
Great Northern No. 2 oil	"	31	97
"	Filtrol	31	95
"	Norit A charcoal	31	99

Moreover, as will be seen below, silica gel treatment of a clean fuel of WSIM 99-100 apparently improved it further, since it lessened the reduction in WSIM caused by the addition of Santolene C.

It is noteworthy that, as shown in Table 9 (page 27), purification of the No. 2 diesel oil gave very little increase in its interfacial tension against water.

2. Effect of Surfactant Additives

The WSIM's of JP-5, CITE, and Jet A with different concentrations of various surfactants have been listed above in Table 8 (page 25).

Subsequent WSIM data on different JP-5 and Jet A fuels with Santolene C, AFA-1, and Aerosol OT, alone or in combination, are listed below in Table 17. (For these fuels, there was no corresponding measurement of the IFT.)

Three tests were made in diesel fuels. In the Delta fuel containing their FOA 208 (amount not specified), the WSIM was 41 compared with 81 for the fuel without that additive. In the purified Great Northern fuel, 25 ppm Santolene C lowered the WSIM from 99 to 68 and 200 ppm of Ethyl's MPA-D lowered it to only 23.

Addition of 10% NATO F-75 diesel oil to Sun JP-5 lowered the WSIM from 99 to 82, 85. Further addition of 25 ppm Santolene C to this mixture gave a WSIM of only 53.

Examination of the data in Tables 8 and 17 leads to several conclusions:

1. Petronate L and Aerosol OT had a much stronger effect than any of the other surfactants. With 1 ppm Aerosol OT, the WSIM varied from 41 to 68, depending on the base fuel. Addition of Santolene C to the Aerosol OT fuel had no effect, but addition of AFA-1 showed some improvement (as been reported elsewhere, ref.5).

2. Santolene C had less effect than the other corrosion inhibitors. The very small reduction in WSIM in the purified Ashland fuel is difficult to explain, particularly since the same fuel gave a very low index on addition of Aerosol OT.

TABLE 17

EFFECT OF SURFACTANTS ON THE WSIM

Fuel	Additives, ppm	WSIM's	Notes
Jet A	25 Santolene C	90,85	
Same, purified	"	94	
Sun JP-5	"	77 ±4	1
Same, + 0.1% Antiicer	"	98?	2
Ashland JP-5 (purified)	25 Santolene C	98,94,96,97	
"	14 AFA-1	72,75	
"	1 Aerosol OT	41	
"	25 San. C + 1 AOT	43	
"	14 AFA-1 + 1 AOT	53	
Bronoco 140	25 Santolene C	78,85,77	
Same, purified	"	94	
Same, + 0.15% antiicer	"	87	
Same, Plexiglas cell	"	89	3
Bronoco 140	1 Aerosol OT	66,69	
"	25 San. C + 1 AOT	34	4

1. Average of 11 runs ranging from 73 to 83.
2. This result may be erroneous; compare it with the corresponding result with Bronoco 140. The antiicer alone had little or no adverse effect.
3. This was the cell described above on page 37.
4. This was the value obtained at the time these runs were made. Much later in the program, as described below (page 104), the machine consistently gave a higher WSIM of 64 ±9 for this fuel.

Silica gel treatment of the apparently very clean Bronoco 140 greatly reduced the effect of Santolene C therein.

3. Addition of antiicer definitely reduced the effect of Santolene C. This will be confirmed and more clearly defined in the record of tests in the larger cells.

4. Heavy contamination of clean JP-5 with diesel oil lowered the WSIM less than might have been expected, but the further addition of Santolene C, had a more severe effect than anticipated.

5. The reliability of these WSIM's on fuels containing specific surfactants (as an index of their behavior in full scale filter/coalescer elements) is open to suspicion. This will be discussed later, after presenting the data obtained in the larger cells.

III. EXPERIMENTAL MATS AND PROCESS VARIABLES IN THE SEPAROMETER CELL

1. Introductory Remarks

Over 300 experimental runs were made using the separometer No. 2 (modified) cell, usually at the standard WSIM water input and fuel flow rate. The mat materials and often the mat depth were varied.

Although we recognized that the WSIM operating conditions are unrealistically severe, we felt that the effects of process variables and the discrimination between different coalescer media would be magnified thereby. Up to a point, this is undoubtedly true. However, some caution should be used in interpretation of the results with respect to anticipated performance under realistic conditions. Specifically, it does not follow that the best coalescer mat for operation at 0.0625 inch mat depth and 25 cm/sec fuel velocity will also be the best at a depth of 0.5 inch and a velocity of 1 cm/sec. Nonetheless, this research provided valuable background information and guidelines for subsequent development of improved coalescer media for full scale elements.

Since no visual observations were possible, apart from inspection of the fallout chamber, performance was appraised solely by the separometer meter readings. As explained above, page 43, attempts to analyze the effluent for water content were unsatisfactory. The meter reading will be designated as "index" in the following text and tables.

The results of these experiments were reported in detail in GR's 67-2, 67-28, and 68-3, plus a few more in GR 68-33. No attempt will be made here to repeat all these results, many of which proved to be of no significance.

Instead, the salient data and conclusions will be summarized under separate headings. These will comprise the effects of: (1) flow rate; (2) input water content; (3) packing density, for both variable weight at constant volume and constant weight in variable volume; (4) single coalescer media in clear fuel, both at uniform low ΔP and at higher ΔP's; (5) effect of Santolene C corrosion inhibitor; (6) correlation of individual mat performance with previous data; and finally and of most importance, (7) combination mats in surfactant fuels. A brief summary concludes this section.

2. Effect of Fuel Flow Rate

In many runs, after a steady reading at 150 ml/min had been obtained in the prescribed 8 min time, the flow rate was reduced to 20 ml/min. The index then rose to a new equilibrium level after 6 to 10 min of continued operation. The increase at the low flow rate was at most 25 to 30 units for indexes in the middle range from 35 to 60, and was progressively lower at indexes from 60 to 100.

One special experiment showed that these indexes measured at 20 ml/min represent equilibrium conditions. A mat of 2 Std. coarse glass disks was run on clear JP-5 at 20 ml/min from the start for a total of 24 min. After 15 min, the index remained unchanged at 89, a value no greater than that observed after prior operation at 150 ml/min.

Addition of Santolene C to the fuel gave, on the average, a slightly greater difference in the indexes at 150 and 20 ml/min.

Flow rates higher than 150 ml/min showed a substantially lower index. At rates below 20 ml/min, there was apparently very little further increase in the index, although this seemed unlikely. However, when the average velocity was decreased to 10% of the normal rate by operating at 150 ml/min in the No. 1 (unmodified) cell, a mat consisting of 1 Std. fine disk showed an increase in index from 82 to 99. This is a larger effect than would have been expected from the results in the modified No. 2 cell. It suggests that there may be an adverse wall effect in the small diameter cell.

3. Effect of Water Content

Very little investigation of this factor was made. The WSIM of clear JP-5 was lowered perhaps 1 unit by increasing the water input to 1%. Using a superior mat (FM 45 + FM 225, 0.25 inch depth), JP-5 containing 25 ppm Santolene C gave an index of 99 at 0.1% water, but only 86 at 1%. Using an

inferior mat (2 Std. coarse glass disks) with clear JP-5, the index was lowered from 78 to 63 by raising the water input to only 0.2%.

4. Effect of Packing Density

It has long been recognized that there is an optimum packing density for each type of coalescer material. In commercial filter/coalescer elements, the density of the fine glass layers is generally about 0.05-0.10 g/cc, while that of the coarse glass layers is 0.20-0.25.

A few tests were made with clear fuel using single types of glass at different densities in the usual 2/32-inch mat. Also one run was made where the density was lowered by increasing the mat depth to 7/32 inch. Table 18 gives these results.

TABLE 18

INDEX VS. PACKING DENSITY OF SINGLE LAYER MATS

Material	Density	ΔP cm*	Index	No. of Runs
Fine glass				
Std. WS	0.022	5.9	48	1
	.050	17.0	82	2
	.104	52.5	93	1
Coml. A	.036	7.2	57	1
	.072	20 est.	80	1
Coml. B-2	.016	2.3	37	1
	.028	7.1	64	1
Coarse glass - Std. WS	.101	2.1	73	3
Same, 7/32 inch	.202	5.9	78	8
	.054	4.9	90	1

* In No. 1 cell at 8 lit/min.

These data show a consistent trend toward increase in index with packing density for each type of glass; the optimum densities remained undetermined. In the 7/32-inch cell experiment, the reduction in density should presumably have been far more than enough to offset the expected improvement from the longer residence time. On the contrary, the net result was a marked increase in the index. This implied that the mat depth per se is an important factor. Why this should be so was not at all evident.

Further experiments in variation of packing density were made using combination fine plus coarse glass or glass-steel mats.

In the standard WSIM combination of fine and coarse glass disks, if each layer occupied one-half of the cell volume, the density of the fine layer would be 0.107 and that of the coarse layer would be 0.198, in good agreement with commercial practice. We found that this is not true. The two disks were separated by a thin, rigid metal shim, and the assembly was squeezed between two flat glass plates to a thickness of 2/32 inch. It was observed that the fine glass layer occupied only one-third of the space. Accordingly, both layers after compression had about an equal density of 0.15. This is undoubtedly above the optimum for the fine glass layer, as will be shown below.

A series of tests with clear fuel was made at 2/32 inch mat depth using various weights of FM 4 and 3 (Coml. A fine and coarse glass), in an effort to establish the optimum values. The results were erratic, but did indicate that the best combinations had a lower weight of glass and pressure drop than the WSIM disks. In another test with fuel containing Santolene C, the WSIM was 80. When the amount of coarse glass was reduced 46%, giving a reduction in the compression and ΔP of the fine glass layer, the index rose to 93.

Subsequent experiments were made with combination mats of constant weight at variable cell depth. The mats comprised one Std. fine disk plus either one Std. coarse disk or about 270 mg of FM 236+235 steel wool. The Bronoco 140 fuel contained 25 ppm Santolene C + 1 ppm Aerosol OT, in order to provide a severe test. Table 19 shows the measured ΔP and index data.

TABLE 19

INDEX VS. CELL DEPTH AT CONSTANT MAT WEIGHT

Fuel Containing 25 ppm Santolene C + 1 ppm Aerosol OT

Mat	Cell depth, 32nd inch	ΔP cm[1]	Index
Fine + coarse glass	2	47	34
	4	27	63
	7	9	69
	9	7	63
	16	5	39[2]
Fine glass + steel	4	49	34
	7	21	64
	9	14	80

(Continued)

TABLE 19 - Continued

Mat	Cell depth, 32nd inch	ΔP cm[1]	Index
Fine glass + steel (Cont'd.)			
	9	18	64
	9	22	65
	14	12	80
	14	12	78
	16	5	39[2]

(1) In No. 2 cell at 1 lit/min.

(2) At a reduced flow rate of 20 ml/min, these indexes rose to 91-92.

Although the results for the glass-steel mat were erratic, there was clear indication that both types of mat gave an optimum performance when the pressure drop was reduced to about 10 to 15 cm by lowering the compression of the fine glass. (The coarse glass and steel contributed almost nothing to this pressure drop.)

Since the all-glass mat at 7/32 inch cell depth was presumably below its optimum packing density, one experiment was made in which the amount of glass was increased 3-fold. This gave a high ΔP of >60 cm but the index remained at 70.

Thus it was concluded that the optimum packing density depends on both flow rate and cell depth. The data obtained were not sufficient to make a precise evaluation for the separometer cell, but it was tentatively concluded that a density of 0.12 for fine glass and 0.20 for coarse glass would be near the optimum values for a total depth of 14/32 inch at a low flow rate. Further consideration of this problem was deferred until the larger cells were constructed and tested.

5. Index of Individual Coalescer Media in Clear Fuel

A large number of glass and other materials were tested for intrinsic ability to remove and coalesce water from clear JP-5 fuel. The tests were made in the separometer No. 2 cell at 1/16 inch mat depth and 150 ml/min fuel flow. To provide a common basis for comparison, the mats were adjusted to have a uniform pressure drop of approximately 6.5 cm (No. 1 cell, 8 lit/min air flow). Table 20 lists these results. The table also includes a few combinations of fine and coarse glass, at the same low pressure drop, to

illustrate the important fact that combination mats (which will be reviewed later) can be far more effective than either component alone. In combination mats, the upstream layer is always listed first.

The principal conclusion drawn from these preliminary tests in Table 20 was in a sense a negative one: the performance of a material by itself was no indication whatever of its potential usefulness in a composite mat. The steel wool, nylon felt, and polyurethane foam which were excellent coalescing agents in composite mats (as will appear below) had almost no effectiveness when used alone. Likewise, the fine glass (at the low packing density required to obtain the stipulated low pressure drop) was not as good as the coarser fibers with their greater surface area.

TABLE 20

INDEXES GIVEN BY INDIVIDUAL MATERIALS IN CLEAR FUEL

Material	FM No.	Wt. mg	ΔP cm	Index
Glass				
Std. fine (0.4 disk)	--	18	5.9	48
Coml. A fine	4	30	7.2	57
Coml. B-2 fine	--	23	7.1	64
Std. coarse (2 disks)	--	170	5.9	78
Uncoated	1	142	7.3	66
Uncured coated	2	255	6.7	50
Coml. A coarse	3	301	7.0	86
Coml. B-1 coarse	--	219	5.6	83
Coml. B-2 coarse	--	253	6.8	67
Coml. B-3 coarse	--	136	5.8	85
Std. fine + coarse	--	15+33	6.2	91
Std. coarse + fine	--	36+14	5.7	75
Coml. A fine + coarse	4 + 3	23+38	6.5	98
Coml. A coarse + fine	3 + 4	38+23	5.6	58
Coml. B-2 fine + coarse	--	18+59	6.9	93
Acrilan				
Wool	46	137	7.5	49
Wool	47	72	6.4	48
Fabric	48	338	6.9	36
Cotton				
Wool	5	150	6.4	60

(Continued)

TABLE 20 - Continued

Material	FM No.	Wt. mg	ΔP cm	Index
Nylon				
Felt	12	166	4.4	35
Cloth	19	402	7.3	45
Cloth	21	271	7.1	69
Wool	49	106	7.3	35
Filaments	8+11	328	5.3	25
Polyester				
Paper	43	229	6.6	73
Paper	44	311	7.0	65
Wool	45	136	6.4	78
Dacron staple	56	488	7.9	46
Polyurethane				
Foam (3/32 inch depth)	53	305	6.4	36
Polyvinylchloride				
Roving	24	527	5.5	53
Staple	25	184	5.9	57
Wool	26	261	6.0	54
Wool	38	227	7.0	47
Cloth	39	435	6.9	23
Stainless Steel				
Wool	236	463	6.0	37
Wool	236+235	141+168	low	26
Fiber sheet, 0.04 in.	123	2600	3.7	19
Fiber sheet, 0.1 in.	250	1930	6.8	21

Even at higher packing densities and pressure drops, none of the individual media approached the performance of the composite glass mats. The standard fine plus coarse mats gave a WSIM of 99+ at a ΔP of 29.7 cm, and the Commercial A fine plus coarse glass gave a index of 100 at 15.6 cm ΔP. Not one of the numerous metallic media by itself showed any effectiveness whatever, with the unique exception of the 0.1-inch FM 235 fibermetal sheet. It gave an index of 83 at a ΔP of 64 cm.

6. Effect of Santolene C

An extended series of runs, reported in GR 67-28, was made to determine the effect of 25 ppm Santolene on glass and other coalescer media. As above, these runs were made in the No. 2 cell at a mat depth of 1/16 inch and 150 ml/min flow of fuel containing 0.1% water.

From another project, we had a reliable value of 77 ±4 for the WSIM of the Sun JP-5 fuel. For the mat composed of two Std. coarse disks, the index was lowered from 78 ±4 (8 runs) in clear fuel to about 40 (average of 6 values from 27 to 53) in the Santolene C fuel.

None of the various polymeric media tested was notably resistant to the surfactant. The reduction in index was proportional to the index obtained for the clear fuel, up to a peak reduction of nearly 40 points at a clear fuel index of about 80. The more effective glass mats were somewhat less depreciated. Only the FM 225 steel fibermetal sheet was outstandingly resistant; using it, the index fell only 9 points, from 83 to 74.

In many of these runs, after the test the mat was washed well with isopropanol and then retested in clear fuel, to determine whether the surfactant was permanently adsorbed. The results showed that the Santolene C was strongly retained by polyvinylchloride wool and more or less so by the polyester media, but none of the other materials was permanently affected.

7. Correlation of Individual Mat Performance

It has always been tacitly assumed that the chemical nature of the fiber surface is an important factor in determining its performance. For reliable evaluation of different materials, it was evident that they should be compared in mats having similar structural parameters. From the preceding data, this could be done, at least to an approximate degree, for wool-like mats of fibers in the 5-40 μ range. Table 21 lists the indexes of such mats, for fuel both clear and with Santolene C. It was evident that there was indeed a wide variation in performance of different surface materials, with resin-coated glass and polyester being the best, and nylon and steel the poorest.

The table also lists the previously-determined values of the contact angles of water on these surfaces, when submerged in fuel. It was obvious that there was no observable correlation whatever between these values and the indexes. Nor was there any evident relation of the indexes to the previous observations of droplet adherence and detachment for single filaments (page 53 et seq.).

TABLE 21

PERFORMANCE OF MATS OF SIMILAR STRUCTURE

Material	FM No.	Contact angle deg.	Fiber D,μ	Wt. Mg	ΔP cm	Index Clear	Index + San. C
Polyester	45	--	15	128	6.4	78	48
Phenolic resin on glass (2 Std. coarse)	--	110	5-20	170	5.9	78	40
Glass uncoated	1	50	3-8	142	7.3	66	--
Cotton	5	--	15-40	150	6.4	60	--
PVC	26	145	37-40	273	6.0	54	30
Acrilan	47	--	4-20	76	6.4	48	35
Steel	236	115	10	463	6.0	37	--
Nylon	49	86	10-14	106	7.3	35	--

Another significant fact to be considered was the outstanding performance of the steel fibermetal FM 225 sheet (index = 83), in comparison with the well-high complete lack of coalescence of other fibermetal sheets and steel wire wool. There is nothing in the manufacturer's specifications that would distinguish the FM 225 from the other sheets.

From this array of evidence, one is led to conclude that there are indeed marked differences in performance of mats of approximately similar gross structure--but that these differences are the result of subtle variations in surface properties that have not yet been identified.

8. Combination Mats in Clear Fuel

As previously shown (Table 20), the combination of Standard WS fine and coarse mats was distinctly superior to an equal amount of either one alone, provided the coarse layer was on the downstream side. Although this fact has been well recognized in the design of filter/coalescer elements, there has been no satisfactory explanation of it.

A number of other combinations were tested with clear fuel under the same conditions. Most of these had relatively coarse materials in the upstream layer and consequently gave poor results. However, one run was noteworthy. Here, a downstream layer of PVC FM 29 cloth raised the index of two Standard WS coarse mats from 78 to 99. Since the PVC alone was somewhat effective (index = 62) and its addition increased the mat depth to 1/8 inch, one cannot be positive that the combination exhibited synergy, but it seems almost certain that it did so.

Finally, a number of composite mats were prepared from binary mixtures of steel chips with nylon or PVC, as described in GR 68-3. These proved to be completely ineffective when used alone.

9. Combination Mats, Excluding Fine Glass, in Sun JP-5 Fuel Containing Santolene C (WSIM 77)

Preliminary runs (GR 67-28) showed that combinations with FM 225 or 627 steel fibermetal sheets on the downstream side were outstandingly effective. A combination of 2 Std. coarse glass plus 1 sheet of FM 627 (total depth 5/32 inch) gave an index of 99+, although the glass alone gave only 40 and the steel alone had no effect at all. The pressure drop (No. 1 cell) of this combination was only 21.9 cm compared with 29.7 cm for Std. fine + coarse glass. On the other hand, replacement of the FM 627 sheet by FM 232 steel wire cloth gave an index of only 44 at a ΔP of 20.5.

Similar combinations of coarse glass with downstream layers of nylon FM 21, Acrilan FM 48, polyester FM 45, PVC FM 29, or polyethylene FM 55 gave indexes of 45, 31, 61, 79, 86, and 63, respectively. The fact that the 4/32 inch disk of inert, low energy polyethylene gave a substantial improvement showed that steel was not unique in this respect.

A reverse combination of steel FM 627 upstream with coarse glass downstream gave an index 10 points higher than the standard fine plus coarse glass mat--despite the fact that the steel alone was previously shown to have no coalescing action whatever. This anomaly remained unexplained.

10. Combination Mats, Excluding Fine Glass, in Purified Ashland Fuel Containing Santolene C

Despite the abnormally high WSIM of the Ashland fuel with Santolene C (96 ±2), it was used to test a number of single and combination mats, in order to determine whether any materials could equal the effectiveness of the

standard fine glass for use as the upstream layer. In the combinations, standard coarse glass or the effective steel FM 627 fibermetal plate were used as the downstream layer.

These results clearly indicated that none of the three selected plastics (nylon FM 21, polyester FM 45, PVC FM 29) showed good performance when used as the upstream layer; even coarse glass was better than these polymers. As the downstream layer, the steel FM 627 plate was again clearly superior to coarse glass.

In view of collective results up to this point, all further efforts were concentrated on combinations having a standard fine glass mat as the upstream layer.

11. Combination Mats Including Fine Glass, with Ashland Fuel Containing 25 ppm Santolene C

In this series, a few selected plastics and a number of metal fibers were tested as downstream layers, in combination with one standard fine glass mat upstream. In addition, two samples of very fine wire stainless steel wool, FM 235 (12 μ) and FM 236 (8-10 μ), became available at this time, and were investigated at different cell depths and packing densities. These steel wools came in the form of thin blankets, from which the 1-inch diameter mats were cut out. The mats varied considerably in weight and uniformity; the average weight was 136 mg for FM 235 and 106 mg for FM 236. In many instances, as indicated in the following tables, two or three mats of a given kind were superimposed in order to vary the packing density.

Note that in these and all subsequent runs, the pressure drop is that measured in the No. 2 (or larger) cell at 1 lit/min air flow (cf. page 33).

The results, given in Table 22, indicated that the various plastic media were inferior to standard coarse glass, when used as the downstream layer. Three fibermetal specimens of relatively large pore size--steel FM 123, nickel FM 131, and copper FM 1006--were completely ineffective; indeed, the indexes were even lower than the value of 49 obtained for one fine glass mat alone. The results given by the effective steel media will be discussed later, following the tabulations of the remaining data.

TABLE 22

INDEXES OF COMBINATIONS INCLUDING FINE GLASS WITH ASHLAND FUEL CONTAINING SANTOLENE C

Mat Materials	Wt., mg	Cell depth 32nds in.	ΔP, cm	Index
1 Standard fine glass plus:	avg. 44			
Nylon FM 21	318	4	76	86
Polyester FM 45	152	2	>100	32
Polyvinyl chloride FM 29	414	4	40	85
Polyethylene FM 55	659	5	18	49
Steel FM 123	2596	4	low	31
Steel FM 225	1960	4	47	92
3 Steel FM 627	5548	7	>60	98[1]
Nickel FM 131	9640	-	low	31
Copper FM 1006	2428	7	low	24
Steel FM 57 + Polyester FM 43	506 + 40	4	27	97
Steel FM 236 + PVC FM 29 + 2 Steel 235	95 + 420 + 259	7	est. 60	100[2]
" + " + 1 "	93 + 437 + 121	7	49	98
" + "	345 + 416	5	64	87
" + "	186 + 423	7	44	73
PVC FM 29 + 2 Steel FM 235	434 + 262	7	69	92
Steel FM 236 + "	93 + 243	7	46	99
2 " + "	237 + 303	7	53	99
2 "	185	2	51	86
2 "	249	4	44	98
1 "	79	2	34	89
3 Steel FM 235	400	2	high	38
2 "	240	2	81	74
2 "	260	4	52	98
1 "	149	2	50	89
1 St. coarse glass (WSIM)	avg. 85	2	avg. 64	95±2

1. Using 2 standard fine glass, at the same cell depth, the index of the combination was 97.

2. This was an arbitrary combination. It also gave an index of 99+ with 1% water in the fuel. Omission of the fine glass layer, at the same cell depth, lowered the ΔP to 6 cm and the index fell to 55. Replacement of the glass by second layer of steel FM 236 wool gave the same decreases in ΔP and index.

12. Combination Mats Including Fine Glass, with Bronoco Fuel Containing 25 ppm Santolene C

This series of runs, like the preceding, were all made with one standard fine glass mat upstream. The runs comprised: (1) tests of various granular and other new downstream media; (2) confirmation of the effectiveness of the fine steel wool; and (3) further observations of the effect of packing density. In appraising the results in Table 23, it must be recalled that the WSIM of this fuel with Santolene C added was only about 80, in contrast to the value of 95 for the preceding Ashland fuel.

The granular solids were selected because their shape and surface texture were notably different from the various fibers. While these materials would hardly be practicable for use, we hoped that their performance might be helpful in defining optimum characteristics for the downstream layers of coalescer mats. A test was made to insure that the solids would not readily absorb suspended water, which could have invalidated a short time run. As shown in Table 23, the coalescer test results were disappointing. None of the three solids approached the FM 57 steel chips in effectiveness.

The bronze wool was too coarse to be of value. The sintered carbon disk, like the FM 57 steel, was quite effective and the composite steel-PVC disk was excellent.

TABLE 23

INDEXES OF COMBINATIONS INCLUDING FINE GLASS, WITH BRONOCO FUEL CONTAINING SANTOLENE C

Mat Materials	Wt., mg	Cell depth 32nds in.	ΔP, cm	Index
1 Standard fine glass plus:	avg. 44			
Chromosorb FM 101 + FM 43[1]	478 + 42	3	76	62
Alumina FM 102 + FM 43	846 + 42	3	65	76
Sand FM 103 + FM 43	1455 + 42	3	69	50
Bronze Wool FM 100	445	2	80	31
Carbon FM 65	730	4	29	93
Teflon FM 61		2	51	31[2]
Teflon FM 62		2	65	43[2]
Steel FM 236 + PVC FM 29 + 2 Steel FM 235	116 + 406 + 269	7	73	99+
2 Steel FM 236 + 2 Steel FM 235	242 + 268	7	48	99
1 " + "	125 + 154	4	59	98
1 Steel FM 235	158	2	63	79
1/2 Steel FM 235	80	2	42	90
Steel FM 58 wool mat	576	4	75	67
Steel FM 57 + steel screen	549	3[3]	53	90
67% Steel FM 57 - 33% PVC FM 29 Composite[4]	560	4	33	99
1 St. coarse glass (WSIM)	avg. 85	2	avg. 64	80[5]
"		4	23	99
1/2 St. coarse glass	46	2	40	93
2 St. Fine + 3 St. coarse glass	80 + 233	4	>100	98

1. A thin sheet of polyester paper FM 43 was used to retain the granular media.

2. The Teflon paper ruptured during the run (probably as soon as it became covered with water droplets); the observed index is about that anticipated for the fine glass mat alone.

3. Excluding the 1/32-inch thick perforated steel screen.

4. Described in Paragraph 8, above.

5. Average of three runs with WSIM of 78, 85, and 77.

13. Indexes Using Fuels Containing Aerosol OT, with or without Corrosion Inhibitors

A series of runs listed in Table 24 was made with Ashland fuel containing 1 ppm Aerosol OT, with or without an added 14 ppm AFA-1 or 25 ppm Santolene C. In these runs the principal objective was to test the effective glass and steel wool combination with a fuel of much lower WSIM than that provided by Santolene C alone.

TABLE 24

INDEXES FOR ASHLAND FUEL CONTAINING AEROSOL OT, WITH OR WITHOUT CORROSION INHIBITORS

Two coalescer mats were used: standard fine + coarse glass, and the experimental 4-layer combination of fine glass-steel FM 236-PVC FM 29-2 Steel FM 235 described in Table 23.

Additives, ppm	Mat	Cell Depth 32nds in.	ΔP, cm	Index
1 AOT	Stand.	2	65	41
	Exptl.	7	52	76
14 AFA-1	Stand.	2	avg. 64	72, 75
	Exptl.	7	52	99
25 San. C	Stand.	2	avg. 64	95 ± 2
	Exptl.	7	est. 60	100
AOT + AFA-1	Stand.	2	48[1]	53
	Exptl.	7	52	98
AOT + San. C	Stand.	2	65	43

1. There is no evident reason for this low value; the weights of the mats were normal.

14. Upstream Layers of Ultrafine Glass or Steel

A few tests were made (GR 68-33) using the <1 μ FM 0 glass fibers or the 4 μ FM 237 steel wool in place of Std. fine glass in the upstream layer. The fuel was Bronoco containing 25 ppm Santolene C plus 1 ppm Aerosol OT. The downstream layer was FM 236-235 steel.

The ultrafine glass showed no evident advantage, although the results were somewhat inconclusive. A subsequent test in the 0.5-inch cell led to the same conclusion.

The fine steel showed no effectiveness whatever, possibly because its packing density was too low; the pressure drop was only 5 cm. At best, however, it would certainly be no better than the Std. fine glass of comparable fiber diameter.

15. Summary of Separometer Cell Test Data

At this point in the program, it was evident that further work should be carried out in larger cells at lower flow rates. It was felt that the water separometer cell had been a very useful research tool. However, as indicated above in the introduction to this section, it was now clear that caution had to be used in interpretation of the results.

Perhaps the principal contribution from these tests was the clear demonstration that the performance of an individual material had no relation whatever to its effectiveness in a combination mat.

Second, it was evident that the optimum packing density of a given material depended on the flow rate, the cell depth, and the other materials used in a combination mat. This complex interrelationship was difficult to define. For example the effect of a decrease in flow rate shown in the footnote of Table 19 was vastly greater in a low density 1/2-inch mat than in a normal 1/16-inch mat.

In a 2-layer combination mat, the standard resin-coated fine glass at a packing density of about 0.10 was the best choice for the upstream layer. All coarse fibers were clearly inferior.

For the downstream layer, the data allowed valid comparisons at equal flow rates in cells of equal depth and equal pressure drop -- the latter implying an equal degree of compression of the upstream fine glass. These data showed a small but definite superiority of the steel FM 627 plate or FM 235 wool, compared with standard coarse glass. Apart from the various

steels and the porous carbon plate, none of the other materials tested approached the glass in effectiveness. However, it was evident that the possibilities for further improvement had by no means been exhausted. For it was clear that the performance of the downstream mat was critically dependent on its structural properties, and that a multilayer mat might be advantageous.

Finally, there was no indication that the presence of either corrosion inhibitors or the more powerful Aerosol OT would modify any of the above conclusions. If so, this would eliminate the surfactants per se as a factor to be taken into account in the further development of improved coalescer mats.

IV. COALESCENCE UNDER REALISTIC CONDITIONS IN LARGER CELLS

1. Preliminary Runs (GR 68-33)

A series of 8 pilot runs was made in the glass tube cell described on page 13. The results sufficed to show that the effects of packing density and fuel additives could readily be distinguished in such a cell. For example, addition of 1 ppm Aerosol OT lowered an index from 100 to 78. The Bronoco fuel was used in these and all subsequent runs.

While awaiting construction of the steel cell, a group of runs was made in the Plexiglas cell (page 13) to obtain an approximate value of the optimum packing density of Standard all-glass mats and to note the effect of linear flow velocity. The mat thickness was held constant at 0.5 inch. The fuel contained 0.1% water, but no antiicer; 25 ppm Santolene C with or without 1 ppm Aerosol OT was usually added.

Since the indexes in this cell were evidently abnormally high, as shown above on page 37, the data will not be tabulated here. The results indicated that:

(1) The performance was very sensitive to packing density; best results were obtained with a combination of 8 fine plus 4 coarse Std. disks.

(2) The performance was likewise sensitive to flow rate, as anticipated. At a marginal condition (Aerosol OT present), the index was lowered from 97 to 72 by a two-fold increase in flow. On the other hand, at a milder condition (only Santolene C present), the index remained at 100 for both flow rates, indicating excess coalescing capacity at the lower rate.

(3) Thus, in the adverse condition, addition of Aerosol OT drastically lowered the index.

(4) With the optimum packing, at the normal flow rate, the index of 97 for the fuel containing Aerosol OT was abnormally high, in comparison with the pilot run in the glass cell and the later runs in the steel cell.

2. Runs in the 0.5-Inch Steel Cell, without Antiicer in the Fuel

In these and all the subsequent runs in the 0.5-inch cell, the realistic flow rate of 75 ml/min (1 cm/sec or 2 ft/min linear velocity) was employed. If the flow rate was increased to 150 ml/min, the index was considerably reduced. Initially the runs were continued for only 8 min, which was sufficient time to reach equilibrium for mats of good performance. In the later runs, the operating time was extended to 26 min or more. Except as noted, the water input was constant at 0.1%. The pressure drops were measured directly in the cell at 1 lit/min air flow.

In the first series, to provide a basis for comparison, a few runs were made with the above-described combination of 8 fine plus 4 coarse Standard WS glass disks. The results in Table 25 established a base line index of 74 ±3 for the fuel containing 25 ppm Santolene C plus 1 ppm Aerosol OT, with 0.1% water.

TABLE 25

RUNS USING 8 FINE + 4 COARSE St. WS MATS

Fuel flow 75 ml/min for 8 min. Total mat depth 0.5 inch.

Fuel Additives	Mat Wt. mg	ΔP cm	Index
None	108 + 92	45	100
"	106 + 95	38	100
25 San. C + 1 AOT	103 + 98	42	71
"	108 + 92	45	79
"	106 + 95	38	72
"	107 + 105	41	75

The next series of runs was made with various combinations of Std. fine glass and steel, to determine the effect of mat thickness. The packing density of the glass was about 0.12 g/cm^3, and of the steel was 0.23 g/cm^3. The steel section was invariably a layer of FM 236 followed by an equal layer of FM 235, retained by two layers of 16-mesh glass screen. With one exception, the fuel contained 25 ppm Santolene C plus 1 ppm Aerosol OT.

The results in Table 26 showed that 4/32 inch of glass was required, and that 3/32 inch of steel was insufficient. Additional quantities were somewhat beneficial, judging by the data at higher flow rates.

Comparison with Table 25 clearly showed the vast improvement of the glass-steel over the all-glass mat -- the indexes were 99 for the former and about 73 for the latter, under indentical conditions. Also, the pressure drop was lower in the glass-steel mat.

TABLE 26

STANDARD WS FINE GLASS PLUS STEEL FM 236-235

Fuel contained 25 ppm Santolene C + 1 ppm Aerosol OT

Depth, 32nds inch		Wt, mg (1)		ΔP	
glass	steel	glass	steel	cm	Index
6	0	66	-	23	85
0	8	-	184	1	31
1	8	12	191	6	80
2	8	22	188	10	92+
4	8	45	183	17	99+
6	8	77	193	30	99
8	8	110	185	32	99
8	8	110	185	32	77 (2)
12	8	138	186	55	99
6	3	74	69	26	95
6	11	70	242	34	100
8	11	93	259	41	99

(1) Note that the volume of a 1/32-in. layer of 0.5-in diameter is almost exactly 0.1 cm^3, so that the packing density of a given layer can be obtained directly by dividing its weight in mg by the depth in 1/32nds x 100.

(2) Fuel contained 2-fold concentration of additives.

Before preparing a full scale filter/coalescer element, it was necessary to confirm previous indications that the FM 4 glass mat used by the element's manufacturer is just as effective as the Standard WS fine glass disks. This proved to be so.

Also, a few tests were made in which the ultrafine FM 0 glass was substituted for part of the FM 4, or in which some coarse FM 3 glass was used ahead of the steel. The FM 0 was somewhat detrimental, but the combination of coarse glass and steel looked promising. Alternating layers of FM 4 and steel showed no advantage. Insertion of a layer of polyvinylchloride fabric or porous sheet (FM 29, 64) was not helpful. However, an all-glass mat was good, and with the addition of an outer skin of FM 64 gave a very promising result. Table 27 shows these results.

TABLE 27

FM 4 AND OTHER GLASS PLUS STEEL

Fuel contained 25 ppm Santolene C + 1 ppm Aerosol OT

Materials, FM No.	Depth, 32nds	Wt, mg	ΔP cm	Index 8 min	Index 26 min
4 + 236-235	6 + 8	73 + 175	20	97	95
"	6 + 11	70 + 142	20	100	-
"	"	"	"	78(1)	-
4 + 236 + 4 + 236	8 + 3 + 2 + 3	89 + 67 + 25 + 66	28	95	85
4 + 236 + 4 + 235	8 + 2 + 1 + 4	90 + 44 + 13 + 89	28	98	93
0 + 4 + 236-235	2 + 5 + 8	16 + 65 + 176	32	95	92
4 + 3 + 236-235	8 + 4 + 4	88 + 44 + 88	26	97	95
"	8 + 3 + 3	89 + 96 + 65	26	99	96
"	"	48 + 66 + 65	10	99(2)	96
"	8 + 2 + 4	88 + 44 + 89	31	99	97
4 + 236 + 29 + 235	6 + 2 + 2 + 4	72 + 45 + 420 + 89	25	97	93
4 + 64 + 235	8 + 2 + 4	89 + 142 + 90	26	86	79
4 + 3 + 64	8 + 4 + 2	90 + 129 + 136	45	98	97

(1) Fuel contained 2-fold concentration of additives.

(2) Note that the 50% decrease in packing density of the FM 4 fine glass (and consequent low ΔP) did not have any appreciable effect.

No visual rating of the water content in the effluent was reported in these runs. Those with indexes in the 90's would have rated "C" (see page 45 for the code), although there was often enough haze to lower the index below 99. Attempts to measure the water content of these "C" runs by the fluorescent pad method (using a Hydro-Scan unit) gave estimated values of about 20 ppm. In view of the additive content of the fuel, these results were encouraging.

Finally, a series of runs was made using materials taken from commercial elements, with fuel containing, as before, 25 ppm Santolene C plus 1 ppm Aerosol OT. Plugs 0.5 inch in diameter were cut out of two different elements and the sock that came with the element was used as the outer skin. Both plugs gave very poor performance, with indexes of about 65. (One of these plugs was also tested with fuel containing 56 ppm Santolene C only and 1% water; it gave an index of 96 with only a slight amount of water visible in the effluent.) These results confirm the fact that the mats in present-day elements are incapable of satisfactory coalescence in fuels containing powerful surfactants.

The outer 3/16 or 1/4-inch layer of the plugs was removed and replaced with FM 236-235 steel wool at the usual packing density, using the customary 16-mesh glass screen as the outer skin. This improved the performance somewhat, the index rising only to about 75 -- a far from satisfactory level. It therefore appeared necessary to incoporate a layer of FM 4 fine glass beneath the steel.

The remaining experiments were confined to Element A, the one selected as the basis for the full scale experimental models. It had a total mat depth of 18/32 inch. The innermost 4/32-inch glass layer of density 0.28 g/cm^3 was retained. The remainder was replaced with 6/32 inch of FM 4 glass at a density of 0.12 and 8/32 of FM 236-235 steel at an average density of 0.22, plus the final glass-screen retainer. This gave the expected good performance, the 26-min index being 96 and 97 in two tests using the mixed additive fuel. As before, the effluent was clear except for a few medium-size droplets. In a final test, the inner half of the steel layer was replaced by FM 3 coarse glass at a density of 0.32. It gave a 26-mm index of 92.

The foregoing results for fuel containing no antiicer, when tested in the 0.5-inch cell at a realistic flow rate, may be summarized as follows. To appraise the relative effectiveness of different mats under these conditions, it was necessary to degrade the fuel by addition of 25 ppm Santolene C plus 1 ppm Aerosol OT. This provided a severe test. Plugs cut out of two different

commercial elements gave poor coalescence, the index being about 65. The best combination of standard fine and coarse glass disks in a mat depth of 0.5 inch gave a reading of about 74 after 8 min. A better packing of FM 4 and FM 3 glass wools gave a reading of 95, which fell to 87 after 26 min. However, optimum combinations of glass and steel wools gave meter readings of 96-97 after 26 minutes. Also, an FM 4 + FM 3 glass mat with an outer 2/32-inch layer of FM 64 PVC porous sheet gave a 26-min index of 97; it had a high pressure drop, however, and the emergent drops were small. In these last runs, the effluent was free from haze but did contain a few visible droplets that were just too small to fall out in the observation chamber. The amount of this water was estimated to be about 20 ppm.

3. Runs with Antiicer Present--Selection of a Test Fuel (GR 69-1)

At this stage in the program, addition of 0.15% antiicer to the fuel was stipulated. As will be seen, this caused a major reduction in the effect of the sulfonate additives. The first experiments were those aimed at using iron in the water as a tracer for analysis (see page 45). At the conclusion of those runs, it appeared that results obtained in the absence of iron were better than expected. This was confirmed by a number of runs without anti-icer. The fuel contained 25 ppm Santolene C plus 1 ppm Aerosol OT; the cell had 8 fine + 4 coarse Std. glass disks. Previous experience had given a well-established 8-min index of 75 ± 4 for this combination. But the current runs consistenly gave an index of 98. To see whether the coalescer cell or mat was responsible for this anomaly, the WSIM of the fuel was determined. Values ranging from 55 to 73 were obtained, in contrast to the previous value of 34.

The separometer was then completely overhauled and cleaned, and the valves, photocell, and copper lines were replaced. New fuel blends were prepared. Nonetheless, the high ratings continued, both in the 0.5-inch cell and in the WSIM cell. However, two series of WSIM check runs using RF-1 fuel plus 0, 0.5, and 1% Aerosol OT gave exactly normal results, in agreement with previous experience and with the CRC standard curve.

It was finally concluded that the separometer, the cells and mats, and the additives were in no way defective, and that no further effort to explain the discrepancy between current and previous results was warranted.

As a basis for the selection of a test fuel, it seemed desirable to employ a mat that did not include the high cost stainless steel wool. A

series of preliminary experiments was made with downstream layers incoporating FM 3 coarse glass, FM 73 polypropylene, FM 74 nylon felt, or FM 75 carbon felt. The fuel contained antiicer, Santolene C, and 3 ppm Aerosol OT. A combination of the coarse glass and nylon felt gave a better result than either one alone or than any of the other materials. It was therefore concluded that a suitable standard mat would comprise the following:

Layer	Material	Depth, 32nds	Wt, mg	Density, g/cm^3
Upstream	Fine glass FM 4	6	72	0.120
Middle	Coarse glass FM 3	4	82	0.205
Downstream	Nylon felt FM 74	4	62	0.150

This packing has a flow resistance of 25 to 30 cm water at 1 lit/min air flow. All the runs made with this baseline mat are listed below in Table 28. In view of the experience detailed below in Paragraph 6, the condition of each mat is noted in the table. Again, the letter code for the visual ratings is described on page 45.

TABLE 28

EFFECT OF FUEL ADDITIVES, USING A STANDARD TEST MAT

Brenoco fuel, 0.1% water, flow rate 75 ml/min or 2 ft/sec; mat as described in text, except as noted.

Antiicer %	Additives, ppm San. C	ACT	Pet. L	Rating 8 min	26 min	Run No.	Mat	Notes
0.15	--	--	--	100A*	100A*	894	used	
--	56	--	--	100A*	100A*	892	used	
.15	56	--	--	100A*	100A*	893	new	
.15	56	--	--	100A	100B	900	new	(1)
.15	56	--	--	100C	95C	899	new	(2)
--	--	10	--	94D	97D	891	new	
--	56	10	--	93D	94D	890	used	
.15	--	10	--	100A*	97AH	889	used	
.15	56	3	--	100A	99+C	881	new	
.15	56	10	--	100A	99+C	888	new	
--	56	--	10	45F	35G	896	used	
.15	56	--	10	82D-	78E	895	used	
.15	56	--	10	87D-	82D-	901	new	(3)
.15	56	--	3	98D	93D	897	new	
.15	56	--	3	94D	89D	898	--	(4)
.15	56	--	3	96D	89D	902	new	(5)

Continued - -

Footnotes for Table 28

(1) 62 mg of FM 235 in place of FM 74.

(2) 1% water input; run considered defective because accumulation of water in fallout chamber covered much of mat surface.

(3) 82 mg of FM 235 in place of FM 3.

(4) Fresh FM 4 and FM 3; used FM 74.

(5) No. 1 Plexiglas plate placed upstream.

Since fuel containing only antiicer or Santolene C or both gave perfect coalescence, it was clearly necessary to degrade it by further addition of a sulfonate. In the presence of antiicer, even 10 ppm Aerosol OT was insufficient to give the desired degradation but 10 ppm Petronate L gave too much (Run 895). However, 3 ppm Petronate L provided a reasonable level of performance, with opportunity for improvement if a better mat could be discovered. It was therefore selected as the standard "poison" for subsequent use in conjunction with antiicer and Santolene C.

4. Comparison of Mats, with Fuel Containing Antiicer, Santolene C, and 3 ppm Petronate L (See also Paragraph 9 for later runs)

Table 29 gives the ratings of mats in which only the downstream layer was varied; the upstream and middle layers were the standard 6/32 inch (72 mg) of FM 4 and 4/32 inch (82 mg) of FM 3 glass. All mats were freshly prepared.

Prior to one run (No. 942), an additional 4 liters of 0.1% water suspension was prepared in the separometer, set aside, and added to the fuel tank during the run. The mat was the same as that in Run 897, except that the nylon layer was a reused one. It gave a 26-min rating of 89 D⁻ which remained unchanged at 40, 60, and 80 min.

TABLE 29

COMPARISONS OF DOWNSTREAM LAYERS

Upstream layers 6/32 inch FM-4 plus 4/32 inch FM-3. Fuel contained antiicer, Santolene C, and 3 ppm Petronate L.

Material	FM No.	Depth 32nds.	Wt. mg	ΔP cm	Rating 8 min.	Rating 26 min.	Run No.	Notes
None	--	--	--	27	97 D	89 D⁻	916	
Nylon	74	4	61	28	98 D	93 D	897	
Dacron	86	1	52	45	75 D⁻	65 E	905	(1)
Dacron	56	4	62	27	97 D	92 D	906	
Dac.-vinyon	84	4	190	34	99 C	79 E	940	
Dynel	85	2	189	>>100	46 G⁺	44 G⁺	912	(1)
Glass	1	4	62	28	100 B	98 C	926	(2)
"	0	4	63	78	88 D⁻	85 D⁻	937	(1)
"	0	4	13	29	94 D	90 D	938	
"	3	4	77	28	99⁺C	92 D	941	(3)
Quartz	67	4	62	28	99+B	98 C	918	(4)
Cellulose	90	4	82	34	86 E	85 E	917	(2)
Sponge	91	4	25	29	100 B	98 C	939	
Steel	235	4	62	34	95 D	83 D	903	(5)
Nylon + Polypropylene	74-83	4	36-28	18	80 E	72 E	914	(6)
"	"	4	62-	32	95 D	91 D	915	(7)
Nylon-glass	74-1	2-2	34-32	32	98 C	95 D	935	(2)

(1) Density and ΔP too high.

(2) Grapeing occurred near end of run.

(3) An identical result was obtained (Run 945) when the packed cell was first baked in an oven at 350F for 40 min to harden the resin coating on the fibers; the ΔP was not changed by the baking.

(4) Incipient grapeing? - drops evolved in clusters.

(5) Also No. 1 Plexiglas plate upstream.

(6) Abnormally low ΔP - mat defective?

(7) Downstream brass retainer disk replaced by two sheets of FM 83 polypropylene.

Table 30 shows other mats tested with this fuel. In some, the intermediate layer was varied; in others, the total depth was incresed. Also included are plugs cut from two different commercial filter/coalescer elements.

TABLE 30

COMPARISONS OF VARIOUS MATS

Fuel contained antiicer, Santolene C, and 3 ppm Petronate L

FM No.	Depth 32nds	Weight mg	ΔP cm	Rating 8 min	Rating 26 min	Run No.	Notes
4*3*74*	6-4-4	72-9-83-9-62-9	33	94 D	85 D	911	(1)
4-1-74	6-4-4	73-82-62	32	100 C	97 D	925	
4-1-3	6-4-4	73-62-83	27	99 C	93 D	930	
1-4-3	6-4-4	91-47-79	21	92 D^+	88 D^-	929	(2)
4-74	6-8	77-110	27	98 D	92 D	943	
4-3-1	6-4-8	73-82-62	32	100 C	96 C	927	(3)
4-3-1-74	6-4-4-4	73-82-63-64	33	100 C	98 D	931	
4-3-74-1	6-4-4-4	73-84-64-63	29	100 B	99 B	932	(4)
4-3-74-72	6-4-12-1	71-82-190-115	30	96 D	96 D	921	(5)
4-3-93	6-4-10	72-84-303	46	95 D	88 D^-	924	
Coml. element A	16	481	14	84 D^-	76 E	928	
" " B	16	356	12	80 D^-	71 E	944	

(1) * indicates one layer of FM 76 polyester paper.

(2) Only 0.9 ml water collected, instead of customary 1.3 ml.

(3) Grapeing after 16 min; cf. Run 926, Table 29.

(4) Grapeing after 22 min; high water recovery, 1.5 ml.

(5) The ΔP across the cell was measured during the run; it was 2.5 psi.

5. Runs with Fuel Containing Only Antiicer and Santolene C

As shown above in Table 28, fuel containing either or both Santolene C and antiicer gave perfect coalescence with the standard glass-nylon test mat. In two earlier runs with the somewhat inferior all-glass mat (6/32 inch FM 4 plus 8/32 inch FM 3), Santolene C alone or with antiicer gave a 26-min index of 99; no visual rating was made.

Five additional runs were made near the end of the series to observe the manner of water release with hydrophilic quartz and uncoated glass downstream surfaces and with thicker mats, and also to test the effect of increasing the water input to 1%. Table 31 gives the data.

TABLE 31

HYDROPHILIC MAT SURFACE WITH SULFONATE-FREE FUEL

FM No.	Depth 32nds	Weight mg	ΔP cm	Rating 8 min	Rating 26 min	Run No.	Notes
4-3-67	6-4-4	72-83-62	31	100 A*	99 A*	919	(1)
"	6-4-12	73-82-193	34	100 A*	99 A*	920	
4-3-74-1	6-4-4-4	See note		100 A*	100 A*	933	(2)
"	"	"		100 A**	99+A**	934	(2,3)
"	6-4-2-2	"		100 A*	100 A*	936	(4)

(1) Slight grapeing at end of run.

(2) Used mat from Run 932.

(3) 1% water input.

(4) Used mat from Run 935, Table 29.

These results, in comparison with those for comparable mats in Tables 29 and 30, showed that the absence of Petronate L greatly reduced the tendency of hydrophilic surfaces to cause grapeing. In Run 920, it was noteworthy that all the water drops emerged from the bottom 20% of the face area of the mat. This suggests that the additional 8/32-inch layer allowed the water streams to flow downward within the mat structure. It was also noteworthy that raising the water input to 1% had no effect other than to increase the size of the emergent drops. In the four runs with 0.1% water input, the amount collected in the fallout chamber was 1.2-1.3 ml.

6. Reuse of Mats

In a considerable number of instances, in order to save time, at the end of a run the mat assembly was not discarded but was washed in place with isopropanol and with Bayol, and was then reused. Usually no direct comparison between the performance of fresh and reused mats was available. When such comparisons could be made, there was generally no indication of a significant difference. However, in one group of runs there was distinct evidence of inferior performance by the used mats. These runs were made with fuel containing antiicer, Santolene C, and 1 ppm Aerosol OT; the mats comprised 6/32 inch FM 4 plus 8/32 inch FM 3. Two fresh mats gave 26-min ratings of 97 and 100; two other used mats gave 91 and 71. The latter used mat was then soaked in

isopropanol for three days, dried, and again tested; it still gave a rating of C7. All things considered, the most likely explanation is that the process of washing in place in the cell sometimes caused an impairment of the structural integrity of the mats.

7. Test of Two Cells in Series

Two coalescer cells were connected in tandem, the outlet from the first fallout chamber leading directly into the second cell. Each was packed with 6/32 inch FM 4 plus 8/32 inch FM 3 glass. Using the fuel containing Petronate L, a single such mat had given a 26-min rating of 92 D (Run 941, Table 29).

In this tandem cell test (Run 946), visual observation of the effluent leaving the first fallout chamber showed many droplets, in agreement with the previous Run 941. Nearly all of these droplets were removed by the second cell; the combination of two cells gave 8 and 26-minute ratings of 100 A and 99 B.

8. Effect of Antiicer

From the data presented in Table 28, it was evident that the addition of antiicer strongly reduced the degradation caused by Aerosol OT or Petronate L. The same result was obtained when using an all-glass mat. For convenience, the comparative results are listed below in Table 32.

TABLE 32

EFFECT OF ANTIICER

Fuel Contained 56 ppm Santolene C

FM No.	Sulfonate ppm	Antiicer present	Rating 8 min	Rating 26 min	Run No.
4-3	3 AOT	no	80	58	873
		yes	100	96	874
4-3-74	10 AOT	no	93 D	94 D	890
		yes	100 A	99+C	888
4-3-74	10 Pet.L	no	45 F	35 G	896
		yes	82 D-	78 E	895

9. New Data on Comparison of Mats with Fuel Containing Antiicer, Santolene C, and 3 ppm Petronate L

All runs listed here and in the following sections of this report were made since the issuance of the last Interim Report.

Many of these runs involved the use of FM 52 or FM 53 100-pore polyurethane foam at the downstream surface. This material has a fiber diameter and reticulated structure very much like that of natural sponge, which was shown above (Table 29) to be very effective. The foam was used in the form of a 1-inch disk that replaced the customary 16-mesh glass screen retainer. Table 33 gives the data for these runs with polyurethane, and Table 34 presents the other runs made using the Petronate L poisoned fuel.

TABLE 33

COMPARISONS OF MATS WITH POLYURETHANE DOWNSTREAM SKIN

Fuel contained antiicer, 56 ppm Santolene C, and 3 ppm Petronate L

FM Nos.	Depth 32nds	Weight, mg	ΔP cm	Rating 8 min	Rating 26 min	Run No.	Notes
4-3-1-53	6-4-4-3	73-82-61-34	32	100 B	100 C	964	
"	6-3-3-3	58-61-28-38	25	99 C	96 D	990	
"	"	72-35-35-39	27	100 C	98 C	993	
"	"	36-29-27-44	9	99 C	95 D	994	
"	"	72-46-30-35	27	100 C+	99 C	1006	
"	6-3-2-3	73-62-32-33	28	100 C	99 C	969	
"	"	72-60-20-35	29	100 C	97 D	999	
"	"	72-60-10-35	26	98 C	95 C	1001	
"	"	72-31-21-36	26	99 C+	94 D	1002	
"	3-3-3-3	36-61-29-39	14	98 D	89 E	989	
"	"	48-36-27-38	15	85 E	73 E	992	
4-3-1-52	6-3-3-2	72-62-30-24	27	100 A	100 B	984	
"	"	72-82-48-26	28	100 B	99 C	980	(1)
4-3-52-53	6-3-2-3	72-60-26-35	27	97 D	93 D	1000	
4-3-74-52	6-2-4-2	72-20-59-23	22	96 C	89 D	1003	
"	6-4-4-2	71-81-62-25	26	100 B	98 D	979	(1)
4-1-74-52	6-2-4-2	73-20-60-24	22	99 C+	95 D	1004	
"	6-4-4-2	72-81-59-21	26	99 C+	92 D	1005	
4-74-1-53	6-4-4-3	73-80-62-45	29	100 C+	95 D	997	
4-98-1-53	6-4-2-3	38-64-18-43	10	99 C+	89 E	996	
47-46-26-52	6-3-3-2	73-62-30-24	8	96 D	80 D-	985	(1)
75-4-52 / 4-3-75-52	10-3-2 / 5-4-4-2	179-37-20 / 61-79-72-20	31	99 C-	91 D	1016	(2)

(1) A second cell in tandem contained the FM 106 Teflon coated canister screen.

(2) Two separate cells in tandem.

TABLE 34

COMPARISONS OF MATS WITH OTHER DOWNSTREAM LAYERS

Fuel contained antiicer, 56 ppm Santolene C, and 3 ppm Petronate L

FM No.	Depth 32nds	Weight, mg	ΔP cm	Rating 8 min	Rating 26 min	Run No.	Notes
4-3-1	6-4-4	73-82-64	31	100 A	99 C	947	
4-3-74-1	6-4-4-4	72-84-63-61	31	100 A	100 C	948	
"	"	72-83-62-62	31	100 B	100 C	953	(1)
1-4-3	4-6-4	63-74-82	35	91 D	79 D⁻	1011	
"	"	12-72-82	23	88 E	76 E	1012	
0-4-3	"	63-73-83	>100	95 D	87 E	1013	
"	"	12-74-83	38	97 D+	92 D	1014	
4-3-74	6-4-4	74-83-62	33	97 D	92 D	949	
"	"	72-82-71	26	100 A	99 B	951	(2)
"	"	72-83-72	29	99 C	95 D	956	(2)
"	"	72-81-73	31	100 C	99+C	961	(3,4)
"	"	72-83-53	30	99+D	99 D	968	(3)
3-4-3-74	4-6-4-4	93-73-83-72	36	98 C	95 D	955	
4-3-98	6-4-4	74-82-63	35	99 C	92 D⁻	995	
4-3-46	"	71-82-62	32	99+B	97 D	966	
4-3-235	"	73-83-62	35	99 C	97 D	950	
4-3-94	"	73-81-61	31	96 D	92 D	957	
4-3-*	6-4-2	71-82-103	30	93 D	80 D⁻	963	(5)
Plug	12	418	12	86 D⁻	76 E	954	(6)
"	18	588	27	87 D⁻	82 D⁻	960	(6)
94	12	165	1	27 G	24 G	958	

(1) No. 2 Plexiglas disk (page 37) placed downstream.

(2) Innermost layer (4/32 inch, 94 mg) of commercial element placed upstream.

(3) Same as (2), but 7/32 inch, 207 mg layer.

(4) Run was continued for 80 min; rating remained 98 D from 40 to 80 min.

(5) * is a layer of yellow pine wood, across the grain.

(6) Plug cut from a commercial element.

10. Principal Conclusions from Tables 29-34

The most important results in this collection of data on the performance of different mats in the poisoned fuel would seem to be as follows:

1. For the upstream layer, the uncoated FM 0 and FM 1 glass are inferior to the regular FM 4 that is used in a commercial element. For the latter, a depth of 6/32 is much better than 3/32 inch. The optimum density is 0.12 or perhaps somewhat less.

2. For the internal layer, the regular FM 3 coarse glass is as good as any.

3. For the downstream layer, the most effective materials were natural sponge, quartz wool, and uncoated FM-1 glass; slightly inferior were nylon FM-74 and an additional amount of FM 3 coarse glass (Table 29). Polyurethane alone was less effective (Table 33). The glass-nylon mats were frequently used, and this provided a measure of variability -- their 26-min ratings ranged from 93 D (Table 29) to 99 B (Table 34). A longer run showed a decline in rating from 100 C at 8 min to 99+C at 26 min and then down to 98 D at 40 min where it remained constant.

4. Interleaves of FM 76 polyester paper between the glass and nylon layers had a quite harmful effect, although they did not greatly increase the pressure drop.

5. The 100-pore polyurethane skin repressed the grapeing that often (Tables 29-30) developed on the hydrophilic uncoated glass and quartz surfaces. The 4-layer mats with uncoated glass downstream (Table 34, top) also did not form grapes. They might well have done so at a higher water input, but this was not tested. Removal of the Petronate L poison (Table 31) greatly reduced the tendency to grape formation, even with 1% water input.

6. The best 26-min rating obtained with the poisoned fuel was 100 B for a mat of only 14/32 depth, comprising fine, coarse, and uncoated glass, with a polyurethane skin (Table 33, Run No. 984). In retrospect, it appears that a 5-layer mat with nylon between the coarse and uncoated glass might have been even better, but this was not tested.

7. Plugs cut from commercial elements were greatly inferior to the experimental mats (Tables 30 and 34).

8. Two cells in tandem gave a marked improvement, although not 100% complete removal of water (Paragraph 7).

9. The great improvement cuased by the presence of antiicer (Table 32) should not be ignored.

11. [illegible] Containing Only Additives and Stabilizer C

A few of the mats listed in Tables 33 and 34 were also tested without tetraethyl lead in the fuel. The results, given in Table 35, were almost invariably excellent.

TABLE 35

PERFORMANCE OF MATS IN FUEL CONTAINING ANTIICER A-3 PLUS STABILIZER C ONLY

FM No.	Bench 22 hr	Weight, mg	ΔP cm	Rating 8 min	Rating 26 min	Run No.	Note
4-3-1-33	6-3-3-3	58-61-38-38	25	100 A*	100 A	991	
"	"	72-46-30-35	27	100 A	100 B	1007	
"	6-4-4-3	73-82-61-34	32	100 A	100 A	965	
"	6-3-3-3	72-63-32-31	29	100 A**	100 A**	970	
4-74-1-33	6-4-4-3	73-80-62-45	29	100 A*	99-A	988	
4-3-74	6-4-4	72-82-71	26	100 A*	99-B	972	(1)
"	"	72-81-73	31	100 A	100 A	982	(2)
"	3-7-4	37-144-61	13	100 A*	96 AB	1035	(3)
92-4-3-74	3-3-4-4	18-36-81-62	17	100 A	98 AB	977	(4)
94	12	165	1	39 C	28 C	959	

(1) Inner-most layer (4/32 inch, 94 mg) of commercial element placed upstream.

(2) Same as (1), but 7/32 inch, 207 mg layer.

(3) 16-Mesh [illegible] screen used as downstream retainer.

(4) A second [illegible] in tandem contained the FM 165 Teflon coated canister screen.

12. [illegible] Grade

Four runs were made on the untreated Great Northern No. 2 oil of MIXM 31, using both [illegible]ylon and glass-polyurethane mats. All gave poor results, the 26-min ratings varying from 35 E to 65 E. One run made with the tenth cell deposited in the last line of Table 16 gave a much better result, the final rating being 95 E. However, there was no assurance that this degree of efficiency would be maintained in continued operation.

One run on the more fully after purification with charcoal (MIXM 30) gave a 8-min rating of 100 A**, but at 26 min this had fallen to 65 E. Thus, the high [illegible]

Earlier (GR 68-33), runs made on the Nato F-75 diesel fuel in the No. 2 separometer cell gave very low indexes. In the present series in the 0.5-inch cell, this fuel was treated with silica gel and tested with a glass-nylon mat. The 8 and 26-min ratings were 100 A** and 99 B.

V. PERFORMANCE OF OUTER CANISTER SCREENS

1. Test Conditions

A series of 17 qualitative observations of the behavior of isolated separator screens was made at the end of the program. The test cell was the 0.75-inch i.d. glass tube illustrated in Figure 3, page 16. A good coalescer mat was used: it comprised 6/32 inch FM 4, 3/32 inch each of FM 3 and FM 1 glass and FM 53 polyurethane. (An inferior mat might have served the purpose better). The fuel normally contained 0.1% water, antiicer, Santolene C, and 0, 1, or 3 ppm Petronate L. The final run had 1% water.

With no Petronate L, there was of course no water in the effluent and the only observations were of the pressure drop across the screen. With 3 ppm of the poison, the water droplets in the effluent were too small to be affected even by a 400-mesh screen, but merely flowed through unhindered. However, by reducing the Petronate L content to 1 ppm and operating at high fuel flow rates, it was possible to transport a small number of medium size droplets across the fallout chamber and onto the screens. These droplets were roughly 50 μ in diameter.

The screens used, and their pressure drops (converted to cm of water) at a fuel flow of 112 ml/min are listed in Table 36. This flow corresponds to a face velocity of 0.67 cm/sec, which is that at the surface of the canister screen around a full scale filter/coalescer element delivering 20 gal/min.

TABLE 36

SEPARATOR SCREENS EXAMINED

FM No.	Screen Material	ΔP cm of water	Notes
106	100-mesh Teflon coated steel	0.12	(1)
107	100-mesh brass	0.11	
--	Same, coated with acrylic resin	0.43	
108	400-mesh stainless steel	0.32	
109	325-mesh bronze	0.22	
76	polyester paper	2.52	
77	polyvinylchloride paper	1.46	
52	100-pore polyurethane (3 layers)	0.24	
--	80-pore polyurethane, sprayed with Scotch-gard	--	(2)
111-53	0.75 inch depth of 10-pore polyurethane in fallout chamber plus 1 layer of 100-pore screen	0.12 est.	(3)

(1) This sample was taken from one of the present-day filter/separator canister screens.

(2) It was questionable whether the foam was actually coated with the silicone.

(3) The 10-pore open mesh packing was inserted to see what effect it had on the flow of water droplets across the chamber.

2. Observations

The pressure drops across the water-free screens at normal flow rate are listed above in Table 36. The two samples of paper obviously were too high in resistance to be considered. On the other hand, even a 3/16-inch layer of 100-pore polyurethane was acceptably low, as was the 325-mesh screen.

With the FM 106 Teflon coated screen, after passage of 6 lit of suspension, the pressure drop at 190 ml/min (1.13 cm/sec) rose to 0.39 cm, compared with 0.16 cm for water-free fuel at the same flow rate. The smaller droplets readily streamed through the screen; the larger ones stuck to the screen for a time and eventually rolled down. Chains of successive droplets were broken up as they struck the screen. With 1% water input, the behavior was similar. The 100-mesh brass screen was clearly less satisfactory; its pressure drop reached 0.55 cm.

At the other extreme, the FM 108 400-mesh screen became badly clogged with water. After only 14 min of operation at the low rate of 112 ml/min, the pressure drop had risen from 0.24 to 1.90 cm. Likewise, the FM 109 325-mesh screen was noticeably clogged. At the high flow rate, the pressure drop rose from 0.32 to 1.36 cm. Water could be seen on the screen, and some coalescence appeared to be taking place there. Meanwhile, small droplets flowed through readily.

The FM 52 100-pore foam showed a behavior intermediate between that of the 100-mesh and 325-mesh screens. At the high flow rate, the pressure drop was 0.39 cm after passage of 2 lit of suspension, and rose to 0.71 cm after 4 lit. Accumulations of coalesced water were clearly visible on the upstream surface, forming large drops that rolled down and off the screen; only small droplets appeared in the downstream effluent.

In the experiment with the 10-pore foam in the fallout chamber, there was some indication that less water reached the 100-pore screen.

The two tests using acrylic and silicone coated screens failed to yield useful information.

Based on the limited number of experiments made, it is difficult to generalize as to optimum material to do the water shedding job. It is regrettable that time did not allow further experiments along this line, for we speculate that improvement of the existing system can be made. Further discussion of this possibility will be included in the final section on conclusions.

FULL SIZE EXPERIMENTAL FILTER/COALESCER ELEMENTS

To fulfill the requirements of the contract, a small number of full scale experimental elements were constructed and sent to USA MERDC, Fort Belvoir, for examination.

All these had as their basis a present-day commercial element whose fabrication had been completed up to the final point of applying the outer fabric jacket and end caps. The outermost 14/32 inch layer was then removed and replaced by an experimental mat and outer skin. Then the ends of the mat were trimmed flat and end caps were cemented on.

For the sake of the record, Table 37 lists the materials used and the thickness of each layer. It will be recalled that FM 4 and 3 are the resin-coated fine and coarse glass obtained from the manufacturer of the basic element; FM 1 is uncoated glass; FM 236-235 is the dual layer of medium and coarse steel wool; FM 74 is nylon felt; FM 52 and 53 are 100-pore and FM 111 is 10-pore polyurethane foam. The nominal packing density of each material was held constant throughout, at the following values:

FM No.	4	3	1	236-235	74	52-53	111
g/cm^3	0.12	0.205	0.10	0.23	0.15	0.066	0.030

TABLE 37

MATERIALS USED IN EXPERIMENTAL ELEMENTS

Elements No.	Coalescer Mat and Outer Skin FM Nos.	Depth, 32nds	Notes
1-2	4-236,235	6-8	(1)
3-4	4-3-74	6-3-4	(1)
5-6	4-3-1-52	6-3-3-2	
7	4-3-1-53	6-3-3-3	
8	4-1-74-52	6-2-4-2	(2)
9	4-3-74-53	3-4-4-3	
10	4-3-74	3-7-4	(1)
11	4-3-1-53-111-53	3-4-4-3-16-3	(3)

(1) The outer skin was 2 layers of 16-mesh glass or PVC screen.

(2) A detachable outer skirt of FM 53, 5-inches in diameter and 21 inches long was fastened to the top cap.

(3) The outer layers of FM 111 and 53 were clamped onto the top cap and were open at the bottom.

For the first six elements, an effort was made to use plastic end caps provided by the manufacturer of the basic element. Despite considerable effort, we were unable to obtain a permanently leak-proof seal beneath the caps. This leakage made it impossible to obtain meaningful test data.

For the remaining five elements, we used aluminum caps made in our shop and sealed on with Duro EPF-200 "EpoxE" cement. This provided a tight seal.

Elements Nos. 7 and 8 still gave some evident leakage from isolated spots in the body of the mat. This was evidently a result of a structural failure, although subsequent examination failed to reveal the nature or cause of it.

The remaining three elements showed no indication of leakage during their initial testing at MERDC. No report of the test data will be made here, since the testing is still in progress. Suffice it to say that the initial observations were gratifying.

CONCLUSIONS AND RECOMMENDATIONS

I. MATERIALS AND EQUIPMENT

1. Fuels

The study of both JP-5 and diesel fuel covered a sufficiently wide range with respect to ease of water removal.

The WSIM of a non-additive fuel is apparently a good index of its "purity" with regard to components that affect coalescence. There may be unusual exceptions, such as the purified diesel fuel that had a WSIM of 99 but showed poor coalescence after 26 min of operation (page 114).

With additives present, the WSIM may be misleading. For example, with 25 ppm Santolene, JP-5 had a WSIM of only 77, but excellent coalescence was obtained in a moderately good mat (Table 28, page 105).

The ready purification of low grade fuels by treatment with silica gel or charcoal is noteworthy. Even a fuel of high WSIM was further improved by this means: the WSIM of the high quality Bronoco with Santolene C added was increased from 77 to 94 by such pretreatment (Table 17, page 82). It might prove worthwhile to attempt an analysis of the components removed by these adsorbents. This might suggest a modification in refinery processing that would improve fuel quality.

In any event, it is clear that every effort should be made to avoid contamination in transit and storage. Given a "clean" JP-5 containing anti-icer, even the existing filter/coalescer elements should be able to cope with the addition of a high concentration of Santolene C without much difficulty (page 103 shows an index of 96 <u>without</u> antiicer).

For diesel fuels, either with or without the customary additives, there appears to be no prospect of <u>complete</u> removal of water in a single, small diameter filter/coalescer element. Larger or multiple units might do so, but is that necessary? It would be desirable to measure the actual water content in the effluent from a DoD element for a realistic diesel oil with high water input. If a diesel engine can run on such an effluent fuel without serious difficulties, there should be no objection to it. Alternatively, the cleaner CITE fuel could be used.

2. Surfactants

The individual surfactants employed covered a wide range of chemical types. The only ones not isolated and tested were the natural components already present in low quality fuels.

Anionic, nonionic, and cationic compounds seemed to be about equal in their effect. The petroleum sulfonate Petronate L was considerably more harmful than the standard Aerosol OT, although both lowered the interfacial tension to about equally low values (Table 9, page 27). The corrosion inhibitors were much less harmful.

3. Coalescer Media

A wide variety of material filaments or fibers were tested in the form of wool, felt, or paper. It seems unlikely that any further types would exhibit unexpected properties, particularly since it appears that fiber diameter and geometry are more important than the chemical nature of the material. On the other hand, only a limited number of "3-dimensional" materials such as the sponges, foam, sintered metal plates, and granular compounds were used. These showed a wide range of effectiveness and it is therefore possible that further exploration of such structures might uncover some of value.

Composite media, containing widely different materials in intimate contact, were originally suggested by Dr. Zisman at NRL. These proved to be difficult to prepare, and only a few tests were made. Although completely ineffective when used alone, one steel-PVC plate gave very good performance when used as a downstream layer (Table 23, page 96). Further work on such materials might be very useful, as will be discussed below.

4. Equipment

The water separometer is a very satisfactory research tool, if care is taken to follow the instructions and to check the performance at frequent intervals. The 0.5-inch experimental coalescer cells used in the separometer were likewise satisfactory. However, for further research, it would be desirable to increase the fuel tank capacity to 10 liters so that a one-hour run could be made with a larger cell of 0.75-inch diameter. A run time of one hour should be ample to reach equilibrium conditions.

Such small scale equipment is far lower in cost and quicker and easier to operate than a full scale single element test loop. The effluent fuel is not worth reclaiming, and can readily be disposed of.

On the other hand, the study of external fallout and separator screens really requires a long vertical unit. The existing single element test facilities are recommended for this purpose.

The glass observation cell (page 54) used for the single fiber studies was highly satisfactory. However, a more advanced photographic study of a multiple fiber matrix will require a different design. This might involve transparent plates having a hydrophobic surface, placed close together in parallel.

II. PHYSICAL PROPERTIES AND EFFECT OF ADDITIVES

1. Contact Angles

The data obtained (page 18) are of questionable value for making generalizations, because the results were highly specific with respect to both individual fuel components and surface materials. To be meaningful, it would be necessary to measure the angles for a large number of fuel-water-solid systems and to determine the coalescence behavior for each of these systems -- altogether, a major effort.

2. Interfacial Tensions

These IFT data (pages 24-27) are of more direct significance, provided the measurements are made on systems that have brought into equilibrium. It is well recognized that a fuel having a low IFT against water generally shows a low WSIM, the IFT being indicative of fuel "purity." The disengagement of water drops at the coalescer surface is necessarily affected by the IFT, and in fuels of lower IFT the drops did tend to be smaller. However, even with an IFT below 1 dyne/cm (page 27) in fuel with antiicer, Santolene C, and 10 ppm Aerosol OT, most of the water drops were still large enough to fall out (Table 28, page 105).

3. Porosity, Capillarity, Pore Size, and Pressure Drop

It is now clear that both coalescence and disengagement of water are governed to a major degree by the structure or geometry of the coalescer mats. It is therefore important to have means of characterizing the different mat structures.

What might be called the "gross structure" is determined by the readily observable properties -- depth of mat, packing density, fiber diameter or cell wall thickness, and general form. The last term distinguishes different

types of structure, such as random wool-like arrays of filaments (like fiberglass), partly or wholly oriented fibers (paper, felt, and bundles), woven fabrics and screens, cellular foams, etc.

A description of the gross structure is useful as a means of broad classification. However, it is insufficient to predict the performance of materials such as fibrous mats and fabrics. For these, a closer view of the "micro structure" is required. This is not readily obtained by direct observation. It was hoped that it might be deduced from measurement of capillarity and resistance to fluid flow. (Other measurable properties such as permeability to solids might also be useful, but were not investigated in the present work.)

The capillary rise measurements failed to provide a clear-cut definition of the micro structure, in relation to the gross structure parameters. However, the data were sufficient to indicate that the size of the channels or pores in a given mat varies widely, perhaps over a 5-fold to 15-fold range, and that all the eight mats examined had pore sizes of the same order of magnitude.

Flow resistance is readily and accurately measurable, and should be closely related to micro structure. No special study of this subject was made, but the data obtained in passing were sufficient for some preliminary analysis. For example, it was anticipated that there might be a simple relationship between the flow resistance of the fine and coarse fibers, but this was not so. In general it appeared that, in flow resistance, the fiber mats are intermediate in character between screens and capillary channels, and that the degree of resistance varies with both the diameter of the fibers and the average distances between them.

Altogether, it was not possible to find a useful, quantitative correlation of these structural properties with the effectiveness of the materials as components in a coalescer mat.

4. Electrokinetic Properties

The effect of Plexiglas surfaces, though quite irreproducible, was undoubtedly real. It is hard to ascribe this to any other than an electrostatic or -kinetic action. Further investigation in this area is certainly warranted, and work is currently underway elsewhere (ref. 12).

5. Determination of Water

It would be highly desirable to develop a simple, rapid method that would determine the total free water in a fuel, regardless of the droplet size. In a crude experiment just now made, it was observed that addition of dry indigo carmine dye to a dilute suspension of fine droplets in fuel rapidly coagulates the water. This is in marked contrast to the behavior of the granular solids mentioned on page 95. It suggests that an absorption method of this kind might be developed that would be an improvement over the fluorescent pad.

6. Effect of Organic Dyes

The strong beneficial effect of adding dyes to the input water was presumably due to their adsorption on the fibers, inasmuch as it was difficult to wash them off after making a run. This suggests the possibility of modifying the resin coating on the glass fibers to make it more resistant to surfactants, while retaining its useful effects (increased rigidity of the mat and reduction of the overly hydrophilic nature of the glass surface).

7. Effect of Antiicer

The marked reduction in the effects of both weak and strong surfactants resulting from addition of antiicer remains unexplained. The antiicer certainly did not have a pronounced effect on the interfacial tension (Table 9, page 27). Perhaps, like the dyes, it is adsorbed on and modifies the fiber surfaces.

8. Effect of Surfactants

Even though the surfactants were not strongly adsorbed on most of the solid materials tested (pages 90, 109), they clearly modified the surfaces. Hence, both the solid-fuel and solid-water as well as the water-fuel interfacial tensions were more or less altered. The net effect on the work of adhesion of water was specific with respect to both the surface material and the surfactant structure, as described above (pages 27-28).

As a result, three effects were apparent. First, the ease of attachment of the inflowing small droplets (which at best is difficult, as shown on page 62) was reduced. With strong surfactants or diesel fuel, the result was the appearance of haze in the effluent fuel. This haze almost surely was not formed in the mat, but consisted of original droplets that flowed through without attachment.

Second, within the mat, the merging of water rivulets into larger streams was evidently impeded. As a result, the emerging drops were smaller.

Finally, if the outer skin had small pore diameters and the outflowing water streams were constricted, the growth of a large drop at the surface was inhibited by the lower fuel-water IFT.

III. PROCESS OF COALESCENCE AND REMOVAL OF WATER

1. Outline of Process

It is now generally agreed that the overall process of coalescence in a mat involves: (a) complete attachment of inflowing droplets onto upstream fiber surfaces; (b) growth of the attached drops and their eventual collection into rivulets that join together into larger streams during their flow through the mat; and (c) an unhampered discharge of the streams in large drop form at the exposed downstream surface of the mat or skin.

The details of the process in the upstream and interior still remain unknown, being wellnigh out of the range of visual observation. It seems certain that subtle differences in the interior structure or environment can have major effects. The same is clearly true at the downstream surface or skin.

2. Extension of Single Fiber Study

The observations made on single fibers in a flowing suspension, although interesting, were inadequate to explain the overall coalescence process. Nor did they help in the selection of materials for use in mats.

An extension of these studies, however, might well be profitable. One such approach was mentioned above in the conclusions regarding equipment (page 122): it would permit transverse observation of fuel flow through a "2-dimensional" fiber matrix. Another approach would be to examine both the upstream and downstream surfaces and observe the performance of very shallow mat layers, using different input water droplet sizes.

3. Value of Physical Property Studies

Altogether, the considerable effort spent in studying the various physical properties, together with the other auxillary observations, proved to be of little value as a guide to the selection of effective coalescer media.

In theory, given sufficient knowledge of the mechanism of the process and the properties of the fuels and coalescer media, one should be able to design a complete mat without recourse to trial tests. In practice, this appears to be impossible. Instead, a systematic trial-and-error test program seems to be the only effective approach to achieve optimum performance.

4. Selection of Coalescer Media

For the upstream droplet attachment layer, the FM-4 resin-coated 1 to 5 μ glass wool was the best of the many materials tested. It appears unlikely that smaller diameter fibers would offer any overall advantage. Possibly a very thin layer of finer fibers at the surface would be helpful; this was not investigated.

For the intermediate layers, the best materials (in approximate order of descending merit) were: natural sponge, FM 627 sintered fibermetal steel plate, FM 236-235 8 to 12 μ stainless steel wool, FM 75 16 μ carbon felt, FM 74 and FM 98 40 to 50 μ nylon and dacron felts, the FM 65 porous carbon plate, and FM 3 6 to 24 μ resin coated glass.

At the outer layer, FM 1 3 to 8 μ uncoated glass and FM 67 quartz wool strongly promoted the formation of large drops. At the same time, the outer surface tended to become too wet with water, often resulting in the formation of "grapes." This usually occurred only when the fuel contained Petronate L. An outer skin of FM 52 or FM 53 100-pore polyurethane foam was effective in prevention of grapeing. Steel wool and nylon felt also gave good results with only a layer or two of 16-mesh glass or PVC screen as the outer skin.

There may well be materials of other structures that would be still better than the foregoing. In general, closely woven fabrics and papers are too dense, and loosely woven fabrics lack the tortuous channels that are clearly desirable. Some examination of oriented filaments should be considered, as this area was not explored in any detail. For example, layers of screens, parallel to or at a small angle from the direction of fuel flow, might be of interest.

Composite media, as noted above (page 121) should be investigated. If one could separate the fuel and water flow channels (especially near or at the downstream surface) by means of a composite mat, this would surely be superior to the behavior of a mat of uniform cross section. How this might be done is by no means clear.

5. Removal of Water

A 360 gal/min filter/separator vessel of 26.25 in. i.d. contains 18 canister screens of 5 in. o.d. and a down pipe of 4 in. o.d. This leaves an open area for upflow of fuel of only 175 in^2 and the average fuel flow velocity at the top level of the screens is 20 cm/sec, which is greater than the terminal velocity of even large water drops. Thus it is essential to provide a fallout zone wherein the fuel flow is relatively slow and horizontal. This, of course, is the function of the canister screen. It must also act as a barrier to stop the lateral flow of the medium size drops that do not plunge directly to the bottom sump.

The present 100-mesh Teflon coated screen appears to be a good selection for this purpose, except for the fact that it has only 35% open area. This necessitates a 3-fold increase in fuel flow velocity at the surface of the screen. Other rigid screens examined were no better in this respect.

The measured openings in the Teflon screen were 140 to 160 μ. Thus the small drops of the kind observed in the poisoned fuel outflow readily passed through this screen or even through a 400-mesh screen. To retain these would require an additional coalescence, such as was observed on the 100-pore polyurethane screen.

This suggests the possibility of interposing a coalescing layer of low resistance between the element and the outermost barrier screen. If this could be accomplished without raising the total pressure drop to an overly high level, the result would be advantageous. The maximum allowable pressure drop between the element and the outside of the barrier obviously depends on the depth of immersion of the outer screens in the bottom layer of water in the tank. A pressure drop of 0.5 cm would require at least a 1-inch head of water to force the fuel through the screens.

On the whole, it does not seem likely that coalescence of the small 25 to 150 μ water drops can be accomplished at such a low pressure drop. An alternative possibility that has been considered is to divert the lateral flow of these drops into a downward flow to a region where they could be collected. However it is not easy to add to the force of gravity. The drops are probably too small, and their density is too close to that of the fuel, to be able to utilize inertial separators of the kind used in dust collection, etc.

These considerations inevitably lead to the concept of multistage removal of water. The effective performance of the tandem cells suggests the possibility of designing a single 5-inch diameter closed end element embodying multistage action. Separate coalescer mats would be supported between rigid screens, with an open space between them for water to fall out to the bottom plate and then to flow out laterally into the sump. The experimental full scale element No. 11 represented an initial step in this direction. Further work in this area is certainly warranted.

6. Conclusion

Considering only the coalescence of water from jet fuels containing surfactants, it is clear that mats of the kind described here are far superior to present day commercial materials.

Whether such new mats would be practicable or even feasible in other respects remains to be determined. Such respects include effect on solids removal, durability, problems of full scale construction, and cost.

For diesel oils or badly contaminated jet fuel, even the best known coalescer mats in elements of present dimensions would not be fully effective. A modified approach based on the tandem or multistage principle should give better performance, within the confines of existing filter/separator vessels. It seems certain that operation of existing units in tandem, or of single units at a lower flow rate, would give substantial improvement. This should be measured.

Finally, there remains the distinct possibility that even better coalescers than those described here can be developed. Since the detailed mechanism of the process still remains unknown, further direct investigation of this might open up new avenues of approach. The foregoing paragraphs give several suggestions for possible improvements in both the materials and structure of the mats.

Eventually, it seems certain, continued research will result in the development of superior units suitable for use in the field.

BIBLIOGRAPHY

1. Bascom, W. D., and Singleterry, C. R. (Naval Research Laboratory), "The Effect of Polar-Non-Polar Solutes on the Water Wettability of Solid Surfaces Submerged in Oil," J. Phys. Chem. 66, 236 (1962).

2. Beatty, H. A. (Ethyl Corporation), "Jet Fuel Decontamination Studies," reports listed in the Introduction.

3. Belk, T. E., "Coalescence: Effect of Physical Chemical Parameters," Chem. Eng. Progress 61, No. 10, 72 (1965).

4. Bert, J. A., and Porter, H. R., "Surfactants in Jet Fuels -- Symptoms, Sources, and Solutions," Proc. Amer. Petroleum Inst. 43, III, 165 (1963).

5. Bitten, J. F. (IIT Research Institute), "Study of Aviation Fuel Filter/Separators," yearly summary reports No. IITRI-C6088-4 and C6088-8, April 1967 and 1968.

6. Bitten, John, "New Method for Determining Free-Water Content in Fuel," Anal. Chem. 40, 960 (1968).

7. Brooks, D. B., "Military Research on Jet Fuel Contamination," Proc. Amer. Petroleum Inst. 43, III, 172 (1963).

8. Brown, R.N., and Blakeney, S. A., "Comparative Evaluation of Four Methods for Detecting Minute Quantities of Free Water in Hydrocarbon Fuels," U.S. Army Mobility Equipment Research and Development Center report No. 1858, May 1967 (for official use only).

9. Coordinating Research Council, "Development of Research Technique for Assessing the Water Separation Characteristics of Fuels Containing Surfactants," February 1964.

10. Hazlett, R. N. (Naval Research Laboratory), "Factors in the Coalescence of Water in Fuel," NRL report 6669, February 1968; "An Examination of the Steps Involved in the Separation of Water from Fuel in a Fibrous Bed," presented at Jet Fuel Quality Symposium, San Antonio, October 1968.

11. Hostetler, H. F., and Powers, E. J., "Bugs, Surfactants, and Woes," Proc. Amer. Petroleum Inst. 43, III, 122 (1963).

12. Jefferson, T. H. (U.S. Army MERDC, Fort Belvoir), "Investigation of New Concepts for the Decontamination of Military Hydrocarbon Fuels," presented at Jet Fuel Quality Symposium, San Antonio, October 1968.

13. Johnston, R. K., and Cuellar, J. P., Jr., "Effect of Jet Fuel Additives on Filterability and Water Separation Characteristics," U.S. Air Force ASD Technical Report 61-345, June 1961.

14. Johnston, R. K., and Monita, C. M., "Evaluation of a Detector for Free Water in Fuel," U.S. Air Force Technical Report AFAPL-TR-66-39, April 1966.

15. Johnston, R. K., Neville, C. M., and Brown, L. B., "Data Tests on Filter/Separator Elements," U.S. Air Force Technical Report AFAPL-TR-68-149, January 1969.

16. Johnston, R. K., Tyler, J. C., and Weichlein, R. G., "Fuel Contamination Survey at Air Force Bases," U.S. Air Force Technical Report SEG-TR-65-7, March 1965.

17. Langdon, W. M. (Armour Research Foundation, IIT), "Study of Filter/Separator Phenomena," reports No. ARF 3169-11 and -18, January 1961 and March 1962.

18. Lepera, M. E., "Investigating Petroleum Fuel-Water Contact Interaction Effects," U.S. Army Coating and Chemical Laboratory CCL Report No. 250, July 1968.

19. Lindenhofen, H. E., and Shertzer, R. H., "Mechanism of Water Coalescers -- Studies of Coalescence in a Full Scale Single Element System," U.S. Naval Air Engineering Center report No. NAEC-AEL-1858, July 1967; cf. ref. 28.

20. Minor, F. W., et al., "The Behavior of Liquids on Single Textile Fibers," Textile Res. J. 29, 940 (1959).

21. Peek, R. L., and McLean, D. A., "Capillary Penetration of Fibrous Materials," Anal. Chem. 6, 85 (1934).

22. Redmon, O. C., "Cartridge Type Coalescers," Chem. Eng. Progress 59, No. 9, 87 (1963).

23. Redmon, O. C., "Industry Developments on Filtration Equipment for Jet Fuel," presented at Jet Fuel Quality Symposium, San Antonio, October 1968.

24. Reiman, P. A. (Arthur D. Little, Inc.), "Investigation of Parameters Affecting Aircraft and Missiles Fuel Filtration," U.S. Air Force WADD Tech. Report 60-263, Part II, May 1961.

25. Sareen, S. S., Rose, P. M., Gudesen, R. C., and Kintner, R. C., "Coalescence in Fibrous Beds," A.I. Ch. E. Journal 12, 1045 (1966).

26. Schwartz, A. M., "Capillarity -- Theory and Practice," Ind. Eng. Chem. 61, 10 (1969).

27. Schwartz, A. M., and Minor, F. W., "A Simplified Approach to Capillarity," J. Colloid Sci. 14, 572, 584 (1959).

28. Shertzer, R. H., and Lindenhofen, H. E., "Laboratory Investigations of Mechanisms of Water Coalescers," U.S. Naval Air Engineering Center report No. NAEC-AEL-1852, April 1967; cf. ref. 19.

29. Somer, T. G., "Distribution of Adhesive Drops within Fiber Bundles," J. Appl. Chem. 16, 149 (1966).

30. Stark, L. L. (U.S. Army MERDC, Fort Belvoir), "Military Fuels Decontamination," presented at Jet Fuel Quality Symposium, San Antonio, October 1968.

31. Weatherford, W. D., Jr., "Coalescence of Single Drops at Liquid-Liquid and Liquid-Solid Interfaces," U.S. Air Force Technical Report AFAPL-TR-67-3, February 1967; "Basic Studies of Coalescence," Southwest Research Institute report No. RS-505, August 1967.

32. Zisman, W. A., "Relation of the Equilibrium Contact Angle to Liquid and Solid Constitution," Advances in Chemistry Series No. 43 (1964), chapter 1.

Ethyl Corporation
[illegible]
Ferndale, Michigan 48220

2a. REPORT SECURITY CLASSIFICATION
UNCLASSIFIED

2b. GROUP

3. REPORT TITLE

JET FUEL DECONTAMINATION STUDIES

4. DESCRIPTIVE NOTES (Type of report and inclusive dates)
Final Technical Report, 10 June 1965 - 10 August 1969

5. AUTHOR(S) (Last name, first name, initial)

Beatty, Harold A.

6. REPORT DATE	7a. TOTAL NO. OF PAGES	7b. NO. OF REFS
1 September 1969	vii + 132	32

8a. CONTRACT OR GRANT NO.	9a. ORIGINATOR'S REPORT NUMBER(S)
DA-44-009-AMC-1165(T)	69-11
b. PROJECT NO. 1M643324159209	9b. OTHER REPORT NO(S) (Any other numbers that may be assigned this report)
c.	
d.	

10. AVAILABILITY/LIMITATION NOTICES - "U.S. Government agencies may obtain copies of this report directly from DDC. Other qualified users shall request through Commander, USAMERDC, Fort Belvoir, Virginia."

11. SUPPLEMENTARY NOTES	12. SPONSORING MILITARY ACTIVITY
	U.S. Army Mobility Equipment Research and Development Center, Fort Belvoir, Virginia

13. ABSTRACT

In a 4-year laboratory bench study of coalescence of free water in JP-5 and other fuels with added corrosion inhibitors and strong surfactants, measurements were made of contact angles on surfaces submerged in fuel, water-fuel interfacial tensions, capillarity and porosity of coalescer media, and of the attachment, growth, and detachment of water on single fibers in a flowing suspension. Many coalescer media were tested in small cells, both under water separometer operating conditions and in larger cells at realistic mat depths and flow velocity. Tests of individual media are meaningless, for effective performance is obtained only in composite mats with layers of varying structure. Certain experimental mats were far superior to plugs cut from commercial filter/coalescer elements. Antiicer greatly reduced the deleterious effect of surfactants. Water removal from diesel fuel is difficult, but may be done by using two coalescers in tandem. A few experimental full scale elements were sent to Fort Belvoir for testing.

14. KEYWORDS

*Jet Engine Fuels, Decontamination
*Fuel Filters, Jet Engine Fuels
Antiicer
Corrosion Inhibitors
Diesel Fuels
Fibers
Surfactants
Water Removal

DD FORM 1473

UNCLASSIFIED
Security Classification